

University of Szeged

Faculty of Pharmacy

Department of Pharmaceutical Technology

Head: Prof. Dr. Habil. Piroska Szabó-Révész DSc.

MANUFACTURING AND INVESTIGATION OF COATED PELLETS
CONTAINING WATER-SOLUBLE ACTIVE INGREDIENTS

Ph.D. Thesis

Krisztina Nikowitz

Supervisor:
Dr. Géza Regdon jr.

2014

PUBLICATIONS RELATED TO THE THESIS

- I. **Krisztina Nikowitz**, Friederike Foltmann, Markus Wirges, Klaus Knop, Klára Pintye-Hódi, Géza Regdon jr., Peter Kleinebudde
Development of a Raman method to follow the evolution of coating thickness of pellets
Drug Development and Industrial Pharmacy (in Press, accepted manuscript
DOI:10.3109/03639045.2013.795583)
IF: 1.539 (2012)
- II. **Krisztina Nikowitz**, Klára Pintye-Hódi, Géza Regdon jr.
Study of the recrystallization in coated pellets - Effect of coating on API crystallinity
European Journal of Pharmaceutical Sciences 48(3):563-571, 2013
IF: 2.987 (2012)
- III. **Nikowitz Krisztina**, Hódi Klára, *ifj. Regdon Géza*
Rétegzéses technológia elve és alkalmazási lehetősége multipartikuláris rendszerekben
Gyógyszerészet, July 2011, publication for continuing education.
IF: -
- IV. **Krisztina Nikowitz**, Péter Kása jr., Klára Pintye-Hódi, Géza Regdon jr.
Study of the preparation of a multiparticulate drug delivery system with a layering technique
Powder Technology 205(1):155–159, 2011
IF: 2.080
- V. Tamás Sovány, **Krisztina Nikowitz**, Géza Regdon jr., Péter Kása jr., Klára Pintye-Hódi
Raman spectroscopic investigation of film thickness
Polymer Testing 28(7):770-772, 2009
IF: 1.667

PRESENTATIONS RELATED TO THE THESIS

- I. **Nikowitz Krisztina**, Friederike Foltmann, Markus Wirges, Klaus Knop, Peter Kleinebudde, Hódi Klára, ifj. Regdon Géza
Bevonatvastagság jellemzése Raman spektrumok multivariáns analízisével
XVII. Országos Gyógyszertechnológiai Konferencia és
IX. Gyógyszer az Ezredfordulón Konferencia 2012, Siófok
- II. **Krisztina Nikowitz**, Markus Wirges, Klaus Knop, Peter Kleinebudde, Klára Pintye-Hódi, Géza Regdon jr.
Physicochemical investigation of a multiparticulate drug delivery system
4th BBBB Conference, 2011, Bled, Slovenia
- III. **Géza Regdon jr.**, **Krisztina Nikowitz**, Klára Pintye-Hódi, Ulrich J. Griesser
Study of the recrystallization in coated pellets
8th Central European Symposium on Pharmaceutical Technology 2011, Graz, Austria
- IV. **Krisztina Nikowitz**, Péter Kása jr., Klára Pintye-Hódi, Géza Regdon jr.
Study of the preparation of a delayed release drug delivery system
7th World Meeting on Pharmaceutics, Biopharmaceutics and Pharmaceutical Technology, 2010, Valetta, Malta
- V. **Nikowitz Krisztina**, Hódi Klára, ifj. Regdon Géza
Diltiazem-hidroklrid tartalmú bevont multipartikuláris rendszerek előállítása és vizsgálata
Congressus Pharmaceuticus Hungaricus XIV., 2009, Budapest
- VI. **Nikowitz Krisztina**: Bevonási körülmények és kristályosodási jelenségek vizsgálata bevont pelletekben
10th Clauder Ottó Emlékverseny, 2011, Budapest
- VII. **Nikowitz Krisztina**, Sovány Tamás, ifj. Kása Péter, Hódi Klára, ifj. Regdon Géza
Különböző bevonatvastagságú rétegzett pelletek előállítása és vizsgálata
MKE Analitikai Napok, 2010, Budapest

Table of Contents

1. Introduction.....	1
2. Current state of the art.....	1
2.1. The production of multilayered pellets	1
2.2. Processing in fluid bed equipment	2
2.3. Film coating in fluid beds	4
2.4. Composition-related factors affecting dissolution	7
3. Aims	9
4. Materials	9
4.1. Raw materials	9
4.2. Samples	9
5. Methods.....	10
5.1. Preparation of samples	10
5.2. Measurement of layer thickness	10
5.3. Differential scanning calorimetry and thermogravimetric analysis	11
5.4. Powder X-ray diffractometry (XRPD)	11
5.5. Hot-stage microscopy	12
5.6. Fourier-transformed infrared spectroscopy (FT-IR)	12
5.7. Dissolution studies	12
5.8. Raman spectroscopy	13
5.9. Data analysis	13
6. Results and discussion	14
6.1. Section I – Pellets containing pyridoxine hydrochloride	14
6.1.1. Preparation of samples	14
6.1.2. Determination of drug content and film thickness.....	15
<i>6.1.2.1. Particle size and film thickness</i>	15

6.1.2.2. <i>Dissolution</i>	17
6.1.2.3. <i>Raman spectroscopy</i>	18
6.1.3. Summary	25
6.2. Section II – Pellets containing diltiazem hydrochloride	26
6.2.1. Preparation of samples	26
6.2.2. Determination of film thickness	26
6.2.3. Study of the API migration and recrystallization	26
6.2.3.1. <i>Thermal analysis</i>	26
6.2.3.2. <i>X-ray analysis</i>	29
6.2.3.3. <i>FT-IR analysis</i>	32
6.2.3.4. <i>Hot-stage microscopy</i>	32
6.2.3.5. <i>Stability</i>	35
6.2.3.6. <i>Dissolution studies</i>	37
6.2.4. Measurement of the degree of crystallinity	38
6.2.4.1. <i>ssNMR</i>	38
6.2.4.2. <i>X-ray characterization of samples</i>	38
6.2.4.3. <i>Determination of the crystalline content by univariate methods</i>	39
6.2.4.4. <i>Determination of the crystalline content by multivariate methods</i>	42
6.2.5. Summary	44
7. Final conclusions, novelty, practical usefulness	45
8. References	47

1. Introduction

Pharmaceutical dosage forms have to meet several requirements in order to be released on the market. Most of these involve parameters that, while key in determining product performance, are not specific to the product itself and have little to no connection to the natural laws and phenomena that determine the functionality of the final dosage form. This probably contributes to the fact that despite the tight quality control maintained in the pharmaceutical industry many of the recalls happen because of failures to meet specifications. While specific formulation properties and their investigation have received a lot of attention and several advanced characterization techniques have been developed a better understanding of the final product is required to improve design and manufacturing and thus avoid unnecessary batch failures and recalls.

Dissolution is arguably the most important parameter of a modern pharmaceutical formulation as it is the value that determines the efficacy of the product. Modified release formulations that are preferred nowadays by patients and prescribers are designed to provide a dissolution profile tailored to fit disease and patient characteristics, thus the factors influencing dissolution are of particular importance in their case. Our work attempts to investigate some properties of a model pellet formulation that potentially influence dissolution and translate the findings into a deeper understanding of the internal affairs of modified release multiparticulates.

2. Current state of the art

2.1. The production of multilayered pellets

Multiparticulate drug delivery systems consist of many individual drug-containing units as opposed to a single drug carrier entity. These units are typically spherical pellets between 100-2000 μm [1] that are further processed into capsules, tablets or dedicated pediatric dosage forms [2-3]. The concurrent use of pellet fractions with different APIs, drug contents, release properties, etc. offers a very wide range of possibilities for drug development. Multiparticulate drug delivery systems are also gaining popularity as their nature provides several benefits over single-unit dosage forms [4-5]. These include but are not limited to a lower irritative effect due to the decreased local concentration, less individual differences in plasma concentration, a reduced risk of dose dumping, improved bioavailability, a decreased variation

between doses, an easy solution for interactions and a large scale of dosage forms that can be produced from one intermediate [6-8].

Pellets are good candidates for the development of multiparticulate dosage forms: they are small, spherical and smooth, therefore possess exceptional flow properties and processibility, especially in coating operations [9-10].

Pellets can be produced by extrusion and spheronization or in a rotary fluid bed (matrix pellets) and by the so-called layering technique (layered pellets) [11-12]. The latter technique uses API-containing or inert (generally sugar or MCC) cores and processes them further, typically in a fluid bed equipment [11-12], where the materials of the next layer are sprayed onto the cores either as a (generally aqueous) solution, suspension or as dry powder [9, 13-14]. Layers typically contain one or more polymer components as binder [15]. Pellets retain their shape and flowability after layering.

A critical parameter in suspension and powder layering is the particle size of the dispersion or powder. Achieving the smooth surface required for further processing and avoiding the abrasion and porosity issues generally calls for micronized substances where particle size has to be cross-referenced with the size of the cores used for production [15-16].

2.2. Processing in fluid bed equipment

Fluidized bed systems have been widely used not only in the production of pellets but for drying and granulation as well. Regardless of purpose the system contains a (usually conical) chamber in which the solids used in the process are suspended in the so-called fluid state by the heated air flow blowing upwards. This constant movement and heating makes the equipment ideal for very quick drying. Main disadvantages are the large number of critical parameters that need to be monitored, multiple-step manufacturing, high production costs, greater need of excipients and advanced technological and human requirements [8, 17]. As pellet size affects the movement patterns of the fluidized solids a wide size distribution (or a badly picked narrow one) can also cause several problems during processing.

The schematic drawings of three fluid bed set-ups are shown in Fig. 1. The first drawing depicts a top-spray equipment that is typically used for the granulation of powders. The second one shows a bottom-spray fluid bed coated equipped with a so-called Wurster column. The third picture is of a tangential spray or rotary fluid bed equipment (described in detail in [18]).

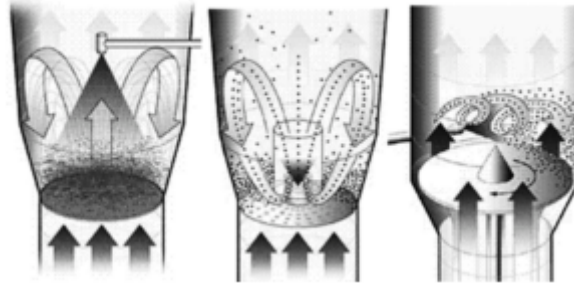


Figure 1: Schematic drawing of common fluid bed types; from left to right top spray, bottom spray with Wurster insert, tangential spray. Figure taken from [19], courtesy of Glatt

Besides the auxiliary systems providing the fluidizing and spraying abilities all three have in common the cone-shaped expansion chamber where the air flow loses some of its velocity, the perforated plate at the bottom of the chamber regulating the air flow and the filters placed at the top of the chamber to prevent solids from escaping with the air flow [19].

The bottom-spray system with the Wurster insert is the optimal the equipment for coating processes [20]. The Wurster column partitions the expansion chamber into two main sections: due to the faster air flow provided by the air distribution plate at the bottom of the chamber particles move upwards inside the Wurster column (and get sprayed during the process) and slowly fall down around the insert due to the more gentle air flow around the perimeter of the partition. Particles are then sucked back into the Wurster column through the gap (the so-called partition height) between the bottom of the insert and the perforated plate by the pressure gradient maintained by the air velocity difference [21-22].

During a coating or layering process the wetting and drying of the particles are in a delicate balance that has a great impact on the final quality of the product [23]. The system is mainly defined by its drying capacity [24-25]. In the case of fluid beds the critical parameters that mainly determine drying capacity are inlet air temperature and volume. (Inlet air humidity is also a critical factor playing part but not all equipment – including both fluid beds used in this work – contains dehumidification pieces to be able to control this parameter.) Spray rate is limited by the drying capacity as too high rates will lead to particle agglomeration [26].

Droplet size of the sprayed substance is determined by nozzle diameter and atomizing air pressure [27] but is also affected by the viscosity of the sprayed solution

or suspension. Suboptimal droplet size affects the quality of the product by either overwetting the particles (and thus facilitating their agglomeration) or spray drying where only the freshly dried solid content reaches the particles resulting in a rough and abrasive surface.

Inlet air temperature and spray rate together determine product temperature which is often difficult to monitor inside the equipment. Product temperature must be chosen according to the thermal behavior of the materials involved in the process: low enough so as not to introduce degradation and high enough to provide for reasonable process durations [19].

Inlet air volume or more accurately inlet air velocity is also a key factor through maintaining a higher humidity gradient between the drying air flow and the particles. Fluidization patterns are governed by inlet air velocity therefore the movement of the particle bed can be optimized through this parameter. Too high velocity causes the particles to get stuck in the filter while too low velocity results in overwetting and agglomeration. The air distributor plate is also very important in determining fluidization patterns by distributing the air evenly thereby providing good gas-solid mixing and drying and minimizing dead zones and channeling [28].

Spray rate has to be chosen according to the factors described above. It is the most critical factor in determining process time and as such the maximal spray rate by which good product quality can be maintained can be considered the optimal choice.

2.3. Film coating in fluid beds

Coating is often the final step in the preparation of a multilayered pellet. As pellets are usually processed further into a dosage form that is more convenient to handle for the patient the coatings in question are usually functional. This means that their quality is of utmost importance in achieving the desired release profile and therapeutic response.

Functional coatings can be categorized according to the release profile they convey. The most common ones are sustained release and delayed release but by combining polymers of different characteristics and suitable excipients a multitude of other release profiles become available [29].

Film coating was traditionally done by spraying an organic (or rarely aqueous) solution of the coating polymer on the core materials but due to toxicity and environmental concerns aqueous dispersions have become the standard solution [30].

Dry powder coating – similarly to powder layering - involves the spraying of plasticizer solution although solutions without the use of any kind of solvent have been described [31-32].

Coatings obtained through these three methods are drastically different both in quality [33] and in the method of formation. In an aqueous or organic solution the coating polymer chains are swollen and the single chains overlap. Upon solvent evaporation this degree of chain mixing remains and a uniform film is formed [34].

Aqueous dispersions contain the polymer in the solid state in globular form. Polymer chains in this state mainly form secondary connections within the molecule and do not interact with each other. Thus upon evaporation individual polymer grains remain, ideally densely packed on the cores' surface. The evaporation of the water contained in the capillaries between the grains lead to particle deformation and under certain conditions film formation through coalescence of the polymer particles [35-36]. Polymer dispersions exhibit a so-called minimum film forming temperature below which coalescence does not take place [37]; suspension coatings performed under the minimal film forming temperature of the polymer result in coatings that do not fulfill their intended role in esthetics, taste masking or controlling drug release. For most polymers plasticizers are required to reach a sufficient molecular mobility to achieve coalescence [38-39].

In the case of dry powder coatings the small amounts of liquid used in the process are generally not enough to facilitate film formation even with sufficient heating. Thus a curing step is required post-production, where the coated particles are heated above the glass transition temperature (T_g) of the coating polymer [40-41]. Above glass transition temperature polymer films transform from glassy to rubbery state where molecular mobility is enhanced and viscosity is decreased. This state can permit polymer particles to coalesce even without the aid of capillary forces but usually elevated humidity is employed during the process.

As even in a glassy state polymers essentially behave similar to a very high-viscosity liquid [41-42] coalescence can occur over long term storage. Uncoalesced or poorly coalesced films are porous and as such do not perform as well as coalesced films in dissolution tests therefore the slow coalescence over the lifetime of the product brings with itself a change in the dissolution characteristics that must be avoided at all costs [43]. Curing of the films helps achieving complete continuity and stability of the coatings and equalizes any potential differences in film structure.

Beside film structure film thickness has been identified as a critical parameter in the performance of functional coatings [44-45]. Many different techniques have been found suitable for the determination of film thickness with each one having distinct advantages and disadvantages over the others. For the direct measurement of the film thickness image analysis is the most common technique but recently tomographic methods have also gained recognition. Traditional static image analysis in the case of pellets is very labor-intensive especially in the case of scanning electron microscopic images where cross-sections are needed [46]. It is mostly for this reason that there is no agreement in the literature about a generally acceptable sample size that can accurately represent the whole batch [10, 47]. Computerized image analysis has been investigated as a tool to solve this problem but the skills needed for its application limit its usefulness. Also, both software and operator choice has been shown to influence results [48-49].

Dynamic image analysis is an emerging technique that specializes in the size range of most multiparticulate products. It alleviates the work load associated with image analysis and provides a more comprehensive view of particle properties but it usually requires the purchase of an expensive piece of equipment and (mainly due to the method making it possible to measure such amounts) requires a large amount of sample compared to the usually investigated quantity [50]. In both cases problems associated with particle projection and image focusing are present, and in addition dynamic image analysis may suffer from the difference between the calibration and the measurement method as well [51].

Raman and NIR spectroscopic methods have been proven to work both offline and inline [52-54] however these methods need to be calibrated to another (preferably direct) method and they rely on either a small sample or a multitude of particles averaged by their constant movement during processing. This means that while spectroscopic methods are a good general indicator of film thickness they cannot be relied upon when predicting the chance of product failure due to variations in coating thickness (for example on tablet edges).

Tomographic methods are mostly absent of the above-mentioned disadvantages. In order to fully benefit from their advantages however samples need to be turned and repeatedly measured. Also some studies found that their detection limit was higher than for other methods investigated [55-57].

The most traditional method of describing and reproducing film thickness however is through polymer weight gain [58]. While probably the easiest to measure polymer weight gain suffers from the same problems as spectroscopic methods. In addition it does not consider the unevenness and abrasion of the cores during the coating process or the deviations from the average weight gain which have been proven to crop up due to fluidized bed coating [46, 59-60]. As such polymer weight gain is a questionable indicator of film thickness and dissolution behavior at best.

The reasons for deviations from the average have been attributed to several different factors. In the easiest approach larger particles will receive a thicker coating because of their larger specific surface area. Several studies have found however that when normalizing polymer weight gain to specific surface area larger particles still received a larger amount of coating than smaller cores [22, 61].

These further differences are most commonly believed to stem from either the number or the efficiency of passes through the spray zone [22, 46] – unfortunately both of these factors require complicated experimental setups to investigate. They are strongly correlated to particle movement patterns that are governed by the previously described process parameters [23, 62]. Even in a narrow size distribution particle properties contribute a lot to the variation in the fluidization patterns and thus significant differences in coating levels can be detected [22]. Several mathematical models were developed using different approaches to the coating process, for example by considering the fluid bed equipment as a series of compartments [63] or by the Monte Carlo method [64]. By their probabilistic nature these models are more descriptive than predictive and do not include all parameters that can affect coating quality and uniformity. However models usually agree that longer coating times result in a more uniform distribution and that the main contributor to the coating variation is the non-uniform weight gain per pass through the spray zone [65].

2.4. Composition-related factors affecting dissolution

Dissolution of coated dosage forms is affected by many factors. The most obvious one is the nature of the polymer coating: does it dissolve at a physiological pH, how permeable is it, what are its swelling and erosion characteristics? Traditional dosage forms usually exhibit a fast initial dissolution however where a coating was used to delay or retard dissolution at least the first phase of drug release will be characterized by diffusion through a (preferably intact) polymer film. An excellent

overview of the possible mechanisms governing this phase was presented by A.G. Ozturk et al. [66].

Beyond the thickness and quality of the polymer film the excipients used in the coating can also have a great impact on the dissolution behavior. The most common types of excipients are plasticizers (especially important in aqueous coating operations), anti-tacking agents and dyes or pigments.

Plasticizers are necessary for coating from aqueous dispersions as they facilitate the mobility of the polymer chains and as such help in forming a uniform film coat [67]. Different plasticizers work differently on the molecular level [68-69] and as such a generalized approach is difficult to maintain. However several plasticizers have been found to influence (generally increase) dissolution through evaporation or leaching (and consequentially pore formation [70-71] or in the unlikely cases where they form a continuous phase through dissolving the API and thus facilitating diffusion through the film [72]. Some studies have found that higher plasticizer levels resulted in a decreased drug release [73-74] which was attributed to insufficient plasticization and thus incomplete film formation at lower levels [66].

The coated substrate composition (and excipients not present in the sample but used in the production process [75] also have an impact on dissolution properties [76]. Several studies have found that release rate increases with solubility [45, 77-78] although some exceptions have been reported but mainly attributed to other factors [45, 79]. Beyond API-solubility the effects of different core materials through osmotic pressure or adsorption have been recently investigated by several authors [80-82] although conflicting results have arisen due to the water counter-current formed due to high osmotic pressure [83].

Binders like HPMC can also affect dissolution due to their dissolution-enhancing properties found in other technological processes but very few studies have been conducted in this direction [12, 15]. Polymers frequently used as binders have been shown to improve solubility and dissolution rate through wettability [84] and prevent the recrystallization of amorphous drugs [85]. Core shape, size and surface have also been investigated and it was suggested that these parameters are just as important as the coating process itself when determining dissolution of the final, coated product [60, 86].

3. Aims

Pellets are an increasingly popular choice in the development of drug delivery systems, yet comparatively few studies deal with their investigation even by methods routinely used elsewhere in the pharmaceutical industry. Our aim was to study the use of different analytical techniques in the investigation of different characteristics and phenomena influencing dissolution, develop new ones and determine the extent of usefulness of methods that, given their nature and required circumstances, appear to have a limited applicability on pellets.

The first section of this work describes the development of a Raman spectroscopic method for the determination of the film thickness of pyridoxine hydrochloride-containing coated pellets. Two different equipment set-ups were used for sample production and their impact on the outcome of the analysis was examined.

Section two deals with the investigation of an atypical thermal phenomenon observed in diltiazem hydrochloride-containing multilayer pellets. This is divided into two larger parts: the investigation of the thermal behavior and the underlying recrystallization phenomenon and the development of a method to determine degree of crystallinity in intact pellets.

4. Materials

4.1. Raw materials

Diltiazem hydrochloride (Ph. Eur., a gift from EGIS Ltd., Budapest, Hungary) and pyridoxine hydrochloride (Ph. Eur.) were used as model drugs, Cellet 500 (Shin-Etsu Chemical Co., Ltd., Tokyo, Japan, granted as a gift from Harke Pharma) as nonpareil core material, Kollidon 25 (polyvinylpyrrolidone; BASF, Ludwigshafen, Germany) and Pharmacoat 606 (hypromellose; BASF, Ludwigshafen, Germany) was applied as a binder in the layering of the APIs, and Acryl-EZE (Colorcon, Dartford Kent, UK), a fully formulated enteric coating dispersion a methacrylic acid copolymer, was used as coating material.

4.2. Samples

Samples' names consist of two or three letters and two numerical characters. The first letter represents the API contained in the sample where

D – indicates diltiazem hydrochloride

P – indicates pyridoxine hydrochloride.

The second letter indicates the binder used for the production of the sample such that

K – stands for Kollidon 25

P – stands for Pharmacoat 606.

In the case of samples labeled PP the third, additional letter represents the place of production where

S – is for Szeged, Hungary

D – is for Düsseldorf, Germany.

The first number will either be 0 or 1 which indicates the lack of or presence of coating. The second numerical character is the batch number.

5. Methods

5.1. Preparation of samples

The multiparticulate pellet samples were prepared in a Strea-1 (Niro Aeromatic, Bubendorf, Switzerland) fluid bed chamber. In the first, drug-loading step, API was layered onto nonpareil Cellet 500 cores. A solution of diltiazem hydrochloride or pyridoxine hydrochloride as API and Kollidon 25 or Pharmacoat 606 as binder in a mass ratio of 5:3 for Kollidon 25 and 5:2 for Pharmacoat 606 respectively was used. A batch size of 200 g of nonpareils and the above-mentioned solution containing 125 g of API was used. Water content of the solution varied with API solubility.

Between drug-loading and coating the pellets were dried in the spray coater for 10 minutes. Since the Acryl-EZE contains sodium bicarbonate as an excipient, the equipment was disassembled and washed to prevent precipitate formation. Samples of the drug-loaded nonpareils were taken for comparison purposes.

In the second, coating step, a 20% aqueous dispersion of Acryl-EZE (a fully formulated USP copolymer type C coating system containing 60% polymer and various excipients) was prepared and applied as per the guidelines of the manufacturer. 0.1% of dimeticone was added to prevent foaming during the stirring and coating process. The parameters of the coating were the same as for the drug layering step in all cases. Samples of different coating levels were produced.

5.2. Measurement of layer thickness

An image analysis method (Leica Quantimet 500 MC, Leica Cambridge Ltd, Cambridge, UK) was used to determine the thickness of the layers on the pellets. Particle size was specified as the average of the minimal and maximal diameter of the particle projection. The mean film thicknesses were calculated from the mean

diameters of the particles, determined by measuring 8 chords of approx. 300 particles of each batch with a stereomicroscope (Zeiss, Oberkochen, Germany).

For the pyridoxine hydrochloride-containing samples three pellet batches from Düsseldorf and four batches from Szeged (pellets coated with Acryl-EZE® and uncoated pellets) were measured three times using the CamsizerXT image analysis system (Retsch® Technology GmbH, Haan, Germany, X-Fall module, free fall mode). The number of measured pellets per sample was counted during measurement. The value specifying the particle size is defined as width of the particle projection and is the shortest of measured maximum chords in 32 directions. The median of the number size distribution was used as the particle size of the sample. The coating thickness was calculated from the mean of n=3 measurements the half of the difference between the coated and uncoated diameter of the sample.

5.3. Differential scanning calorimetry and thermogravimetric analysis

Differential Scanning Calorimetry (DSC) was performed with a Mettler–Toledo DSC 821e (Mettler–Toledo GmbH, Switzerland) instrument. Thermogravimetric Analysis (TGA) was carried out with a Mettler–Toledo TGA/DSC1 (Mettler–Toledo GmbH, Switzerland) instrument. Sample weight varied between 10-12 mg for the TG measurements. Curves were evaluated with STARe Software. The starting temperatures were 0 °C for DSC and 25 °C for TG measurements respectively and heating rate was 10°C/min for most measurements. Final temperature varied according to the purpose of the measurement. Argon atmosphere was used in all cases. Three parallel examinations were done from all samples. The instrument was calibrated using indium. Samples were measured in a 40 µl aluminum pan.

5.4. Powder X-ray diffractometry (XRPD)

The X-ray powder diffraction patterns (XRPD) were obtained with a Bruker D8 Advance (Bruker AXS, Karlsruhe, Germany) that can be equipped with a Sycos H-Hot (Ansyco GmbH, Karlsruhe, Germany) programmable plate holder. Results were detected with a Vântec-1 detector. The patterns were recorded at a tube voltage of 40 kV, tube current of 40 mA, applying a step size of 0.01 Å 2θ in the angular range of 3 Å to 40 Å 2θ.

5.5. Hot-stage microscopy

Thermomicroscopic investigations were carried out with a Nikon Microphot FXA polarizing microscope (Nikon Corporation, Tokio, Japan) fitted with a Linkam THMSG-600 heating-freezing stage (Linkam Scientific Instruments, Waterfield, UK). Photographs were taken with a digital camera (UBS 2 UI-1640LE-C, IDS Imaging Development Systems GmbH, Obersulm, Germany). Pellets were carefully crushed and intact coating flakes chosen from the grist.

5.6. Fourier-transformed infrared spectroscopy (FT-IR)

FT-IR measurements were performed by an Avatar 330 FT-IR spectrometer (Thermo Nicolet/Thermo Fisher Scientific Inc., Ramsay, Minnesota, USA) equipped with a horizontal ATR crystal (ZnSe, 45°). Spectra were recorded between 4000 and 400 cm^{-1} at 4 cm^{-1} optical resolution. Spectra were collected in absorbance mode using the KBr disk method (~0.5 mg powdered sample in 150 mg KBr disk). 256 scans were co-added. Spectra were collected with the EZ Omnic software and analyzed with GRAMS/AI 9.0.

5.7. Dissolution studies

Drug content determination was done with a UV-VIS spectrophotometer (Unicam Helios α , Thermo Fisher Scientific Inc., Waltham, USA) at pH 6.8 (phosphate buffer) from approx. 500 mg of whole pellets after two hours at 325.0 nm for pyridoxine hydrochloride and 237.0 nm for diltiazem hydrochloride with a bandwidth of 2 nm and a lamp charge of 325 nm. Coefficient of determination (R^2) for the calibration curve was 0.9999 and 0.9983 respectively.

Dissolution studies were carried out according to the Ph. Eur. standards with a rotating basket (Erweka DT 700, Erweka GmbH, Heusenstramm, Germany), in 900 ml of simulated gastric acid at 100 rpm at 37 °C for 2 h, then the acidic medium was replaced with 900 ml of phosphate buffer (pH=6.8) and the dissolution measured at the same parameters as above. Samples were taken of the gastric acid at 2 h and of the phosphate buffer at 5, 10, 15, 20, 30, 45, 60 and 90 min. Three parallel measurements were performed for each sample.

Drug concentration was measured spectrophotometrically at 235 nm for diltiazem hydrochloride and 291.0 nm for pyridoxine hydrochloride in artificial gastric acid by comparison to a calibration curve with an R^2 of 0.9946 and 0.9996

respectively. For the measurements in artificial intestinal fluid the parameters and calibration curves were the same as described for the drug content determination. Results were analyzed with Microsoft Excel 2007.

5.8. Raman spectroscopy

The Raman spectra were measured using a RamanRXN2 analyzer (Kaiser Optical Systems, Ann Arbor, USA) with a non-contact optic sampling device (PhAT probe). The probe beam was generated using a diode laser operating at 785 nm and the laser power at the sample was 400 mW. The laser spot diameter was 6 mm corresponding to a 28.3 mm² circular illumination area. Each sample was measured three times with an exposure time of 10 seconds and the average of the three spectra was used for further analysis. Data collection and Pearson's correction were done using icRaman data collection software package (Kaiser Optical Systems, Ann Arbor, USA).

5.9. Data analysis

Savitzky-Golay smoothing (15 point, 2nd order polynomial), single normal variate (SNV) correction, principal component analysis (PCA) and partial least squares regression (PLS) were performed using Matlab 7.13.0.564 and the Statistic Toolbox. As Matlab utilizes the SVD algorithm for multivariate analysis while SIMCA-P, the software used to gather the results published in our article [87] uses the NIPALS algorithm results of the two calculations are not going to produce exact matches (they are however expected to provide the same conclusions).

6. Results and discussion

6.1. Section I – Pellets containing pyridoxine hydrochloride

6.1.1. Preparation of samples

Preformulation studies began using Kollidon 25 as a binder as described in the Methods section. We found that during API layering this composition resulted in the extreme electrostatic charging of the cores that prevented the circulation of the material. Optimization of the parameters yielded little results so Pharmacoat 606 was used instead of Kollidon 25 in further experiments. No significant agglomeration tendencies were observed for either composition.

Samples have been prepared in two different Strea 1 equipment pieces in the same batch sizes. The main differences between the two equipment were the use of the Wurster insert and the geometry of the column. The stainless steel column was set up to include the Raman probe described in the Methods section for inline measurements. The yield of the processes done with the Wurster insert was significantly higher than but further analysis showed no differences between the qualities of the samples that could not be traced back to production yields.

Table 1: Layering and coating parameters

	Strea 1 in Szeged	Strea 1 in Düsseldorf
Inlet temperature	50 °C	50 °C
Outlet temperature	43 °C	37 °C
Spray rate	6 ml/min	6 ml/min
Air volume	80 m ³ /h (variable)	130 m ³ /h (pre-set)
Nozzle diameter	1 mm	1 mm
Chamber material	Glass	Stainless steel
Wurster insert	Yes	No
Spraying installation	Bottom-spray	Bottom-spray

We have found that while fan capacity and fluid feed rate were critical parameters to the process not optimizing them for the different pieces of equipment only affected the yield of the production and not the quality of the samples. Yield was significantly higher in the Wurster equipment with values of 98-99% for API layering and 96-98% for coating. The lower values of 92-95% for API layering and 91-94% for coating observed in the bottom-spray equipment are most probably aggravated by

the difference in chamber geometry: the shape of the stainless steel chamber results in more collisions between particles and with the chamber wall [88].

6.1.2. Determination of drug content and film thickness

6.1.2.1. Particle size and film thickness

Pyridoxine-containing samples were measured with the Camsizer and the Leica equipment as described in the Methods section. Results are summarized in Table 2. It is very important to note that the standard deviations shown in the table are different for the two measurement methods: SD for the Camsizer method is the SD of three measurements of the same sample between measurements while the SD of the Leica method was calculated from individual particle sizes within one measurement.

Particle size and film thickness results between the two analytical methods show a fairly consistent behavior: while film thickness results can be said to be more or less equivalent between the two methods the mean particle sizes are usually larger when measured with the Leica equipment (and this difference is consistent between coated and uncoated samples as evident from the film thickness results). This is most probably explained by the different nature of the equipment: the Leica equipment employs a stereomicroscope focused on the stationary particles where the shadow cast by the particles distorts the image. The magnitude of the distortion also depends on the image recognition software and the resolution of the images taken of the particles. The Camsizer technology measures the shadow cast by the particles thus the distorting effects are taken into account during the calibration process.

The only exception from this is *Sample PPD12* that gave a larger film thickness result on the Leica equipment than with the Camsizer method. The diameters of the coated sample match our expectations based on the film thickness obtained with the Camsizer method and the diameters of *Samples PPD11* and *PPD13* measured on the Leica equipment which means that the difference must stem from the measurement of the uncoated sample. Photographs taken of the particles during the Leica measurement (Figure 2) show that *Sample PPD02* contains a much larger amount of fragmented particles than *Samples PPD01* and *PPD03*. As the Camsizer is designed to measure large numbers of particles through obtaining 60 high-resolution images per second the statistical significance of the results obtained by it is much better ensured both for individual particles and for the whole batch than in the case of the Leica equipment.

Table 2: Particle size and film thickness results of image analysis by Camsizer and Leica equipment

Sample	Amount of coating dispersion used for sample (g)	Camsizer analysis results (μm)			Leica analysis results (μm)				
		Diameter of uncoated pellets	Diameter of coated pellets	Coating thickness	Minimum diameter of uncoated pellets	Minimum diameter of coated pellets	Maximum diameter of uncoated pellets	Maximum diameter of coated pellets	Leica coating thickness
<i>Sample PPS11</i>	300	718.27 \pm 0.11	788.93 \pm 0.25	35.33	731.78 \pm 37.91	803.63 \pm 48.64	793.04 \pm 43.83	861.74 \pm 67.65	35.13
<i>Sample PPS12</i>	450	695.13 \pm 0.31	781.43 \pm 0.06	43.15	707.41 \pm 65.92	795.11 \pm 42.47	764.27 \pm 58.30	857.69 \pm 46.86	45.28
<i>Sample PPS13</i>	500	722.00 \pm 0.10	823.33 \pm 0.15	50.67	742.12 \pm 53.71	847.61 \pm 42.69	802.47 \pm 42.59	907.71 \pm 50.85	52.71
<i>Sample PPS14</i>	600	695.87 \pm 0.06	813.00 \pm 0.00	58.57	706.83 \pm 38.28	836.15 \pm 41.49	769.50 \pm 48.04	892.08 \pm 45.07	62.97
<i>Sample PPD11</i>	300	721.03 \pm 0.06	774.80 \pm 0.17	26.88	716.04 \pm 35.80	773.61 \pm 34.21	783.18 \pm 41.72	834.92 \pm 40.31	27.33
<i>Sample PPD12</i>	450	721.17 \pm 0.12	798.43 \pm 0.06	38.63	703.73 \pm 32.41	806.50 \pm 30.17	771.52 \pm 33.90	872.02 \pm 37.78	50.82
<i>Sample PPD13</i>	600	724.73 \pm 0.15	821.37 \pm 0.06	48.32	727.12 \pm 34.85	823.52 \pm 38.31	789.73 \pm 40.63	890.84 \pm 59.30	49.38

As the parameters for the production of all *PDD samples* were the same we regarded the anomalous result as a probable sampling error.

The Camsizer film thickness results that were used in further studies show a linear correlation with coating polymer weight gain for pooled data ($R^2=0.9219$).

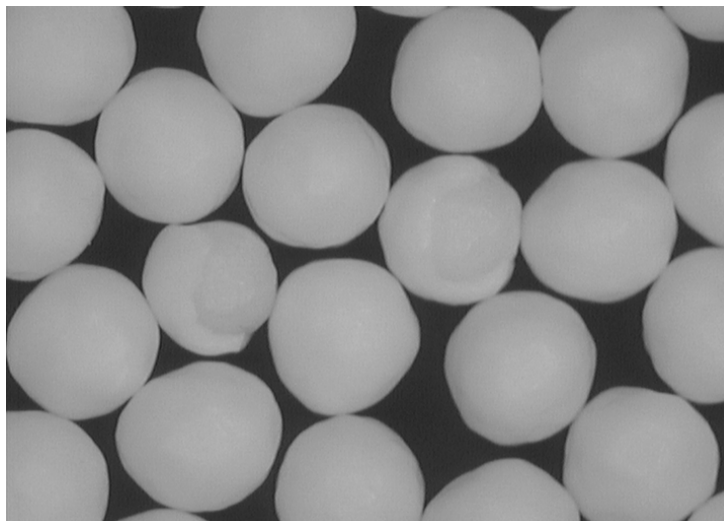


Figure 2: Leica microscopic image of *Sample PPD02*

6.1.2.2. Dissolution

The dissolution curves of the two sample sets are shown in Fig. 3. All samples showed a complete API release after 60 min in the pH 6.8 dissolution medium. Gastroresistance of the film coatings showed a relationship with their thickness where higher coating levels yielded better (in this case lower) results.

Similar levels of coating showed similar levels of dissolution regardless of which equipment was used for sample production, indicating that the coating quality produced in different equipment (but with the same parameters) does not differ in this respect. Coatings of 35 μm or thinner were insufficient in achieving the Ph. Eur. requirements of gastroresistant films. The dissolution testing of *Sample PPD11* was discontinued after observing over 50% drug release in artificial gastric acid.

The possibility of a linear correlation was observed between the percent of drug dissolved in gastric acid and the film thickness was examined but the coefficient of determination (R^2) has proven to be poor (0.6667).

After excluding the data point from the discontinued dissolution test of *Sample PPD11* however the goodness of fit improved to $R^2=0.8798$ (see Fig. 4). Correlation between polymer weight gain and dissolution in artificial gastric acid yielded an R^2 of 0.6842 even after excluding the clearly outlying data point, suggesting that polymer

weight gain is a bad indicator of dissolution results even though it is a good predictor of film thickness [57].

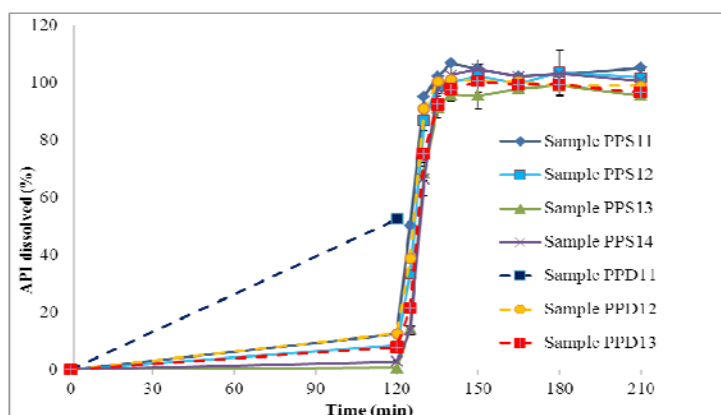


Figure 3: Dissolution of *Sample sets PPS1 and PPD1*

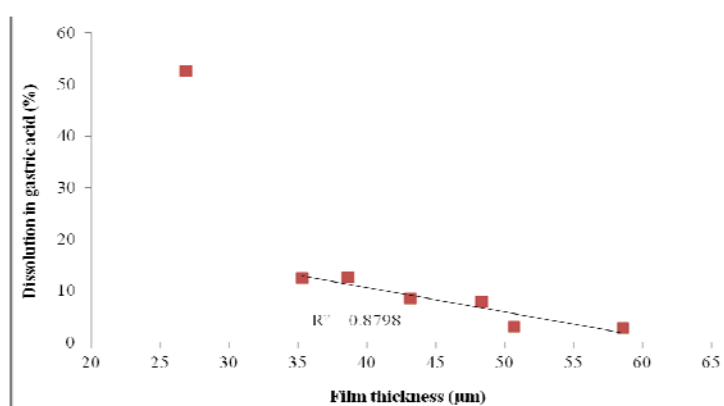


Figure 4: Correlation of film thickness and dissolution in gastric acid; line fitted with the first data point excluded

These results suggest that for gastroresistant films the prediction of dissolution performance based on film thickness measurements may be possible above a threshold value. In the case of the samples used for the study this threshold value is higher than the Ph. Eur. maximum requirement which means that the minimum film thickness can be safely estimated from the correlation.

6.1.2.3. Raman spectroscopy

The Raman spectra of the materials can be seen on Fig 5. The Acryl-EZE film coating system has peaks at 638 cm^{-1} , 515 cm^{-1} and 395 cm^{-1} (henceforth referred to as Peak 1, Peak 2 and Peak 3) that are characteristic of the anatase polymorph of titanium dioxide [89]. These do not overlap with the largest characteristic peaks of pyridoxine hydrochloride which are at 1645 cm^{-1} , 1629 cm^{-1} , 1359 cm^{-1} , 1233 cm^{-1} , 692 cm^{-1} and 329 cm^{-1} [90]. Both API and film coating peaks can be distinctly

observed in the spectra of the samples while signal from the polymer binder and cellulose core cannot be readily identified.

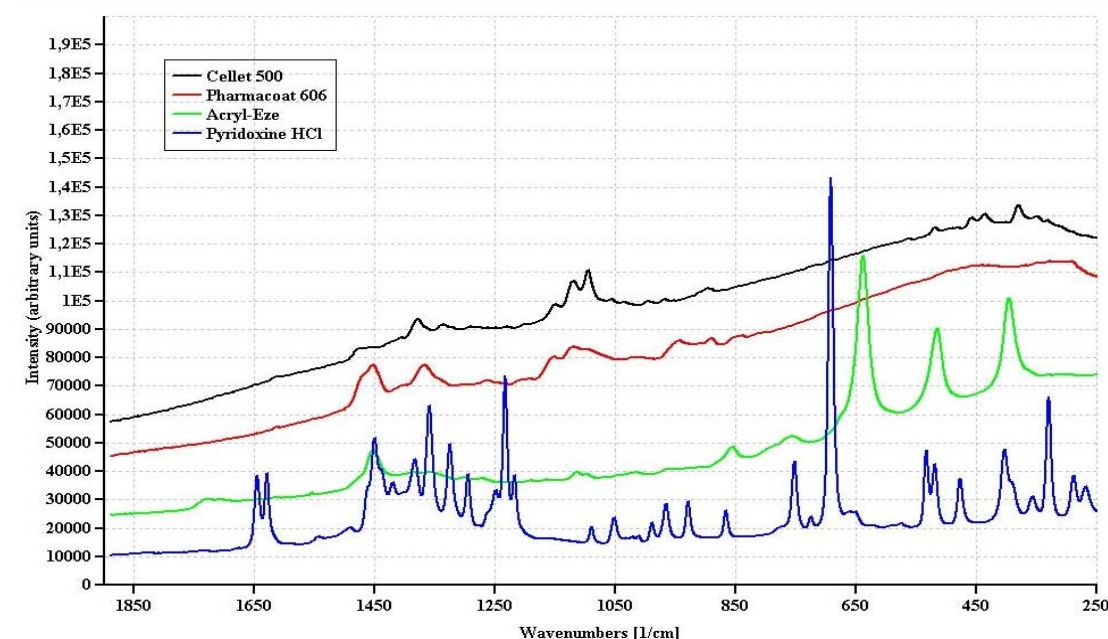


Figure 5: Raman spectra of components

Baseline correction was done with the algorithm described by Pearson [91] that is included in the icRaman software to strip the spectra of the distorting effects of baseline shifts and fluorescence [92]. Peak heights were used for further study to minimize the uncertainty arising from the overlapping smaller peaks.

Univariate analysis of the titanium dioxide peaks showed all three to be good predictors of film thickness where a linear correlation existed between peak area and height and film thickness calculated from the Camsizer analysis results (Fig. 6. a). However this was only true when examining the two sample sets separately – neither sets fit into the others' trend line.

For both sample sets the best fit could be obtained for Peak 1. Peak 2 and Peak 3 gave reasonably good fits for *Sample set PPS1* but showed a decreasing trend in the R^2 value for both sets. Unlike Peak 2 and Peak 3 Peak 1 does not overlap with some characteristic peaks of pyridoxine hydrochloride which – probably being the reason for its better fit – makes it ideal for the univariate determination of film thickness.

The peaks at 692 cm^{-1} , 1233 cm^{-1} , 1629 cm^{-1} and 1645 cm^{-1} corresponding to pyridoxine hydrochloride provided good correlations with the calculated API content (Fig 6. b,) – this was expected due to the attenuation of the API signals being dependent on the film thickness [93].

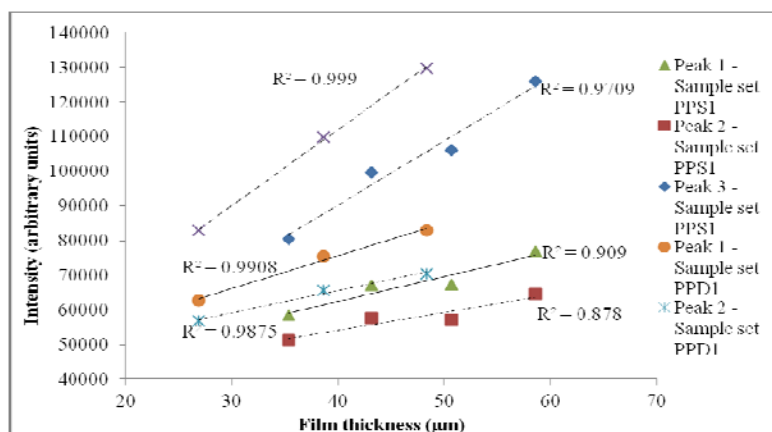


Figure 6. a, Correlation between film thickness and titanium dioxide's Raman peaks

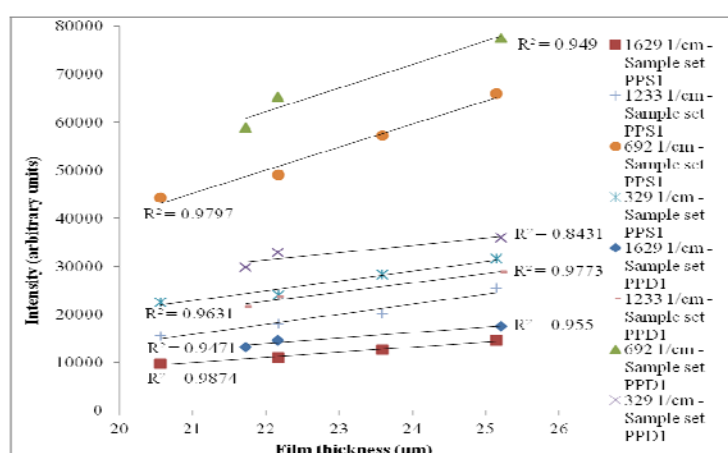


Figure 6. b, Correlation between calculated API content and the API's Raman peaks

The peaks between 1500 cm^{-1} and 1250 cm^{-1} have demonstrated worse results which is probably the result of the baseline correction being insufficient in this spectral region. It can be seen that the regression lines for both film thickness and API content are fairly parallel which means the degree of attenuation is consistent between the two sample sets.

Comparing the raw spectra of the two data sets a trend becomes clearly visible: background fluorescence decreases with the film thickness for both sample sets. An opposite phenomenon was observed for tablets by Kauffman et al. [93] where linear relationship was postulated between the degree of fluorescence stemming from the coating and film thickness. Romero-Torres et al. have also reported small baseline differences in coated tablets [94]; while in their case no systematic pattern was discernible, the effect of incomplete film coverage in thin coatings on highly fluorescent cores they described coincides with our observations of the dissolution and the baseline of *Sample PPD11*.

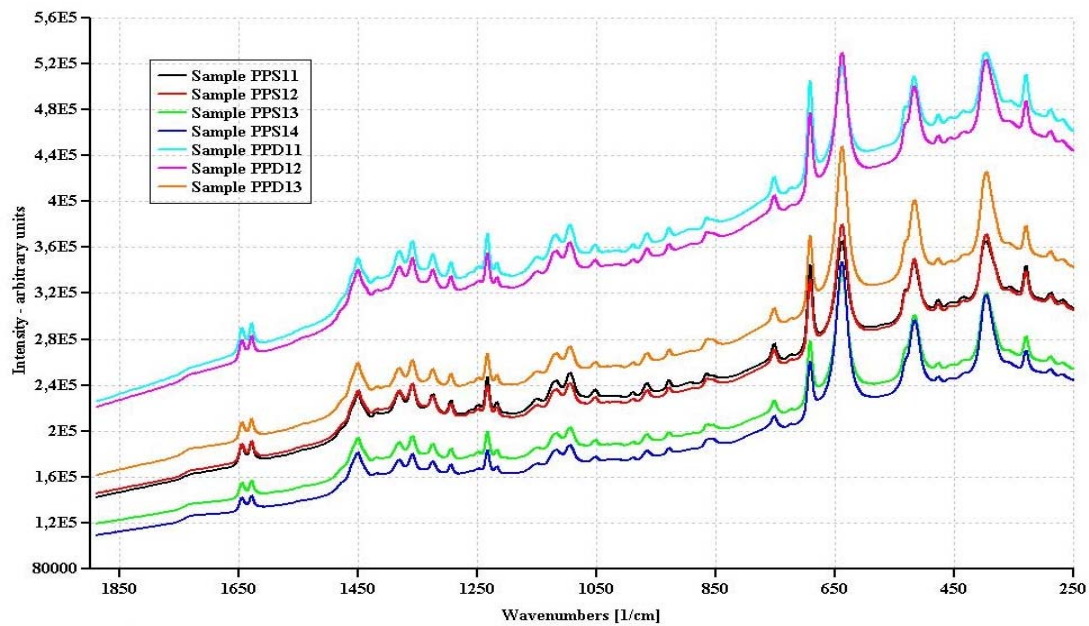


Figure 7: Raw Raman spectra of the coated samples

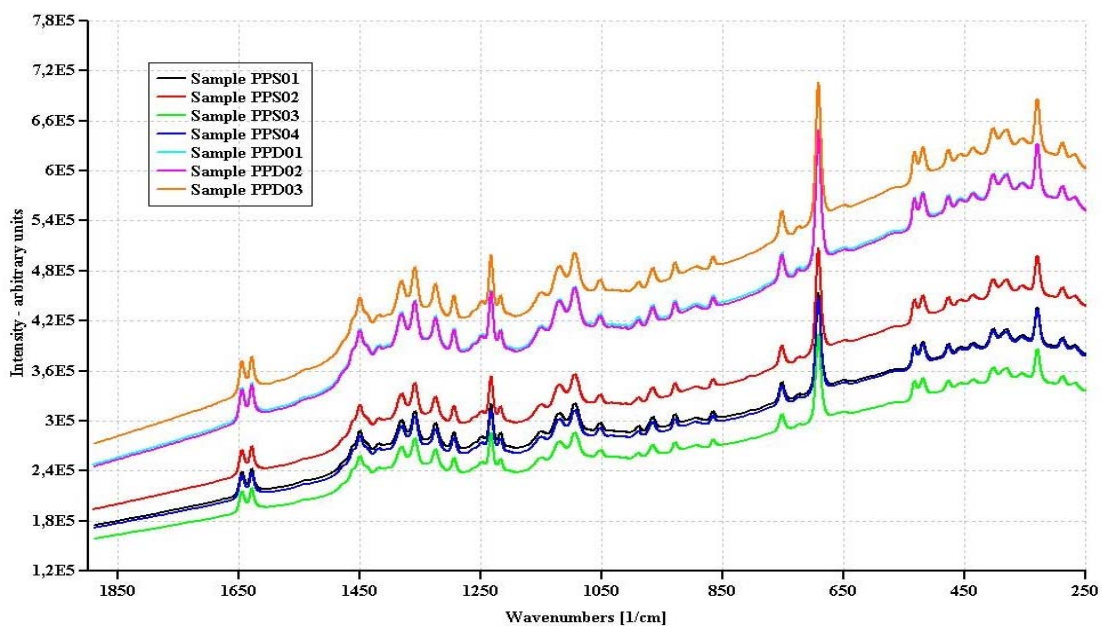


Figure 8: Raw Raman spectra of the uncoated samples

In our case the attenuation of the signal from the highly fluorescent API-layered core can explain the negative trend. *Sample set PPD1* appears to have a distinctively larger offset (see Fig. 7) in all cases.

As long as the detection range is not exceeded fluorescence should not distort the Raman signal [93] but signal-to-noise ratio has been known to influence the efficiency of background subtraction techniques [92]. Other baseline correction methods such as SNV or MSC correction may result in a unified univariate model.

We should keep in mind that peaks indicating coating level are actually caused by the white pigment titanium dioxide and not the coating polymer itself. The closest direct indication of the coating polymer in the spectra would be the fluorescent shift most polymers possess [95] but as the formulation contains several other ingredients showing fluorescence differences in the baseline should be treated very carefully in this case. A look at the raw uncorrected spectra (Fig 8) shows that the systematic difference in the background already exists in the uncoated samples.

While fluorescence is usually treated as problematic noise this systematic variation between the two sample sets suggests that further research might turn up interesting results. Raman spectroscopy has been shown to be suitable to differentiate between tablets coated under different conditions by Cahyadi et al. [96] and our results give a good indication of the same ability in pellets, however for a definitive conclusion further experiments would be needed.

Principal component analysis of the raw spectra showed that 99.85% of the variation between the spectra is explained by the first principal component (PC) which resembles the baseline structure – as expected considering the nature of the calculations involved. Samples are ordered by set along the first PC with *Sample set PPD1* showing positive and *Sample set PPS1* showing negative values and samples of both sets are in decreasing order of film thickness (see Fig. 9).

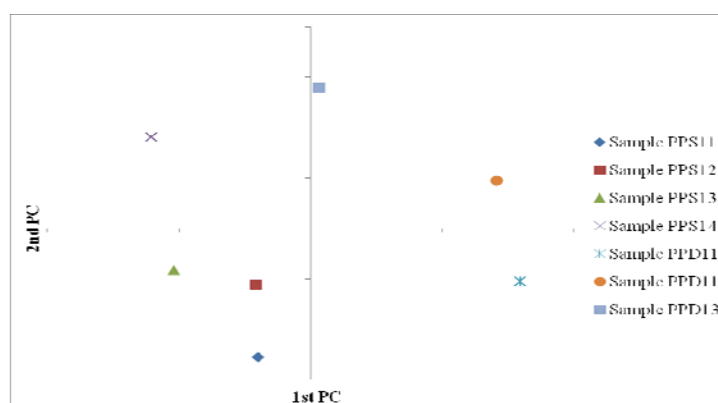


Figure 9. Scores plot of the principal components of raw Raman spectra

For the multivariate analysis spectra were SNV corrected and principal component analysis was performed to observe the variation between the peak structures not confounded by baseline and scaling differences. PLS regression was performed to find a common calibration curve. SNV correction eliminates the basis of the original first PC by subtracting the baseline and normalizing the spectra thereby

providing a better chance to see the latent structures of the peaks. The first PC acquired from this analysis greatly resembles the Raman spectrum of titanium dioxide and corresponds to 91.44% of the variation between the spectra after SNV correction (see Fig. 10. a.). The second PC is very similar to the spectrum of pyridoxine hydrochloride with a small negative trace of the 638.1 cm^{-1} peak of titanium dioxide. This PC explains 6.03% of the variations. The scores plot (Fig. 10. b.) shows that samples are located in order of increasing film thickness along the first PC axis.

These results show that pre-treatment can have a profound effect on the outcome of the analysis. According to the scree plot of the analysis (not shown) two PLS-components were found to give the best results based on the SNV-corrected spectra without signs of overfitting with 97.4% of the spectral variation and 98.61% of the film thickness variation explained.

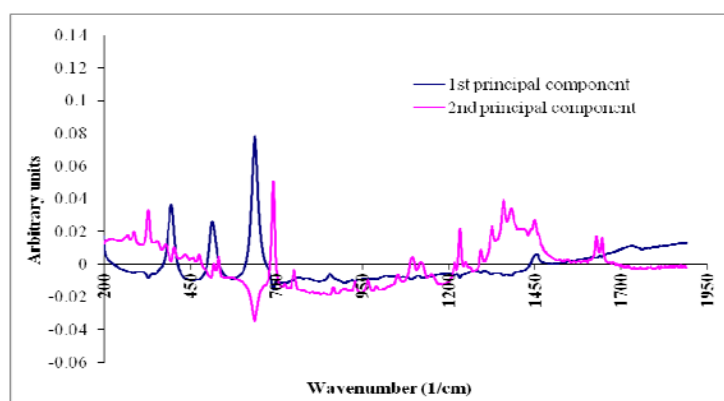


Figure 10: a, Loadings plot of the principal components of corrected Raman spectra

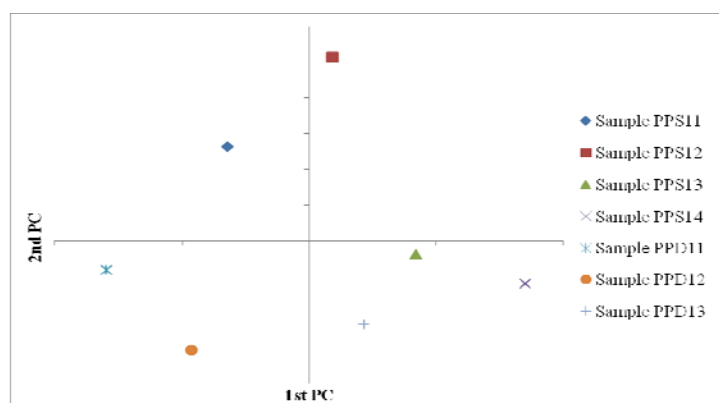


Figure 10. b, Scores plot of the principal components of corrected Raman spectra

The first component again resembles the Raman spectrum of titanium dioxide (see Fig. 11. a). This component is responsible for 91.43% and 96.36% of the X- and Y-directional variations respectively, indicating that the use of just this component can result in a reasonably good model. The second PLS-component contains only 5.94%

of spectral variation and is responsible for 2.25% of the variation in film thickness. The loadings of this component correspond to the Raman spectrum of pyridoxine hydrochloride in the negative. The two PLS-components indicate that the samples contain inversely proportional amounts of coating and API – ideally only one significant PLS-component would be enough to describe such a system.

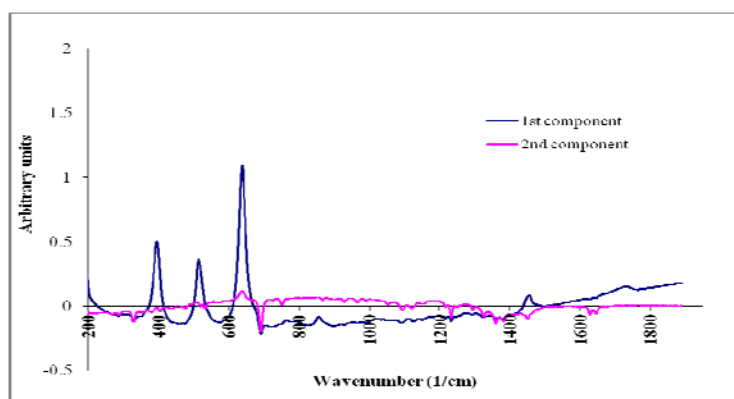


Figure 11: a, Loadings plot of the PLS components of the corrected Raman spectra

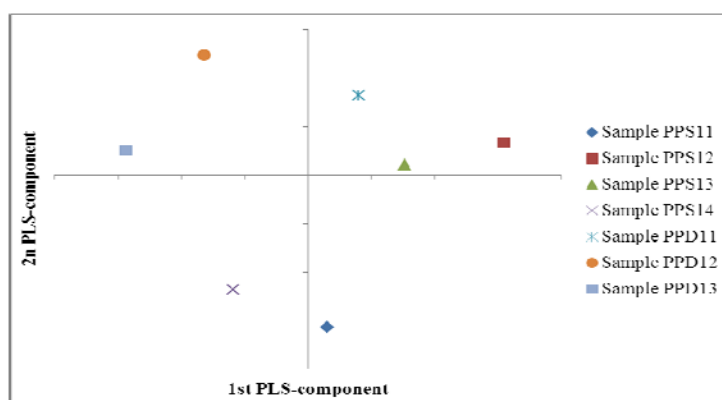


Figure 11. b, Scores plot of the PLS components of the corrected Raman spectra

Our final model included two PLS-components and provided a root mean square error of calibration (RMSEC) of 1.15 and a root mean square error of cross-validation (RMSECV) of 2.29 using the leave-one-out method. The slope and y-intercept of the linear fit also indicate the validity of the model (see Fig. 12). It is worth to mention that using only the first PLS-component in the model also results in a good correlation with an R^2 of 0.9636 but the inclusion of the second component further reduces the mean square error of the leave-one-out cross-validation somewhat.

The lasers utilized for Raman spectroscopy have small sampling area and penetration depth [97]. In our case the illumination area was 28.3 mm^2 , which means that, calculating with the smallest size, less than 100 pellets were measured in every case. This is a significantly lower number of pellets than what the literature generally

suggests [10, 47] and much less than the amount of particles measured with the Camsizer for the development of the method. Nevertheless, Raman spectroscopic data fit well the film thickness data, which in turn showed a linear correlation with the polymer weight gain.

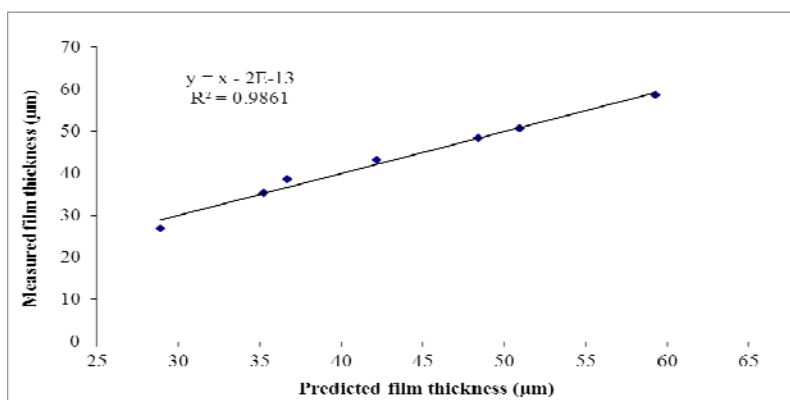


Figure 12: Linear model of the film thickness based on the PLS regression of the SNV-corrected Raman spectra

Contrary to previous studies done on sustained release systems where film thickness was a good predictor of dissolution [51, 57] delayed release coatings appear to be more complicated. Our results suggest that there might be a threshold value above which a correlation exists. One of the reasons for this may be incomplete film formation. The greater mechanical stress the samples suffered in the bottom spray equipment could also have contributed to the poor dissolution performance through the formation of cracks and chips, which in the case of thin coatings (in this case *Sample PPD11*) could affect the preparation more adversely than in thick coatings.

6.1.3. Summary

A Raman spectroscopic method was developed to assess film thickness prepared in two different types of fluid bed equipment. In the dissolution tests no indication of the films formed in the two equipment being different in quality were observed, however circumstances of preparation and Raman spectroscopic results suggest that differences may exist on some level. Multivariate analysis has visualized this as a difference in the slope of the baseline. Results suggest that above a threshold value the results of a dissolution test may be estimated by the measurement of the coating thickness in gastroresistant pellets.

6.2. Section II – Pellets containing diltiazem hydrochloride

6.2.1. Preparation of samples

Diltiazem hydrochloride, being more water-soluble than pyridoxine hydrochloride, could be used in larger concentrations during API layering to reduce loading time. This meant however that the viscosity of the Pharmacoat 606 – diltiazem hydrochloride solution was so high that spraying became very cumbersome. To reduce viscosity Kollidon 25 was used for some of the samples. The loading parameters were: inlet temperature 50 °C, outlet temperature 43 °C, fan capacity 4.5, peristaltic pump speed 4 ml/min, air volume 75 m³/h, blow-out pressure 4.4 bar, atomizing pressure 2 bar and nozzle diameter 1 mm for drug layering and coating.

In both compositions agglomeration was observed during API layering and coating. Fluid feed rate appeared to be the most important parameters that could influence agglomeration tendencies. Agglomeration was observed regardless of how low the fluid feed rate was but with discontinuous spraying the agglomerates broke down shortly after the spraying process was paused [76, 98]. This method has caused the coating time to stretch longer than expected. Higher fluid feed rates resulted in a large agglomerate blocking the Wurster insert so the experiment was discontinued.

6.2.2. Determination of film thickness

Film thickness was measured with the Leica equipment using the method described and examined in the previous section. Obtained values are summarized in Table 3.

Table 3: Film thickness values of diltiazem hydrochloride-containing pellets

Samples	Coating dispersion (g)	Film thickness (mean; μm)
<i>Sample DK11</i>	300	15.5
<i>Sample DK12</i>	300	17.7
<i>Sample DK13</i>	400	23.5
<i>Sample DK14</i>	500	28.9
<i>Sample DK15</i>	600	44.4

6.2.3. Study of the API migration and recrystallization

6.2.3.1. Thermal analysis

The DSC curves of the materials are presented in Fig. 13. The endothermic peak at ~220°C indicates the melting of diltiazem hydrochloride; the second, broad endothermic peak on the curve can be attributed to API degradation. The broad

endothermic peaks on the curves of Kollidon 25 and Pharmacoat 606 are related to the water loss of the polymers. No glass transition temperature could be determined which is probably due to it being obscured by the water loss peak and the changing plasticity caused by the water loss. The T_g of Acryl-EZE is visible at $\sim 60^\circ\text{C}$, but no peaks characteristic of the excipients used in its composition appear on the curve.

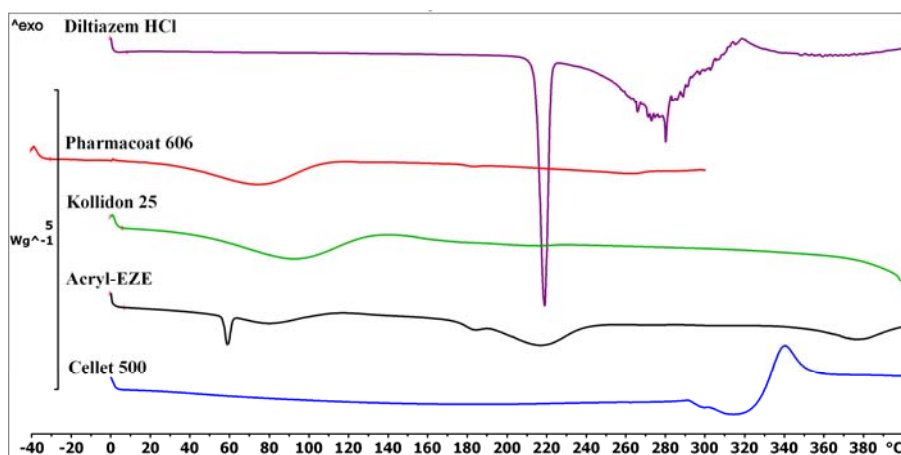


Figure 13: DSC curves of the raw materials

As shown in Fig. 14, the melting point of diltiazem hydrochloride appearing in all the samples has shifted to about 10°C lower than observed in its pure form and an exothermic peak appeared at about 100°C on the DSC curves of the coated pellets. The T_g of Acryl-EZE did not shift significantly and the T_g of the binder polymers did not appear on the curves.

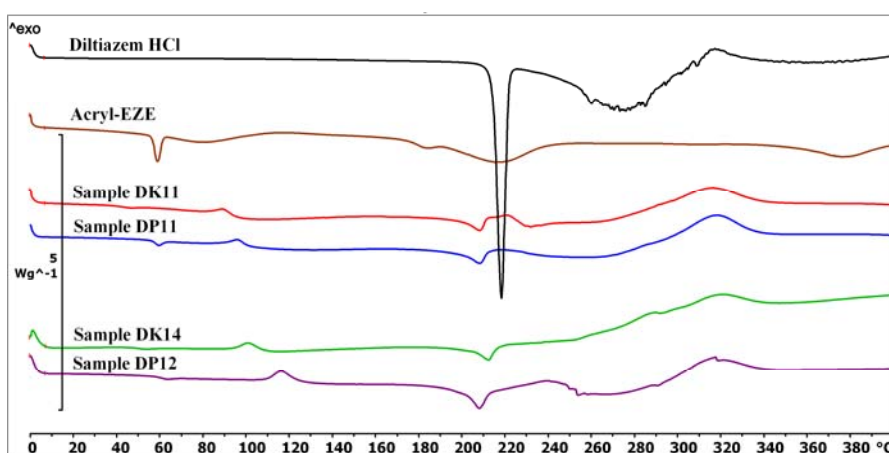


Figure 14: DSC curves of some samples containing diltiazem hydrochloride

The peak at 100°C showed up only in samples containing both diltiazem hydrochloride and the Acryl-EZE coating (see Fig. 15), which suggests that it is a result of an interaction between these two materials. According to its manual Acryl-

EZE contains sodium bicarbonate as an excipient, which precipitates diltiazem base from the aqueous solution of diltiazem hydrochloride [99]. (This concurs well with our previous experience where the same reaction made it necessary to disassemble and wash the equipment between API layering and coating.)

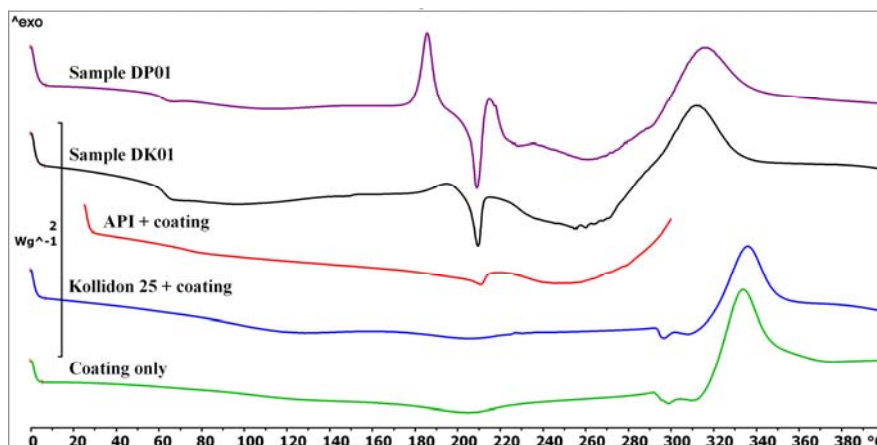


Figure 15: Effect of sample compositions on the DSC curves

The melting point of diltiazem base is in the same thermal range as the exothermic peak, however no melting point appears on the curves in this range and a thermally undetectable amount of sodium bicarbonate does not seem likely to produce detectable amounts of diltiazem base in the first place.

Fig. 15 shows that a similar exothermic peak appeared at about 180°C or directly before the melting point on the curves of the uncoated pellets where no sodium bicarbonate was present in the preparation. This peak is very apparent in the HPMC (Pharmacoat 606)-containing sample and much less present in PVP-containing ones, in some cases it is even completely missing.

An amorphous sample of diltiazem HCl was prepared by quench cooling to measure the T_g which proved to be at 100°C (Fig. 16). The repeated heating of *Sample DK14* also plotted on the same figure showed that the exothermic peak appears only during the first heating cycle.

Fig. 17 shows that a slow weight loss starts approximately at 50°C that accelerates slightly at about 100°C for the uncoated sample. In the case of the coated sample water loss starts much later. Total weight loss up to 100°C is only a few percent in all cases; this concurs with the water loss of the polymers described before and explains why the effect is delayed in coated samples where much of the water is contained beneath the coating. The samples begin to lose weight fast above the

melting point of diltiazem HCl which again concurs with our knowledge of the composition.

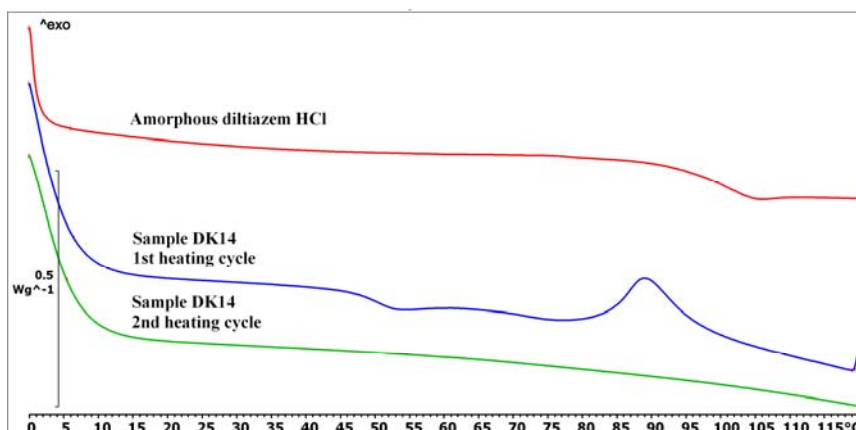


Figure 16: Thermal behavior of amorphous diltiazem hydrochloride

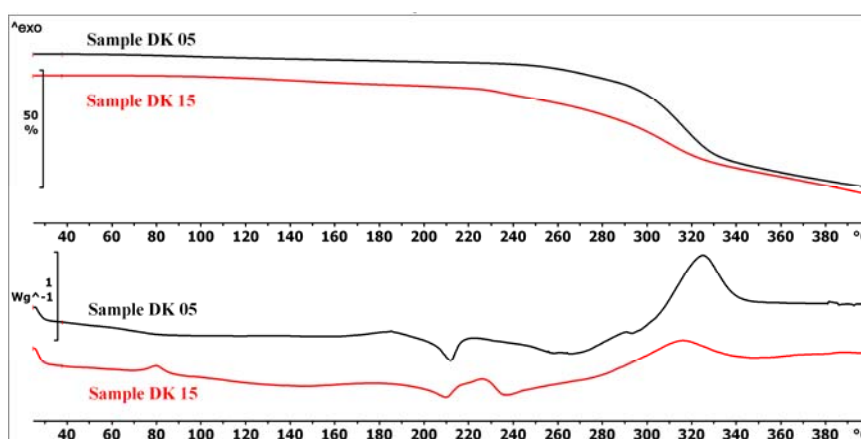


Figure 17: Weight loss of coated and uncoated samples

6.2.3.2. X-ray analysis

As shown in Fig. 18 the XRPD diffractogram of diltiazem HCl comprises several peaks; the larger ones that can also be seen in the samples' diffractograms are at 4.125° , 8.328° , 9.907° , 10.547° , 18.070° , 19.442° , 21.661° and 27.575° 2θ . Cellet 500, Kollidon 25 and Pharmacoat 606 are either polymeric or microcrystalline; hence only very broad peaks appear in their diffractograms which do not hinder the identification of the sharp peaks from other materials. Talc, listed as an ingredient of Acryl-EZE by the manufacturer, produced the two sharp peaks visible in the diffractogram of the coating system.

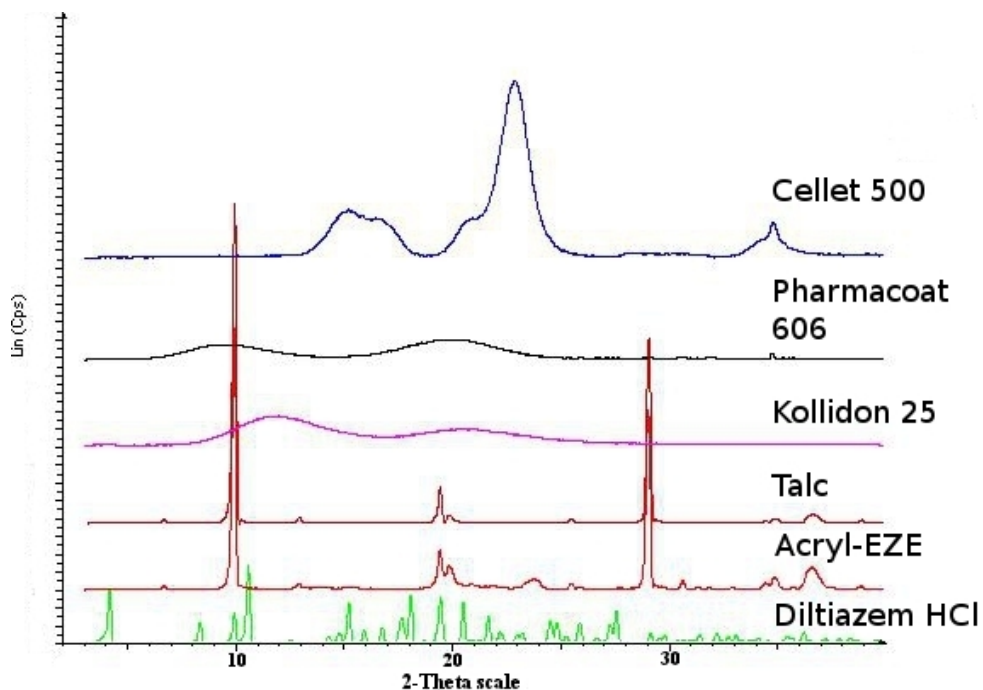


Figure 18: X-ray diffractograms of raw materials

The XRPD diffractograms were detected at room temperature at baseline and heated to 120°C and to 200°C afterward. Results are presented in Fig. 19. The diffractogram of every coated sample shows a sharp peak at 25.648° 2θ. This was identified as titanium dioxide [100], used as white pigment in the Acryl-EZE coating system. The diffractograms of Kollidon-containing samples indicate the presence of crystalline API at baseline while Pharmacoat-containing samples seem to be missing the peaks characteristic of the API indicating that it is in amorphous form.

In all cases diltiazem hydrochloride peaks have become larger (or, in some cases, appeared) after heat treatment. In the case of uncoated samples API peaks appeared/grew only after heat treatment at 200°C whereas coated samples demonstrated the same recrystallization after being heated to 120°C. Comparing 120°C and 200°C heat treated (coated) sample spectra a decrease in API peak heights can be seen which is probably due to the decomposition of diltiazem hydrochloride.

The nature of the sample preparation process closely resembles the procedures employed during the solvent method of the preparation of solid dispersions. This implies that a solid dispersion can be formed during API layering that, depending on the composition and parameters, can contain the API in any and all physical forms [19, 101]. X-ray analysis revealed that the occurrence causing the exothermic peak at

~100°C is recrystallization of the API. In the uncoated samples amorphous API recrystallizes only upon or close to melting (see Fig. 19. b.).

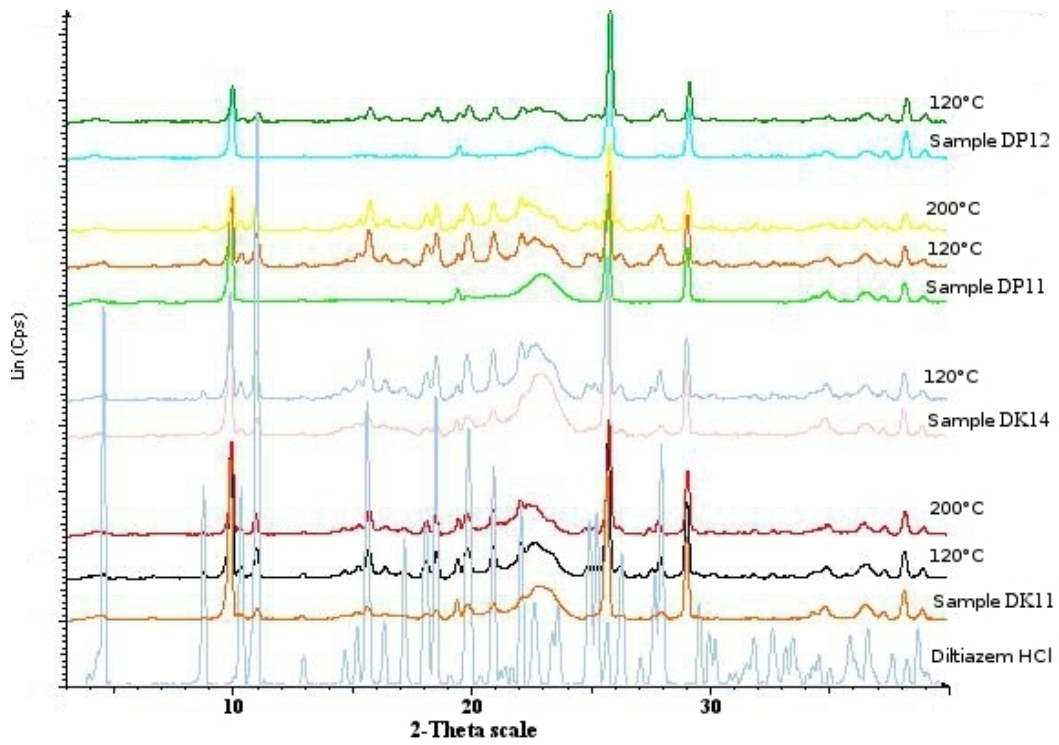


Figure 19. a, X-ray diffractograms of coated samples at different temperatures

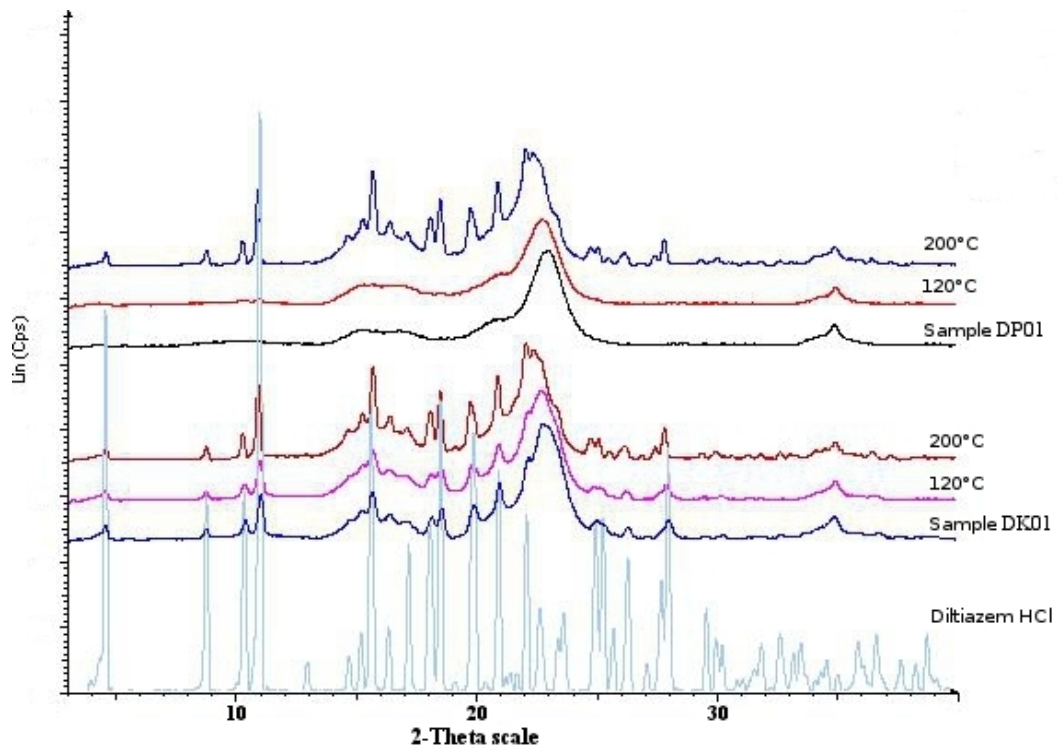


Figure 19. b, X-ray diffractograms of uncoated samples at different temperatures

6.2.3.3. FT-IR analysis

The FT-IR spectra of a Kollidon-containing coated sample before and after recrystallization upon heating are shown in Fig. 20. a. Both the samples and the physical mixture of binder and API exhibit a water peak at 3450 cm^{-1} , although the water content of the sample appears to have significantly decreased heat treatment. In the un-treated sample several peaks are less prominent (if visible at all) and wider, less sharp than in the physical mixture. No shifts in peak positions occurred indicating that no chemical bonds formed between API and polymers. The spectrum of the heat treated sample is mostly the same as that of the physical mixture; slight differences can be attributed to the presence of other excipients. FT-IR spectra of a Pharmacoat 606-containing sample have yielded similar results (see Fig. 20. b.).

6.2.3.4. Hot-stage microscopy

The polarized light microphotograph of a piece of coating (Fig. 21) taken using crossed Nicol prisms shows that the polymeric film layer contains crystalline material even before heat treatment (left side). After the heat treatment (right side) the amount of birefringent particles in the coating increased which indicate that the crystalline material is diltiazem hydrochloride.

The API migrated into the coating and part of it remained amorphous that later crystallized upon heat treatment. The probable mechanism of migration is that the highly water-soluble diltiazem hydrochloride dissolved into the droplets of coating suspension hitting the surface of the API-layered cores during the coating process [102-103]. The plasticization mechanism described by Mizuno et al. can also play a role in the process [104]. Binder polymers might also play a part by improving the speed of dissolution even further by forming solid dispersions with the API upon layering [101, 105-107]. This hypothesis is supported by Fig. 15 (see page 35), which shows that no exothermic peak appears on the DSC curves of a coated sample prepared without binder.

Migration probably occurs mostly before a uniform coating layer forms on the drug-loaded cores [104] and thus affects only a small fraction of the API. Considering the fact that the drug layer already contains an amorphous fraction (see Fig. 15 where recrystallization can be seen in the uncoated samples close to the melting point of diltiazem hydrochloride), migration does not explain the difference in the recrystallization behavior of the coated and uncoated samples.

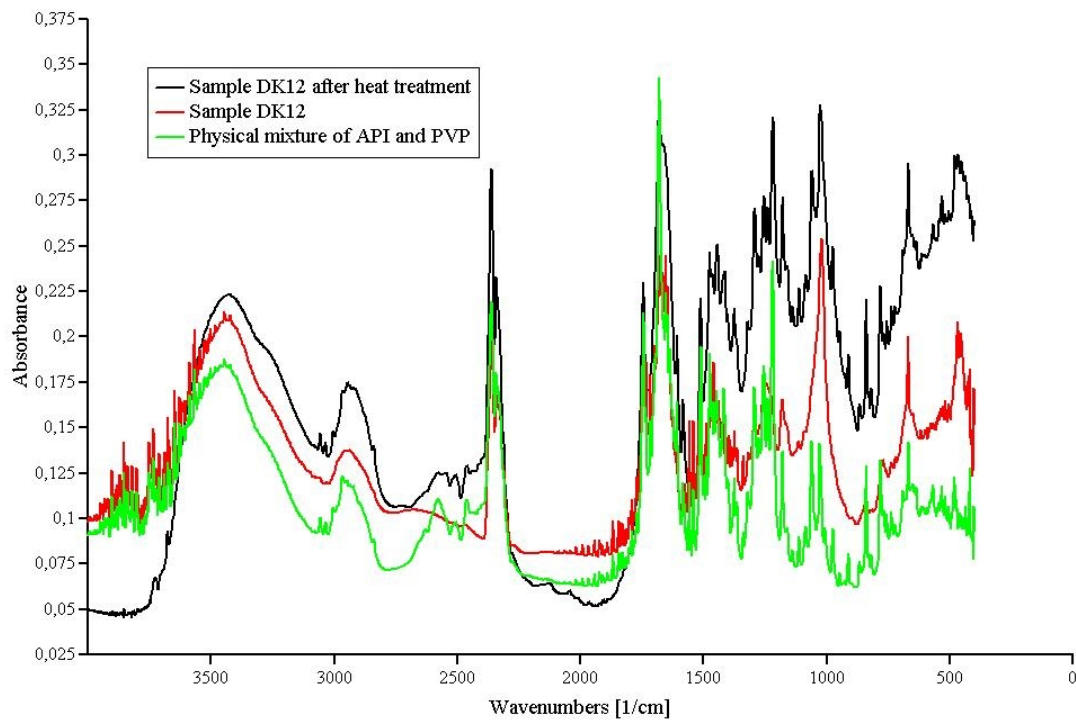


Figure 20. a: FT-IR spectra of interaction between API and Kollidon 25

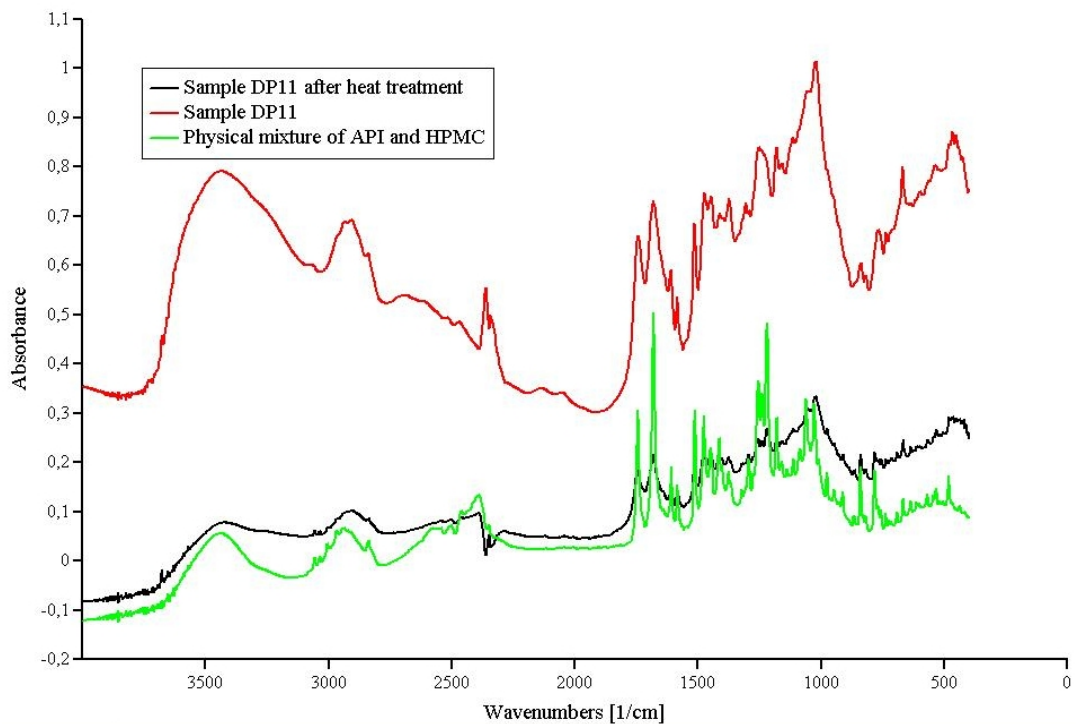


Figure 20 b: FT-IR spectra of interaction between API and Pharmacoat 606

As no chemical bonds between polymer and API were found in either case it can only be physical inhibition that prevents the drug from completely crystallizing during sample preparation and storage [85, 106]. In such cases the main reason of recrystallization is the glassy to rubbery state transition of the API-containing polymer

and the increased molecular mobility of the API that is the result of the increased mobility of the polymer chain segments separating the API clusters [105-106]. It has been described by several authors that the physical stability of a drug depends greatly on the preparation method and the polymer carrier [108-110]. In our case the methods of preparation were the same for all samples but the API (both amorphous and crystalline fractions) is split between the coating layer and the drug layer, which means that based on the above theory we should observe two phases in the recrystallization: one for the drug layer and one for the coating (or only one overlapping one). However, only one recrystallization phase was observed which appeared at significantly lower temperatures in coated samples than in uncoated ones.

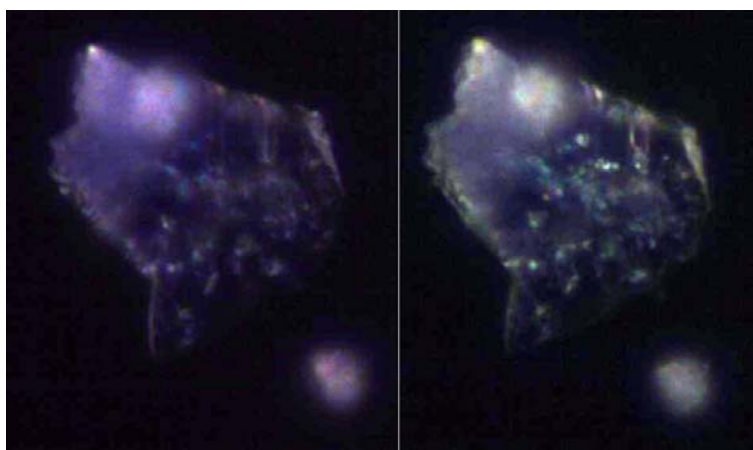


Figure 21: Coating fragment under the polarized light microscope before and after heat treatment

This discrepancy must be explained by the presence of the coating. The DSC curves of the uncoated samples contain a broad endothermic peak that literature attributes to the loss of water in the binder polymers. This peak does not show up on the curves of coated samples and the TG curves indicate that water loss in the coated samples starts close to the boiling point indicating a watertight property of the coating at least on the timescale of the DSC analysis. The exothermic peak attributed to API recrystallization is in the thermal range of the boiling point of water. This raises the question: can water play a role in the recrystallization behavior of the API [111]?

Several theories postulated by other authors can be used to explain the possible influence of water on the behavior of our coated samples [112-113]. Many studies proved that water can act as a plasticizer in polymers; as such it can decrease the T_g of the polymer to the thermal range of our exothermic peak – which it cannot

do for the uncoated samples as most of the water evaporates by the time the sample reaches the temperature range in question [114]. Water can also be trapped in the pores of the microcrystalline cellulose core after API layering. Diltiazem hydrochloride, being highly water-soluble, can dissolve in the water migrating toward the surface of the pellet from the core and crystallize with the eventual evaporation of the solvent. As water boils in the thermal range of the recrystallization peak, the pressure of the forming steam in the pores of the pellet is expected to grow rapidly at the time of the event. As described before, water also acts as a plasticizer, so pores can be easily expanded by the steam essentially removing the physical barriers in the polymer structure that stood in the way of recrystallization. This expansion process is well-known in the food industry (a good description can be found in articles detailing the making of popcorn [115-116]) but a similar effect was noted during the use of supercritical or pressurized carbon dioxide in the pharmaceutical industry [117-119].

6.2.3.5. Stability

These mechanisms can and in reality probably do work independently from each other at the same time. This presents problems regarding the stability testing of samples of this nature. Studies should take into consideration that the high relative humidity used in accelerated stability testing could cause recrystallization by plasticizing the polymer that would not happen under ambient conditions [113, 120]. To compensate for this effect samples were stored at 40°C at 70% relative humidity, at 40°C in a low humidity environment (25±5%), at 75±5% relative humidity at room temperature (20°C±2°C) and at ambient conditions (45±5% and 20°C±2°C).

Fully amorphous samples have fully recrystallized after a day at both highly humid conditions while samples stored at lower humidity levels remained fully amorphous until the closing of the experiment 50 days later. This concurs well with the results of Zelkó et al. [121] where they have demonstrated that only high humidity values cause a change in the structure of PVP.

A study at elevated humidity was conducted to investigate the kinetics of the recrystallization in coated samples. Samples have recrystallized slowly at start but recrystallization speed increased greatly after a lag time (see Fig. 22) that can correspond both to film thickness and initial degree of crystallinity.

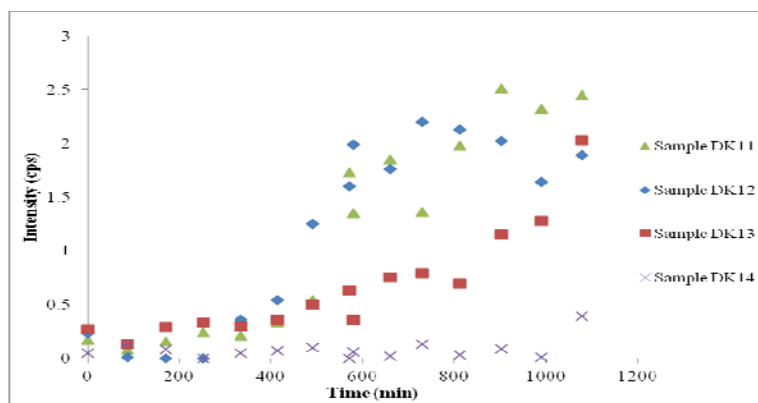


Figure 22: Recrystallization trends as indicated by XRPD peak $9.907^{\circ} 2\theta$

The former was confirmed by a water uptake study where samples of equal volume were stored in open containers in a closed hygrostat containing distilled water on ambient temperature. Samples were weighted at regular intervals and the results plotted in Microsoft Excel.

Uncoated samples exhibited an exponentially decreasing water uptake. Coated samples initially showed linear water uptake that gradually slowed when approaching saturation concentration. This concurs with the equation used to describe diffusion-regulated dissolution from coated pellets [122-123]. Linear trend lines considering the zero intercept were fitted to the data and rate constants calculated for the coated pellets. Rate constants showed a strong inverse relationship with the film thickness with the coefficient of determination being reduced by the fact that *Samples DK11* and *DK12* are very close in coating thickness.

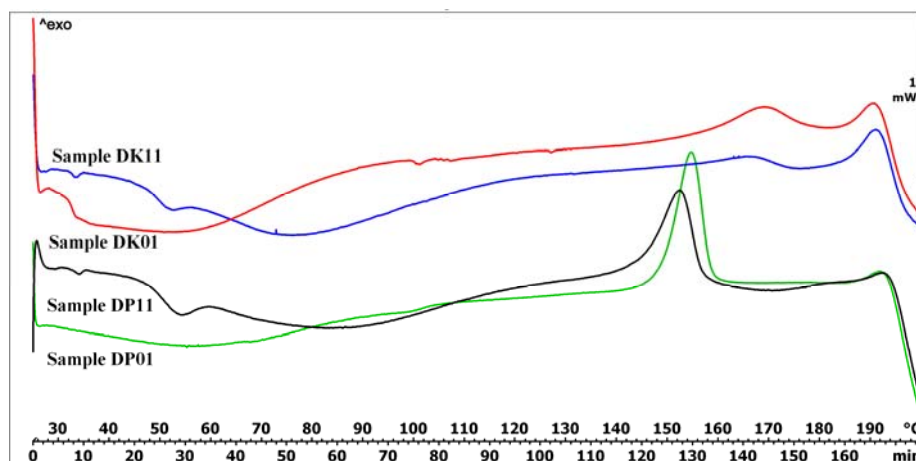


Figure 23. DSC curves of coated and uncoated samples at slow heating rate

The direction of diffusion is determined by the concentration gradient which means that the equations generally used to describe dissolution behavior can be used to describe material influx governed by diffusion. The trends observed for water

uptake will by the same logic be true for loss of water too. This corresponds well with the differences between the weight loss patterns of coated and uncoated samples we have seen during the thermogravimetric measurements. To evaluate the role of water loss in recrystallization a TG-DSC experiment with a low heating rate was performed.

The 1°C/min heating rate was expected to provide enough time for the evaporated water to diffuse through the coating thereby equalizing the water loss trend with that of the uncoated pellets. As can be seen in Fig. 23 DSC curves have both fulfilled that expectation: weight loss rates were even between coated and uncoated samples with only a slight delay for the coated pellets and recrystallization occurs in both coated samples in the same thermal range as in their uncoated counterparts. This confirms that the fast evaporation of water played a crucial part in causing the difference in recrystallization behavior.

6.2.3.6. Dissolution studies

As expected, dissolution in artificial gastric acid is inversely correlated to film thickness with 23.5 µm film thickness already achieving sufficient gastroresistance for *Sample set DK*. As the extent of API migration was not determined in the study no further conclusions can be drawn from the results.

Problems similar to the ones described in the section on stability arise when trying to determine the significance of recrystallization on the dissolution behavior. As intentional recrystallization without the destruction of the sample involves heat treatment, it is logical to assume that curing of the coating also takes place during the process which would improve the outcome of a later dissolution test [43, 114, 124]. Also if the pores expand significantly enough in volume the coating polymer would either rupture [125] or, what is more probable given that it is in rubbery state at the temperatures involved, would stretch thinner (thus decreasing its performance) and transform back into the glassy state upon cooling. The extent of API migration and the starting film thickness would probably also influence the results.

While results in gastric acid improved significantly for *Sample DK11* and *DPI2* the change observed in the case of *Sample DK14* was well beneath the SD value of both tests. These results suggest that no rupturing occurred due to the heat treatment itself which means that heating the samples did not result in significant volume expansion. Overall no clear trend could be seen in the direction of the changes.

6.2.4. Measurement of the degree of crystallinity

Six sub-samples were taken from *Samples DK01-5* and their X-ray diffractograms collected. Diffractograms were then used to attempt to set up a calibration curve for the determination of the degree of crystallinity based on ssNMR results.

6.2.4.1. ssNMR

Spray drying techniques are substantially impacted by environmental factors and as such are hard to control regarding the solid state of the product [126]. To obtain an absolute value of the degree of API crystallinity of the samples solid phase NMR measurements were performed using the CP-MAS technique with a ^{13}C - ^1H coupling.

Table 4: Degree of API crystallinity measured with ssNMR (increasing order)

Sample	Degree of crystallinity of the API (%)
<i>Sample DK03</i>	11
<i>Sample DK01</i>	23
<i>Sample DK05</i>	35
<i>Sample DK02</i>	49
<i>Sample DK04</i>	49

6.2.4.2. X-ray characterization of samples

Pellet formulations were expected to cause difficulties with the measurements due to their size and shape. Packing in the traditional sense of the phrase is less likely to occur as a problem but considerable noise and peak shifting are to be expected due to the air pockets between the particles. Uneven surface and sample displacement cause peak broadening and peak shifting when using Bragg-Brentano equipment [127]; with intact pellets neither can be avoided during measurement. Peak intensity also decreases in rough surfaces compared to smooth ones. When analyzing multilayer pellets starting material concentrations in the focusing circle are not necessarily the same as in the sample bulk due to the different composition of the layers of the sample and are hard to determine because of the unknown but presumably small penetration depth [128-129]. Solid dispersions also have a tendency of exhibiting changes in halo shape and intensity [130] and anisotropic peak shifting has also been observed [131]. Because of these effects whole-pattern fitting and pattern subtraction techniques [132] are very likely to fail. On the other hand pellets

usually have a narrow size distribution, meaning that these features are likely to be fairly consistent between samples. This probably reduces the confounding effects to a level that still makes the analysis of intact pellets possible.

Preferred orientation effects have been known to appear in intact pharmaceutical dosage forms [133-134]. In the case of pellets prepared by solution layering the preference of some directions during crystal growth is likely to be balanced in the three-dimensional space. Nevertheless, samples were rotated during measurement to reduce any possible effects.

A diffractogram of *Sample DK01* representative of most diffractograms obtained from *Samples DK01-5* was shown in Fig. 19. b. *Sample DK03* turned out to be X-ray amorphous but the diffractogram showed no new halo features that could be definitively attributed to amorphous diltiazem hydrochloride. This can be a result of the halos of the polymer components overlapping over most of the 2θ range or differences in the intensity and concentration of the materials. In this case most probably both of these effects occur. Characteristic peaks of diltiazem hydrochloride are shifted in sample diffractograms and the extent of the shift is not consistent for all peaks and samples. The excessive noise (although expected) made the results of any analysis so uncertain that smoothing had to be employed in order to continue [135]. The Savitzky-Golay smoothing algorithm was used with a frame width of 15 data points and a 2nd degree polynomial and diffractograms were normalized to unit area to compensate for weight differences. From here on peaks will be referred to as their maximum observed in pure diltiazem hydrochloride.

6.2.4.3. Determination of the crystalline content by univariate methods

Crystalline and amorphous intensities are proportionate to crystalline and amorphous concentrations [132]. The degree of crystallinity of the sample can be calculated as

$$X_{cr} = \frac{I_c \times 100}{I_c + I_a} \quad [132]$$

where I_c and I_a are usually area under the crystalline peaks and the halo respectively, but peak heights can also be used [130, 132]. The formula requires separation of the amorphous halo from the crystalline peaks. This is a procedure prone to errors [136] as is the definition of the baseline [137] that is required for calculations.

Preliminary calculations were performed to choose the best-performing peaks and also to determine which peak parameter to use for further calculations. The characteristic peaks at $9.907^\circ 2\theta$, $10.547^\circ 2\theta$, $18.071^\circ 2\theta$, $19.442^\circ 2\theta$, $20.521^\circ 2\theta$ and $27.575^\circ 2\theta$ were chosen for their consistently good performance despite some troubling characteristics that shall be discussed later.

Area methods generally provide better results than peak heights because of the wider 2θ range involved [134]. In our case however peak heights almost always provided better results than peak areas. The previously shown formula was used to calculate results from total area parameters. Predicted crystallinity was plotted against the theoretical crystallinity obtained from the ssNMR measurements. The mathematical values used to describe the linear fit are the slope and y-intercept, the coefficient of determination (R^2) and the root mean square error of calibration and cross-validation. For the univariate regressions these have been calculated in Microsoft Excel and are summarized in Table 5. As ssNMR uses very small sample sizes compared to XRPD it is reasonable to assume that sampling errors are more likely to occur during the ssNMR measurement therefore the result may not necessarily be representative of the sample bulk. While the particles were mixed before sampling for XRPD measurements to reduce the chance of obtaining biased sub-samples the actual degree of crystallinity of the sub-samples can differ from each other and from the „theoretical value” for the samples obtained by ssNMR as flow properties and thus drying characteristics are inhomogeneous during production [138-139]. Repeated ssNMR measurements would solve this issue but NMR measurements are both time-consuming and costly and therefore parallel measurements were not performed.

Due to its largest relative intensity the $10.547^\circ 2\theta$ peak was deemed the most promising for quantitative analysis, however it provided the worst results of all the examined peaks. The amorphous halo shows steeply increasing intensity in the region of the $19.442^\circ 2\theta$ and $20.521^\circ 2\theta$ peaks which makes peak and halo separation and thus measurement of the peak parameters prone to errors [140]; in spite of this the peaks provided good linear fit and RMSECV. Considering the amorphous halo as seen on the diffractograms of Cellet 500 and Kollidon 25 it can be said that this is the only region in which the trends in the halo can be clearly identified which makes these peaks more suitable for analysis than similarly sized peaks in other regions.

The peak at $27.575^\circ 2\theta$ is a double peak of moderate intensity in the API diffractogram that fused into one broad peak in the sample diffractograms. Despite this less than ideal quality it showed a good predictive value. This possibly stems from the amorphous halo being fairly even and not very intensive in the region which probably makes peak and halo separation less error-prone.

Baseline correction has resulted in significantly worse slope and R^2 values although this time peaks generally provided better results in order of increasing intensity. This indicates that the definition of the baseline can influence the outcome of the analysis both adding to and compensating for errors from other sources.

Some correlations showed signs of non-linearity; for this reason a log-transformation was performed and calculations repeated. While R^2 , RMSEC and RMSECV values have improved in some cases slopes and y-intercepts show a larger deviation from the expected values of unity and zero respectively. R^2 values still do not reach the generally acceptable level of 0.95 and bias toward the small peaks can still be observed. In general it can be said that the log-transformation worked best for the two smaller peaks examined and the area ratio but even in these cases linear fits clearly perform better in some areas.

While promising, the overall results of the univariate analysis cannot be considered ideal or, in many cases, reliable based on the problems described above. Partial least squares regression was tested to overcome difficulties in parameter selection and to find a good fit based on not confounded information.

Table 5: Regression results for Savitzky-Golay smoothed diffractograms

	Crystalline/ amorphous area ratio	Sum of peak heights	Peak position (2θ)				
			9.907°	10.547°	19.442°	20.521°	27.575°
Slope	1	1	1	1	1	1	1
y intercept	2×10^{-5}	8×10^{-5}	5×10^{-5}	1×10^{-4}	1×10^{-4}	3×10^{-5}	3×10^{-5}
R^2	0.881	0.9028	0.9165	0.8846	0.8972	$\frac{0.927}{7}$	0.9173
RMSEC	5.12	4.62	4.28	5.04	4.75	3.99	4.26
RMSECV	5.38	4.86	4.52	5.29	5.00	4.20	4.51

6.2.4.4. Determination of the crystalline content by multivariate methods

Multivariate analysis is a good technique to avoid the interference of excipients and random noise during quantitative analysis [141] especially in intact dosage forms [142]. First a principal component analysis was performed to see if the method could differentiate between samples. Three principal components were found relevant to the investigation which explained a total of 89.31% of the variation in the diffractograms (see Fig. 24. a.).

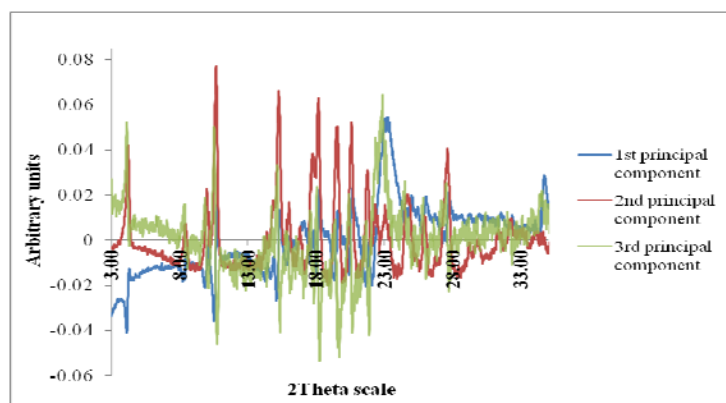


Figure 24. a, Loadings plot of the principal components

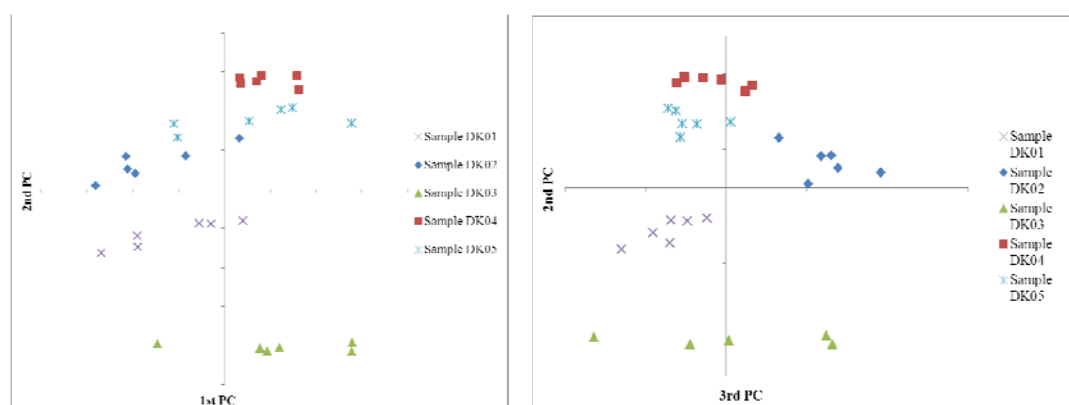


Figure 24. b-c, Scores plots of the principal components

The first PC appears to contain shifts in the amorphous halo and the diltiazem hydrochloride peaks. The second PC very closely resembles the diffractogram of diltiazem hydrochloride. While the third PC resembles the second one it contains the indications and corrections for API peak shifts and an obviously larger amount of noise than the previous PCs. This indicates that while there is still about 11% of variation unaccounted for most of it is likely to be attributed to random noise.

Score plots of the principal components (Fig. 24. b-c.) show that sub-samples are clearly clustered according to their source sample. As the source samples varied in crystallinity this gives us a good indication about the possible positive outcome of

further work. Samples are ordered along the second PC according to degree of crystallinity with the exception of *Sample DK02* and *DK05*.

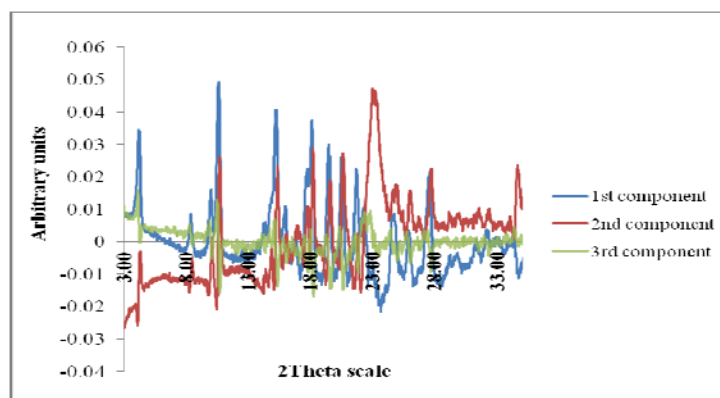


Figure 25. a, Loading plot obtained from PLS-regression

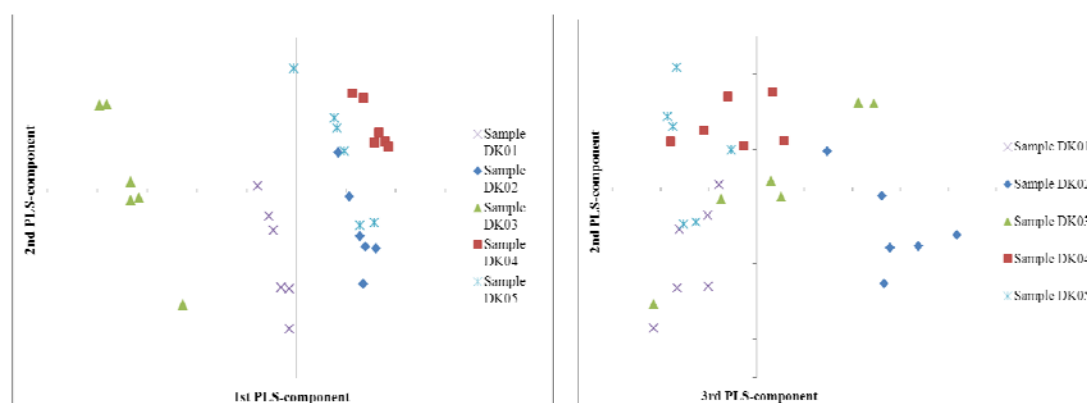


Figure 25. b-c, score plots obtained from PLS-regression

PLS analysis also found three significant components that, while explaining 89.25% of the spectral variation, correspond to 95.81% of the differences in the degree of crystallinity. PLS component weights for the first two components closely resemble the diltiazem hydrochloride diffractogram with the both components containing the amorphous halo from microcrystalline cellulose in negative and in positive respectively (see Fig. 25. a.). The broad microcrystalline cellulose feature and the baseline shift in the lower 2θ region appearing in the first two PLS-components are cancelled out or greatly reduced for most samples when considering both components indicating that they have little actual influence on the outcome variable. Exceptions are some sub-samples of *Sample DK03* and *Sample DK02* where this behavior can either signify an anomaly or unlucky sampling. In the case of the X-ray amorphous *Sample DK02* this may be the result of the other features in the components needing to be zeroed. As a few sub-samples from less affected samples also contain the two components with opposing signs it is likely that the effect is due

to the innate variability of pellets within one sample; an obvious such characteristic would be particle size but more experiments are needed to show a definite connection.

Score plots obtained for the PLS-components again show the same clustering as was described for PCA (see Fig. 25. b.). Samples are approximately in order of increasing degree of crystallinity along the first PLS-component axis. *Samples DK02* and *DK05* are clearly set apart only by the third PLS-component (containing a halo feature and shifted API peaks among some noise) as seen in Fig. 25. c.

The model obtained from the analysis shown in Fig. 26 supersedes all previous attempts to obtain a calibration curve with an RMSEC of 3.04 and an RMSECV of 3.88.

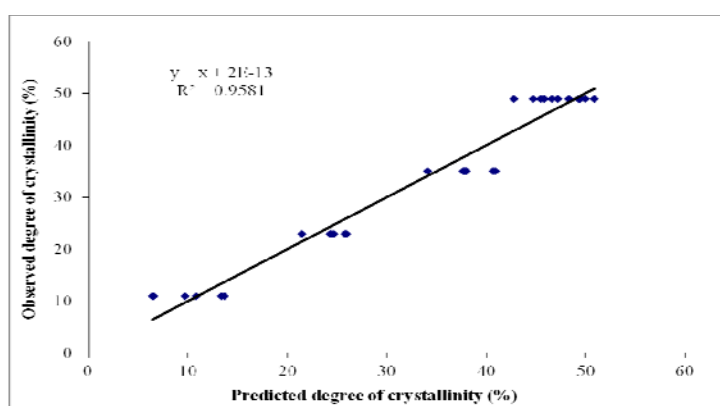


Figure 26. Linear model of the degree of crystallinity based on the PLS regression of the XRPD data of intact pellets

These results have shown that the degree of API crystallinity of intact pellets can be examined by XRPD despite the initial difficulties. Univariate models varied in their predictive quality – often the best models came from the most dubious sources. PLS analysis provided better results and gave much less reason to worry about the validity of the obtained model. Building the PLS model was also less time-consuming due to the lack of preparatory work while for the univariate model not only the peak and halo separation needed to be done but also preliminary calculations were required to avoid choosing the most obvious but in reality not very predictive parameter.

6.2.5. Summary

In this section diltiazem hydrochloride-containing pellets were investigated to find the reason of an atypical behavior and its impact on stability testing and dissolution. We have also attempted to measure the degree of crystallinity of the uncoated samples from intact pellets with both univariate and multivariate methods.

7. Final conclusions, novelty, practical usefulness

The influence of various factors and phenomena on the dissolution of enteric coated pellets was investigated in this study. Pellets were manufactured by solution layering in a fluidized bed and subsequently coated with a fully formulated enteric coating system. Two model APIs and two model hydrophilic binder polymers were used and the four possible compositions were analysed and their characteristics cross-referenced to see the effect of composition, process parameters and other phenomena on the behavior of multilayer pellets.

- API-layered and coated pellets were manufactured in fluid bed equipment in different compositions. Problems encountered during manufacturing were successfully solved and the transfer of the technology to a different device showed the procedure to be robust enough to withstand significant differences in manufacturing equipment. Through this we obtained a solid understanding of what the critical process and product parameters are.
- Differences between the products stemming from the differences between the equipment were described and investigated. This information can be put to good use in the pharmaceutical industry where differences in the manufacturing equipment tend to cause problems during scale-up and technology transfer processes.
- Two image analysis methods for the measurement of particle size were compared and evaluated. For the purpose of film thickness measurements the two methods gave similar results even though they differed substantially in the measurement of particle size characteristics. Results indicate that the automatized method using large sample sizes was more robust to sampling effects and sample characteristics.
- Raman spectroscopy proved to be a good tool for the measurement of the film thickness of coated pellets. Multivariate data analysis made it possible to differentiate samples based on their preparation conditions. It was shown that while the configuration of the fluid bed used for sample preparation probably has an effect on the Raman signal this difference does not indicate a difference in the

performance of the coating. A relationship between film thickness and gastric resistance was postulated.

- An unexpected change in thermal behavior due to the addition of a coating layer was investigated. The effect of API migration on dissolution was analysed and the representativeness of some stability testing procedures were evaluated. The existence of such phenomena and especially their ability to place limitations on standard evaluation procedures emphasizes the importance of understanding product behavior deeply enough to anticipate future problems – a goal that is pursued through similar means by the Quality by Design initiative.
- A multivariate model was developed for the determination of the degree of API crystallinity from intact drug-layered pellets.
- One of the main objectives of model development was to avoid complicated and time-consuming pre-treatment and analysis. The models and methods described in the work can be easily utilized at-line or – under optimal circumstances – even in-line to follow the development of the product during the manufacturing process. By being able to monitor the changes in the product in real time these techniques can fulfill the needs of Process Analytical Technology.

Part of the purpose of the study was to investigate the use of widespread analytical methods in the development of pellets. As multiunit systems are much less researched than traditional dosage forms analytical methods are not usually developed with the goal of making them easy and efficient to use in their development. Our results showed that nevertheless some tools primarily used in the development of other dosage forms can be efficiently employed for pellets if their unique nature is taken into consideration.

8. References

1. Werner D., *Pharm. Technol. Europe* 18(4):35-41, 2006
2. Abdul S., Chandewar A.V., Jaiswal S.B., *J. Control. Release* 147(1):2-16, 2010
3. Haslam J.L., Forbes A.E., Rork G.S., Pipkin T.L., Slade D.A., Khosravi D., *Int. J. Pharm.* 173(2):233-242, 1998
4. Bechgaard H., Hagermann N.G., *Drug Dev. Ind. Pharm.* 4(1):53-67, 1978
5. Bodmeier R., *Eur. J. Pharm. Biopharm.* 43(1):1-8, 1997
6. Krämer J., Blume H., *Biopharmaceutical aspects of multiparticulates*, in: I. Ghebre-Sellassie (Ed.), *Multiparticulate Oral Drug Delivery*, Marcel Dekker Inc., New York, 1994
7. Ghebre-Sellassie I., Knoch A., *Pelletization techniques*, in: Swarbrick J., Boylan J.C. (Eds.), *Encyclopedia of Pharmaceutical Technology*, Marcel Dekker Inc, New York, 2002
8. Roy P., Shahiwala A., *J.Control. Release* 134(2):74-80, 2009
9. Ghebre-Sellassie I., *Pellets: a general overview*, in: Ghebre-Sellassie I. (Ed.), *Pharmaceutical Pelletization Technology*, Marcel Dekker Inc., New York, 1989
10. Larsen C.C., Sonnergaard J.M., Bertelsen P., Holm P., *Eur. J. Pharm. Sci.* 18(2):191-196, 2003
11. Nastruzzi C., Cortesi R., Esposito E., Genovesi A., Spadoni A., Vecchia C., Menegatti E., *AAPS PharmSciTech* 1(2):14-25, 2000
12. Sinchaipanid N., Chitropas P., Mitrevej A., *Pharm. Dev. Technol.* 9(2):163-170, 2004
13. Singh S.K., Dodge J., Durrani M.J., Khan M.A., *Int. J. Pharm.* 125(2):243-255, 1995
14. Vervaet C., Baert L., Remon J.P., *Int. J. Pharm.* 116(2):131-146, 1995,
15. Suhrenbrock L., Radtke G, Knop K., Kleinebudde P., *Int. J. Pharm.* 412(1):28-36, 2011
16. Jones D.M., *Solution and suspension layering.* In: Ghebre-Sellassie I. (Editor), *Pharmaceutical Pelletization Technology*, Marcel Dekker, New York, 1989
17. da Cunha R.L.G, Pereira M.M.C., Rocha S.C.S., *Chem. Eng. Process.* 48(5):1004-1011, 2009
18. Turton R., Cheng X.X., *Powder Technol.* 150(2):78-85, 2005

19. Teng Y., Qiu Z., Fluid Bed Coating and Granulation for CR Delivery in Oral Controlled Release Formulation Design and Drug Delivery: Theory to Practice, Wen H. and Park K. (Eds), John Wiley & Sons, Inc., Hoboken, New Jersey, 2010
20. Teunou E., Poncelet D., Journal of Food Engineering 53 (2002) 325-340.
21. Guignon B., Regalado E., Duquenoy A., Dumoulin E., Powder Technol. 130(2):193- 198, 2003
22. Sudsakorn K., Turton R., Powder Technol. 110(1):37-43, 2000
23. Karlsson S., Niklasson Björn I., Folestad S., Rasmuson A., Powder Technol. 165(1):22- 29, 2006
24. Tang E.S.K., Wang L., Liew C.V., Chan L.W., Heng P.W.S., Int. J. Pharm. 350(2):172-180, 2008
25. Larsen C.C., Sonnergaard J.M., Bertelsen P., Holm P., Eur. J. Pharm. Sci. 20(3):273-283, 2003
26. Maronga S.J., Wnukowski P., Chem. Eng. Process. 37(5):423-432, 1998
27. Werner S.R.L., Jones J.R., Paterson A.H.J., Archer R.H., Pearce D.L., Powder Technol. 171(1):25-33, 2007
28. Depypere F., Pieters J.G., Dewettinck K., Powder Technol, 145(3):176-189, 2004
29. Siepmann F., Siepmann J., Walther M., MacRae R.J., Bodmeier R., J. Control. Release 105(3):226-239, 2005
30. Siepmann F., Hoffmann A., Leclercq B., Carlin B., Siepmann J., J. Control. Release 119(2):182-189, 2007
31. Kablitz C.D., Kappl M., Urbanetz N.A., Eur. J. Pharm. Biopharm. 69(2):760-768. 2008
32. Kablitz C.D., Harder K., Urbanetz N.A., Eur. J. Pharm. Sci. 27(3):212-219, 2006
33. Lorck C.A., Grunenberg P.C., Jiinger H., Laicher A., Eur. J. Pharm. Biopharm. 43(2):149-157, 1997
34. Lecomte F., Siepmann J., Walther M., MacRae R.J., Bodmeier R., Pharm. Res. 21(5):882-890, 2004
35. Williams III R.O., Liu J., Eur. J. Pharm. Biopharm. 49(3):243-252, 2000
36. Kablitz C.D., Urbanetz N.A., Eur. J. Pharm. Biopharm. 67(2):449-457, 2007

37. Bashaiwoldu A.B., Podczeczek F., Newton J.M., *Int. J. Pharm.* 274(1):53-63, 2004
38. Bodmeier R., Paeratakul O., *Drug Dev. Ind. Pharm.* 20(9):1517-1533, 1994
39. Felton L.A., *Int. J. Pharm.* 457(2):423-427, 2013
40. Smikalla M., Mescher A., Walzel P., Urbanetz N.A., *Int. J. Pharm.* 405(1):122-131, 2011
41. Terebesi I., Bodmeier R., *Eur. J. Pharm. Biopharm.* 75(1):63-70, 2010
42. Bartoš J., *Colloid. Polym. Sci.* 274(1):14-19, 1996
43. Muschert S., Siepmann F., Cuppok Y., Leclercq B., Carlin B., Siepmann J., *Int. J. Pharm.* 368(2):138-145, 2009
44. Sreenivasa Rao B. and Ramana Murthy K.V., *Int. J. Pharm.* 231(1):97-106, 2002
45. Sadeghi F., Ford J.L., Rubinstein M.H., Rajabi-Siahboomi A.R., *Drug Dev. Ind. Pharm.* 27(5):419-430, 2001
46. Možina M., Tomažević D., Leben S., Pernuš F., Likar B., *Eur. J. Pharm. Sci.* 41(1):156-162, 2010
47. Paine A.J., *Part. Part. Syst. Character.* 10(1):26-32, 1993
48. Almeida-Prieto S., Blanco-Méndez J., Otero-Espinar F.J., *Eur. J. Pharm. Biopharm.* 67(3):766-776, 2007
49. Podczeczek F., Rahman S.R., Newton J.M., *Int. J. Pharm.* 192(2):123-138, 1999
50. Heinicke G., Schwartz J.B., *Pharm. Dev. Technol.* 9(4):359-67, 2004
51. Heinicke G., Schwartz J.B., *Pharm. Dev. Technol.* 11(4):403-408, 2006
52. De Beer T., Burggraefe A., Fonteyne M., Saerens L., Remon J.P., Vervaet C., *Int. J. Pharm.* 417(1):32-47, 2011
53. Scherzer T., Mirschel G., Heymann K., *Spectroscopy Europe* 20(6):6-8, 2008
54. Bogomolov A., Engler M., Melichar M., Wigmore A., *J. Chemometr.* 24(7):544-557, 2010
55. Spencer J.A., Gao Z., Moore T., Buhse L.F., Taday P.F., Newnham D.A., Shen Y., Portieri A., Husain A., *J. Pharm. Sci.* 97(4):1543-50, 2008
56. Zeitler J.A., Shen Y., Baker C., Taday P.F., Pepper M., Rades T., *J. Pharm. Sci.* 96(2):330-340, 2007
57. Ho L., Müller R., Gordon K.C., Kleinebudde P., Pepper M., Rades T., Shen Y., Taday P.F., Zeitler J.A., *J. Control. Release* 127(1):79-87, 2008

58. Ringqvist A., Taylor L.S., Ekelund K., Ragnarsson G., Engstrom S., Axelsson A., *Int. J. Pharm.* 267(1):35-47, 2003
59. Heinicke G., Schwartz J.B., *Pharm. Dev. Technol.* 12(3):285-296, 2007
60. Ho L., Cuppok Y., Muschert S., Gordon K.C., Pepper M., Shen Y., Siepmann F., Siepmann J., Taday P.F., Rades T., *Int J Pharm* 382(2):151-9, 2009
61. Wesdyk R., Joshi Y.M., Jain N.B., Morris K., Newman A., *Int. J. Pharm.* 65(1):69-76, 1990
62. Shelukar S., Ho J., Zega J., Roland E., Yeh N., Quiram D., Nole A., Katdare A., Reynolds S., *Powder Technol.* 110(1):29-36, 2000
63. Sherony D.F., *Chem. Eng. Sci.* 36(5):845-848, 1981
64. KuShaari K., Pandey P., Song Y., Turton R., *Powder Technol.* 166(2):81-90 2006
65. Turton R., *Powder Technol.* 181(2):186-194, 2008
66. Ozturk A.G., Ozturk S.S., Palsson B.O., Wheatley T.A., Dressman J.B., *J. Control. Release*, 14(3):203-213, 1990
67. Fadda H.M., Khanna M., Santos J.C., Osman D., Gaisford S., Basit A.W., *Eur. J. Pharm. Biopharm.* 76(3):493-497, 2010
68. Klar F., Urbanetz N.A., *Eur. J. Pharm. Biopharm.* 71(1):124-129, 2009
69. Domján A., Bajdik J., Pintye-Hódi K., *Macromolecules*, 42(13):4667-4673, 2009
70. Frohoff-Hülsmann M.A., Lippold B.C., McGinity J.W., *Eur. J. Pharm. Biopharm.* 48(1):67-75, 1999
71. Bando H., McGinity J.W., *Int. J. Pharm.* 323(1):11-17, 2006
72. Sreenivasa Rao B., Ramana Murthy K.V., *Int. J. Pharm.* 231(1):97-106, 2002
73. Steuernagel C.R., Latex emulsions for controlled drug delivery, in: McGinity J.W. (Ed.), *Aqueous Polymer Coatings for Pharmaceutical Dosage Forms*, Marcel Dekker, New York, 1989
74. Goodhart F.W., Harris M.R., Murthy K.S., Nesbitt R.U., *Pharm. Technol.* 8(4):64-71, 1984
75. McConnell E.L., Macfarlane C.B., Basit A.W., *Int. J. Pharm.* 380(1):67-71, 2009
76. Wan L.S.C., Lai W.F., *Int. J. Pharm.* 72(2):163-174, 1991
77. Ragnarsson G., Sandberg A., Johansson M.O., Lindstedt B., Sjögren J., *Int. J. Pharm.* 79(2):223-232, 1992

78. Sousa J.J., Sousa A., Moura M.J., Podczeck F., Newton J.M., *Int. J. Pharm.* 233(1):111-122, 2002
79. Muschert S., Siepmann F., Leclercq B., Carlin B., Siepmann J., *Eur. J. Pharm. Biopharm.* 72(1):130-137, 2009
80. Kállai N., Luhn O., Dredán J., Kovács K., Lengyel M., Antal I., *AAPS PharmSciTech* 11(1):383-391, 2010
81. Tang L., Schwartz J.B., Porter S.C., Schnaare R.L., Wigent R.J., *Pharm. Dev. Technol.* 5(3):383-390, 2000
82. Rivera S.L., Ghodbane S., *Int. J. Pharm.* 108(1):31-38, 1994
83. Muschert S., Siepmann F., Leclercq B., Carlin B., Siepmann J., *J. Control. Release* 135(1):71-79, 2009
84. Dahlberg C., Millqvist-Fureby A., Schuleit M., Furó I., *Eur. J. Pharm. Sci.* 39(1):125-133, 2010
85. Bruce C., Fegely K.A., Rajabi-Siahboomi A.R., McGinity J.W., *Int. J. Pharm.* 341(2):162-172, 2007
86. Chopra R., Alderborn G., Podczeck F., Newton J.M., *Int. J. Pharm.* 239(2):171-178, 2002
87. Nikowitz K., Foltmann F., Wirges M., Knop K., Pintye-Hódi K., Regdon jr. G., Kleinebudde P., *Drug Dev. Ind. Pharm.* - accepted for publication, doi: 10.3109/03639045.2013.795583
88. Yang S.T., Van Savage G., Weiss J., Ghebre-Sellassie I., *Int. J. Pharm.* 86(2):247-257, 1992
89. de Veij M., Vandenabeelen P., De Beer T., *J. Raman Spectrosc.* 40(3):297-307, 2009
90. Cita S., Morari C., Vogel E., Maniu D., *Vib. Spectrosc.* 19(2):329-334, 1999
91. Pearson G.A., *J. Magn. Reson.* 27(2):265-272, 1977
92. Bell S.E.J., *Quantitative Analysis of Solid Dosage Formulations by Raman Spectroscopy* in Šašić S. (Ed.), *Pharmaceutical Applications Of Raman Spectroscopy*, John Wiley & Sons, Inc., Hoboken, 2007
93. Kauffman J.F., Dellibovi M., Cunningham C.R., *J. Pharm. Biomed. Anal.* 43(1):39-48, 2007
94. Romero-Torres S., Pérez-Ramos J.D., Morris K.R., Grant E.R., *J. Pharm. Biomed. Anal.* 38(2):270-274, 2005

95. Lu P., Ding J., Cheng R., Qian R., *Macromol. Rapid Commun.* 15(11):835-840, 1994
96. Cahyadi C., Karande A.D., Chan L.W., Heng P.W.S., *Int. J. Pharm.* 398(1):39-49, 2010
97. Rantanen J., *J. Pharm. Pharmacol.* 59(2):171-177, 2007
98. Wouessidjewe D., *STP Pharma* 7(6):469-475, 1997
99. Pillay V., Fassihi R., *J. Pharm. Sci.* 88(11):1140-1148, 1999
100. Parker R.L., *Zeitschrift für Kristallographie* 59:1-54, 1924
101. Zhang X., Sun N., Wu B., Lu Y., Guan T., Wu W., *Powder Technol.* 182(3):480-485, 2008
102. Yang T.S., Ghebre-Sellassie I., *Int. J. Pharm.* 60(2):109-124, 1990
103. Dansereau R., Brock M., Furey-Redman N., *Drug Dev. Ind. Pharm.* 19(7):793-808, 1993
104. Mizuno M., Hirakura Y., Yamane I., Miyanishi H., Yokota S., Hattori M., Kajiyama A., *Int. J. Pharm.* 305(1):37-51, 2005
105. Konno H., Handa T., Alonzo D.E., Taylor L.S., *Eur. J. Pharm. Biopharm.* 70(2):493-499, 2008
106. Van den Mooter G., Wuyts M., Bleton N., Busson R., Grobet P., Augustijns P., Kinget R., *Eur. J. Pharm. Sci.* 12(3):261-269, 2001
107. Sun N., Wei X., Wu B., Chen J., Lu Y., Wu W., *Powder Technol.* 182(1):72-80, 2008
108. Crowley K.J., Zografi G., *J. Pharm. Sci.* 91(2):492-507, 2002
109. Van Eerdenbrugh B., Taylor L.S., *Mol. Pharm.* 7(4):1328-1337, 2010
110. Bley H., Fussnegger B., Bodmeier R., *Int. J. Pharm.* 390(2):165-173, 2010
111. Wu J.X., Xia D., van den Berg F., Amigo J.M., Rades T., Yang M., Rantanen J., *Int. J. Pharm.* 433(1):60-70, 2012
112. Baird J.A., Taylor L.S., *Adv. Drug Deliver. Rev.* 64(5):396-421, 2012
113. Malaj L., Censi R., Mozzicafreddo M., Pellegrino L., Angeletti M., Gobetto R., Di Martino P., *Int. J. Pharm.* 398(1):61-72, 2010
114. Pirayavaraporn C., Rades T., Tucker I.G., *Int. J. Pharm.* 422(1):68-74, 2012
115. Varnalis A.I., Brennan J.G., MacDougall D.B., *J. Food Eng.* 48(4):361-367, 2001
116. Norton A.D., Greenwood R.W., Noble I., Cox P.W., *J. Food Eng.* 105(1):119-127, 2011

117. Verreck G, Decorte A., Heymans K., Adriaensen J., Cleeren D., Jacobs A., Liu D., Tomasko D., Arien A., Peeters J., Rombaut P., Van den Mooter G., Brewster M.E., *Eur. J. Pharm. Sci.* 26(3):349-358, 2005
118. Verreck G, Decorte A., Li H., Tomasko D., Arien A., Peeters J., Rombaut P., Van den Mooter G., Brewster M.E., *J. Supercrit. Fluid.* 38(3):383-391, 2006
119. Verreck G, Decorte A., Heymans K., Adriaensen J., Liu D., Tomasko D.L., Arien A., Peeters J., Rombaut P., Van den Mooter G., Brewster M.E., *J. Supercrit. Fluids* 40(1):153-162, 2007
120. Fitzpatrick S., McCabe J.F., Petts C.R., Booth S.W., *Int. J. Pharm.* 246(1):143-151, 2002
121. Zelkó R., Orbán Á., Süvegh K., *J. Pharm. Biomed. Anal.* 40(2):249-254, 2006
122. Siepmann J., Siepmann F., *Int. J. Pharm.* 364(2):328-343, 2008
123. Siepmann J., Siepmann F., *J. Control. Release* 161(2):351-362, 2012
124. Gendre C., Genty M., da Silva J.C., Tfayli A., Boiret M., Lecoq O., Baron M., Chaminade P., Péan J.M., *Eur. J. Pharm. Biopharm.* 81(3):657-665, 2012
125. Nevsten P., Borgquist P., Axelsson A., Wallenberg L.R., *Int. J. Pharm.* 290(1):109-120, 2005
126. Savolainen M., Heinz A., Strachan C., Gordon K.C., Yliruusi J., Rades T., Sandler N., *Eur. J. Pharm. Sci.* 30(2):113-123, 2007
127. Chen X., Bates S., Morris K.R., *J. Pharm. Biomed. Anal.* 26(1):63-72, 2001
128. Tian F., Zhang F., Sandler N., Gordon K.C., McGoverin C.M., Strachan C.J., Saville D.J., Rades T., *Eur. J. Pharm. Biopharm.* 66(3):466-474, 2007
129. Priemel P.A., Grohgan H., Gordon K.C., Rades T., Strachan C.J., *Eur. J. Pharm. Biopharm.* 82(1):187-193, 2012
130. Rumondor A.C.F., Taylor L.S., *Int. J. Pharm.* 398(2):155-160, 2010
131. Moore M.D., Cogdill R.P., Short S.M., Hair C.R., Wildfong P.L.D., *J. Pharm. Biomed. Anal.* 47(2):238-247, 2008
132. Shah B., Kakumanu V.K., Bansal A.K., *J. Pharm. Sci.* 95(8):1641-65, 2006
133. Xie Y., Tao W., Morrison H., Chiu R., Jona J., Fang J., Cauchon N., *Int. J. Pharm.* 362(1):29-36, 2008
134. Varasteh M., Deng Z., Hwang H., Kim Y.J., Wong G.B., *Int. J. Pharm.* 366(1):74-81, 2009
135. Zidan A.S., Rahman Z., Sayeed V., Raw A., Yu L., Khan M.A., *Int. J. Pharm.* 423(2):341-350, 2012

136. Nunes C., Mahendrasingam A., Suryanarayanan R., *Pharm. Res.* 22(11):1942-53, 2005
137. Bansal P., Hall M., Realff M.J., Lee J.H., Bommarius A.S., *Biores. Technol.* 101(12):4461-4471, 2010
138. Ohta M., Buckton G., *Int. J. Pharm.* 289(1):31-38, 2005
139. Wesdyk R., Joshi Y.M., De Vincentis J., Newman A.W., Jain N.B., *Int. J. Pharm.* 93(1):101-109, 1993
140. Latsch S., Selzer T., Fink L., Kreuter J., *Eur. J. Pharm. Biopharm.* 57(2):383-395, 2004
141. Bro R., *Anal. Chim. Acta*, 500(2):185-194, 2003
142. Moore M.D., Cogdill R.P., Wildfong P.L.D., *J. Pharm. Biomed. Anal.* 49(3):619-626, 2009

Acknowledgements

Firstly, I sincerely thank my supervisor **Dr. Géza Regdon jr.** for his endless patience, encouragement, and for letting me shape my research along the way. His keen eyes for details have contributed immensely to the quality of all my work.

My deepest gratitude goes to **Prof. Dr. Klára Pintye-Hódi** for her guidance, invaluable advice and for always keeping me on my toes. Her being there was an inspiration for me to pull through.

I take this opportunity to express my appreciation to **Prof. Dr. Piroska Szabó-Révész**, who granted me the opportunity to do research in the Department of Pharmaceutical Technology. I thank her for watching over me and sharing her opinion.

I express my gratitude and appreciation to **Dr. Attila Domján** for his careful solid state NMR spectroscopic measurements, analysis and insights. I am also grateful for the help of **Dr. Félix Schubert** in obtaining the microphotographs presented in Fig. 21.

My heartfelt thanks to **Gabriella Farkas** and **István Farkas** for guiding a stranger in a strange land. Without them I would never have had the confidence to walk my own way. A very special thankyou goes to **Mihály Gottnek**, who always had a few good words, ideas and moments in store for me. I similarly thank **Anita Korbely**, who was always there to patiently hear me out when I needed to vent.

I am indebted to all my former colleagues at the Department of Pharmaceutical Technology who lent me anything from technical support to a shoulder to cry on. I am grateful for their contribution.

Finally, I wish to thank my parents and friends for their support and encouragement throughout my studies.

APPENDIX

PUBLICATIONS RELATED TO THE THESIS

I

RESEARCH ARTICLE

Development of a Raman method to follow the evolution of coating thickness of pellets

Krisztina Nikowitz¹, Friederike Folttmann², Markus Wirges², Klaus Knop², Klára Pintye-Hódi¹, Géza Regdon Jr¹, and Peter Kleinebudde²

¹Department of Pharmaceutical Technology, University of Szeged, Szeged, Hungary and ²Institute of Pharmaceutics and Biopharmaceutics, Heinrich-Heine-University, Düsseldorf, Germany

Abstract

Context: Although several methods have been investigated to measure the film thickness of tablets and its correlation with the dissolution behavior, much fewer such investigations exist for pharmaceutical pellets.

Objective: To study the possibility of measuring the film thickness and predicting the dissolution behavior of pellets produced in different fluid bed equipments with Raman spectroscopy.

Materials and methods: Pyridoxine hydrochloride-layered pellets were produced and coated in two different Strea-1 equipments. Raman spectra were collected and analysed to set up a calibration model based on the film thickness data calculated from Camsizer analysis results. Dissolution tests were done according to Ph. Eur. standards.

Results: Raman spectroscopy proved to be a good tool in the measurement of film thickness. Polymer weight gain showed a linear correlation with film thickness but was a poor predictor of dissolution results below a threshold value.

Conclusion: The Raman spectroscopic measurement of a small sample can provide accurate data of the film thickness. The investigation suggests that a threshold value might exist for the film thickness above which it can be used to judge future dissolution results.

Keywords

Chemometric analysis, dissolution, film thickness, PCA, pellet, PLS, Raman

History

Received 20 December 2012

Revised 8 April 2013

Accepted 10 April 2013

Published online 13 May 2013

Introduction

The use of pharmaceutical pellets provides numerous advantages over single-unit dosage forms^{1–5}. Among these is the smaller variation of the in vivo dissolution profile which results in predictable therapeutic effect. However, the multiparticulate nature causes problems when determining coating thickness which critically affects the drug release⁶. For the direct measurement of film thickness, scanning electron microscopy was often used, but usually a very low number of pellets was measured, and the cross-section images require that the pellets be sliced which makes the measurement very time-consuming^{7–9}. Image analysis can be used to measure a statistically significant number of pellets but there is some disagreement on what this statistically significant number may be. In addition, the methods used to analyse the acquired images are often incomparable^{10,11}. The use of a Camsizer allows the rapid measurement of a large number of particles making it ideal for the calibration of indirect methods to measure film thickness¹².

Weight gain as the most traditional indirect method has been criticized for its lack of specificity stemming from the mass loss of the core material and failure to predict dissolution values^{13–15}. Spectroscopic and tomographic methods have been

used recently to quantify the film thickness of pharmaceutical preparations^{9,16–24}. This study utilizes Raman spectroscopy which has been demonstrated to be suitable for the offline and online (not online in this study) measurement of the film thickness of tablets^{23–25}. Its use regarding pellets however appears to be much more limited²⁶.

In our work we examine pellets of the same composition prepared in two different fluid bed equipments to determine whether a multivariate calibration model that is feasible for the determination of the coating thickness of samples prepared in either equipment can be built.

Experimental section

Materials

Pyridoxine hydrochloride (Ph. Eur.) was used as a model drug. Cellet 500 (Shin-Etsu Chemical Co., Ltd., Tokyo, Japan) was used as non-pareil core material. Pharmacoat 606 (BASF, Ludwigshafen, Germany) was applied as a binder. Acryl-EZE (Colorcon, Dartford Kent, UK), a fully formulated enteric coating dispersion was used as coating material.

Layering of pyridoxine hydrochloride

The pellet samples were prepared in a Strea-1 (Niro Aeromatic, Bubendorf, Switzerland) fluid bed wurster chamber. Two different pieces of equipment were used with slightly different capabilities and chamber layouts (Table 1). As the chamber

Address for correspondence: Peter Kleinebudde, Institute of Pharmaceutics and Biopharmaceutics, Heinrich-Heine-University, Universitätsstr. 1, D-40225 Düsseldorf, Germany. Tel: +49-211-81-14220. Fax: +49-211-81-14251. E-mail: kleinebudde@hhu.de

Table 1. Process and equipment parameters.

	Strea 1 in Szeged	Strea 1 in Düsseldorf
Inlet temperature	50 °C	50 °C
Outlet temperature	43 °C	37 °C
Spray rate	6 ml/min	6 ml/min
Atomizing pressure	2 bar	2.2 bar
Air volume	80 m ³ /h	130 m ³ /h
Nozzle diameter	1 mm	1 mm
Chamber material	Glass	Stainless steel
Wurster insert	Yes	No
Spraying installation	Bottom-spray	Bottom-spray

Table 2. Particle size of uncoated and Acryl-EZE[®] coated pellets ($n = 3$; mean), calculated film thickness.

Sample	Particle size of uncoated pellets [μm] ($n = 3$; mean)	Particle size of Acryl-EZE [®] coated pellets [μm] ($n = 3$; mean)	Coating thickness [μm]	Polymer weight gain [g]
Set1 sample1	718.27 \pm 0.11	788.93 \pm 0.25	35.33	52.9
Set1 sample2	695.13 \pm 0.31	781.43 \pm 0.06	43.15	73.9
Set1 sample3	722.00 \pm 0.10	823.33 \pm 0.15	50.67	87.0
Set1 sample4	695.87 \pm 0.06	813.00 \pm 0.00	58.57	131.1
Set2 sample1	721.03 \pm 0.06	774.80 \pm 0.17	26.88	43.8
Set2 sample2	721.17 \pm 0.12	798.43 \pm 0.06	38.63	67.7
Set2 sample3	724.73 \pm 0.15	821.37 \pm 0.06	48.32	90.3

geometry of the Düsseldorf equipment is such that it prevents the use of a Wurster, insert experiments in these cases were performed using bottom-spray mode.

A solution of pyridoxine hydrochloride and Pharmacoat 606 in 5:2 mass ratio with a total solid content of 12.28% was sprayed onto 200 g nonpareil cores (between 500 and 710 μm in diameter as specified by the manufacturer) until 175 g dry material was applied. The pellets were dried in the spray coater for 10 min.

Coating of layered pellets

Acryl-EZE dispersion was prepared and applied following the guidelines provided by the manufacturer as 20% aqueous dispersion. The manufacturer lists the ingredients of the Acryl-EZE ready-to-disperse fully formulated coating system as USP type C methacrylic acid copolymer, sodium bicarbonate, talc, SiO₂, titanium dioxide, sodium laurylsulphate and triethyl citrate. Only a small amount (0.1%) of dimeticone was added to prevent foaming during the process. Samples were prepared with different coating levels using the same equipment and parameters as for the drug layering. In the two different equipments two sets of samples were prepared. Four batches were made in one and three in the other. The sets differ only in the equipment used for manufacturing; samples within the set differ in coating levels (Table 2).

Measurement of particle size and film thickness

Three pellet batches from Düsseldorf and four batches from Szeged (API-layered pellets coated with Acryl-EZE[®] and uncoated API-layered pellets) were measured three times using the CamsizerXT image analysis system (Retsch[®] Technology GmbH, Haan, Germany, X-Fall module (free fall mode)). The number of measured pellets per sample was counted during measurement. Due to differences in the sampling method the size of the samples varies thus the number of measured uncoated pellets lies between 53 000 and 103 000 and the number of coated pellets is between 35 000 and 62 000. The value specifying the particle size is defined as the width of the particle projection and

is the shortest of measured maximum chords in 32 directions. The median of the number size distribution was taken for further evaluation. The coating thickness was calculated from the mean of $n = 3$ measurements as follows:

$$A = \frac{(d_{\text{min coated pellets}} - d_{\text{min uncoated pellets}})}{2}$$

where A is the coating thickness (μm), $d_{\text{min coated pellets}}$ is the particle size of uncoated pellets (μm) ($n = 3$; mean) and $d_{\text{min uncoated pellets}}$ is the particle size of Acryl-EZE[®] coated pellets (μm) ($n = 3$; mean).

Drug content and dissolution

Drug content determination was done with a UV-Vis spectrophotometer at pH 6.8 (phosphate buffer) at 325.0 nm from approx. 500 mg of whole pellets after 2 h. R^2 of the calibration curve is 0.9999. Dissolution studies were carried out according to Ph. Eur. standards with a rotating basket (Erweka DT 700, Erweka GmbH, Heusenstramm, Germany), in 900 ml of simulated gastric acid at 100 rpm at 37 °C for 2 h, then the acidic medium was replaced with 900 ml of phosphate buffer (pH = 6.8) and the dissolution measured at the same parameters as above. Samples were taken of the gastric acid at 2 h and of the phosphate buffer at 5, 10, 15, 20, 30, 45, 60 and 90 min. Concentration was measured with a spectrophotometer (Unicam Helios α , Thermo Fisher Scientific Inc., Waltham, MA) at 291.0 nm with an R^2 of 0.9996 in artificial gastric acid (pH 1.2). In the phosphate buffer, the same parameters and calibration were used as for drug content determination.

Raman and chemometric analysis

The Raman spectra were measured using a RamanRXN2 analyzer (Kaiser Optical Systems, Ann Arbor, MI) with a non-contact optical sampling device (PhAT probe). The probe beam was generated using a diode laser operating at 785 nm and the laser power at the sample was 400 mW. The laser spot diameter was 6 mm corresponding to a 28.3 mm² circular illumination area. Each sample was measured with an exposure time of 10 s. Data collection, calculations, mean centering of the entire dataset, baseline correction (SNV, standard normal variate), spectral comparison (PCA, principal component analysis) and the construction of the predictive model (PLS regression, partial least squares regression) were done using icRaman[®] data collection software package (Kaiser Optical Systems, Ann Arbor, MI), SIMCA 13.0[®] (Umetrics, Umea, Sweden) and Excel[®] (Version 2007, Microsoft Corporation, Redmond, WA).

Calibration and validation development

In order to detect the amount of enteric coating material calibration was developed based on the offline results of two coated pellet sets ($n = 3 + 4$). A multivariate model was built based on the data sets and the results of the film thickness measurement obtained by the CamsizerXT image analysis system was used as reference analytical method.

Results

Particle size and film thickness

The pellets without the final enteric coating vary in size from 695 μm to 725 μm (Table 2) due to different thicknesses of the pyridoxine hydrochloride layer. These uncoated API-layered pellets show a standard deviation in particle size of 0.06–0.31 μm ($n = 3$). The standard deviation in particle size of the Acryl-EZE[®] coated pellets ($n = 3$) varies between 0 and 0.25 μm .

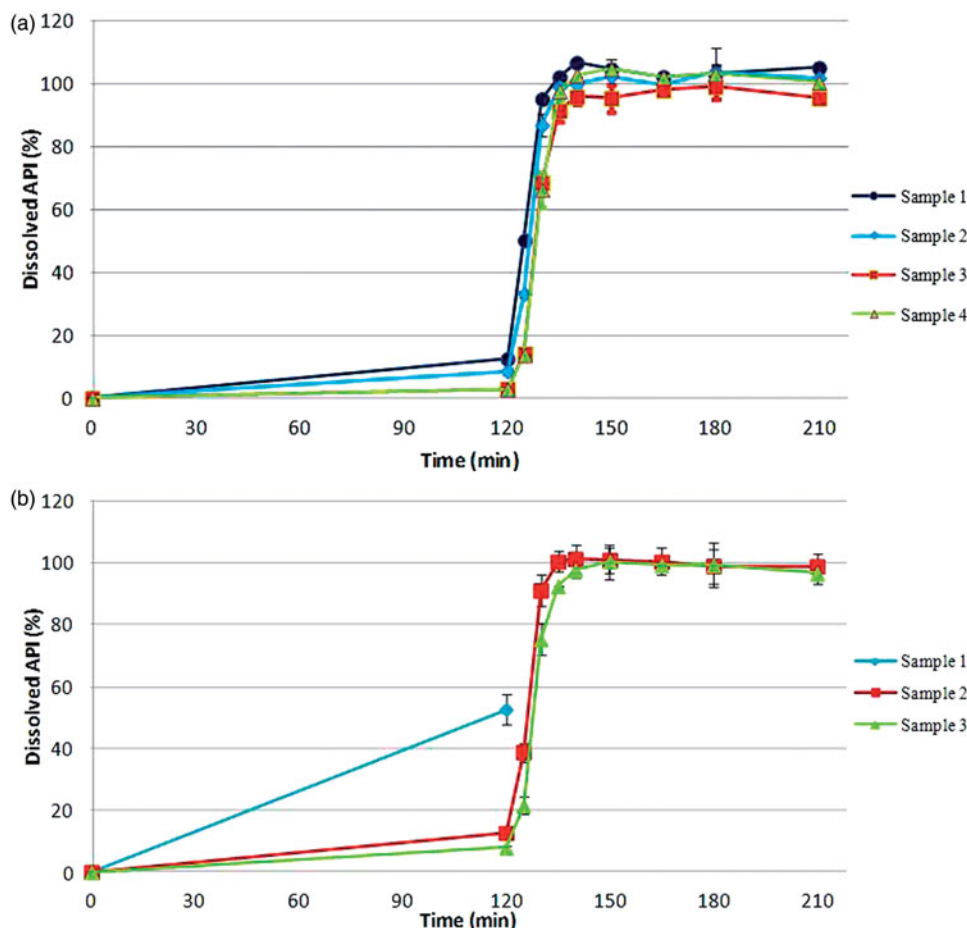


Figure 1. Dissolution of coated pellets (a) set 1 prepared in Szeged and (b) set 2 prepared in Düsseldorf, in order of increasing film thickness.

The coating thickness in sample set 2 increases in steps of almost $10\ \mu\text{m}$ per sample. The coating thickness of the samples in set 1 differs by $8\ \mu\text{m}$ in the order of the numbering.

Drug content and dissolution

All samples released the API completely after 60 min in the pH 6.8 dissolution medium. Drug release in artificial gastric acid was greatly influenced by the thickness of the film coating with higher coating levels yielding better results. Similar levels of coating showed similar gastric resistance regardless of the equipment used for sample production, indicating that the quality of the coatings produced in different equipments does not differ much in this respect. Samples with a film thickness of $38\ \mu\text{m}$ or above have demonstrated dissolution values below 10% that satisfy the requirements of gastroresistant films. The dissolution testing of Set 2 sample 1 was discontinued after observing over 50% drug release in artificial gastric acid (Figure 1).

Raman and chemometric analysis

A PLS predictive model was constructed using the SNV normalized spectra data from the two sample sets with enteric coating levels from 27 to $59\ \mu\text{m}$ (Table 2).

Figure 2 shows the SNV preprocessed Raman spectra ($n=3$; mean) of pyridoxine HCl (ingredient of the first pellet layer), Acryl-EZE[®] (enteric coating material of the second pellet layer) and two pellet sets with different enteric coating levels (four batches produced in Szeged, three batches produced in Duesseldorf) in a spectral range $150\text{--}1890\ \text{cm}^{-1}$. The spectra comprised dominant Raman shifts of the first layering as well as shifts of the final enteric coating. Pyridoxine HCl shows

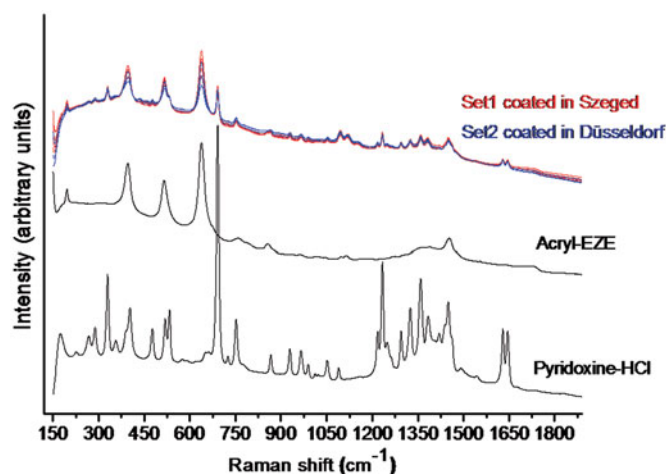


Figure 2. Standard normal variate (SNV) preprocessed Raman spectra ($n=3$; mean) of pyridoxine-HCl, Acryl-EZE[®] and two pellet sets with different enteric coating levels ($n=3+4$), spectral range $150\text{--}1890\ \text{cm}^{-1}$.

characteristic Raman shifts ($692\ \text{cm}^{-1}$, $1234\ \text{cm}^{-1}$) which can be assigned to the quadrant stretching vibrations and the deformation of the 3-Hydroxypiperidin ring according to Cita S et al. (1999)²⁷ ($692\ \text{cm}^{-1}$ vs: tors(C2-C3-C9-H19) + stretch quadrant (C2-C4-C5-N7) + tors(C3-C2-C4-C5), $1234\ \text{cm}^{-1}$ vs: $\delta(\text{O-H})$; $\delta(\text{N-H})$ i.p.). Acryl-EZE[®] is a preformulated aqueous acrylic coating containing the pigment TiO_2 and Eudragit L100-55 as enteric coating polymer²⁸. Titanium dioxide can be used in two different polymorphic forms in pharmaceutical formulations.

The polymorphic form anatase used in this study shows intensive Raman shifts (637 cm^{-1} , 513 cm^{-1} , 395 cm^{-1}). These shifts are caused by the bending vibration and the symmetric stretching vibration of the polymorph (636 cm^{-1} vs: $\delta(\text{TiO}_2)$; 513 cm^{-1} m: $\nu(\text{TiO}_2)$; 395 cm^{-1} m: $\delta(\text{TiO}_2)$)²⁹. The intensity of titanium dioxide Raman shifts increases whereas the intensity of the pyridoxine–HCl shifts decreases with the increasing amount of enteric coating material, clearly visible in the spectral range of $310\text{--}715\text{ cm}^{-1}$ (Figure 3).

Principal component analysis (PCA) of the offline acquired Raman spectra were performed to discriminate sample sets by

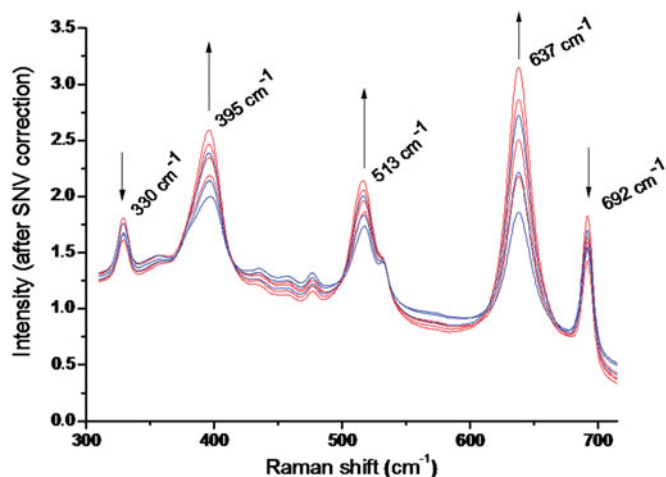


Figure 3. Standard normal variate (SNV) preprocessed Raman spectra ($n=3$; mean) of two pellet sets with different enteric coating levels ($n=3+4$), spectral range $310\text{--}715\text{ cm}^{-1}$, decreasing Raman shifts (330 cm^{-1} , 692 cm^{-1}), increasing Raman shifts (395 cm^{-1} , 513 cm^{-1} , 637 cm^{-1}).

increasing mass of coating material. With the exception of data point 2 and 3, PCA scores on the first principal component (PC1) are able to order the samples with respect to the theoretical amount of enteric coating along the first principal component (Figure 4a). PC1 explains 91.4% of the variance. Loadings on PC1 mainly correspond to spectral information from the titanium dioxide anatase polymorph in the Acryl-EZE[®] layer (Figure 4b). The construction of PC1 can therefore be explained by the increasing amount of enteric coating material coated onto the pyridoxine hydrochloride layered pellet core. In Figure 4(c), each data point displays a sample with certain amount of Acryl-EZE[®] coating, which was measured by Raman spectroscopy and analyzed by a PLS regression algorithm. The coating thickness as predicted by the multivariate model derived from Raman measurement is plotted against the corresponding data as obtained by the CamsizerXT reference method. Best predictive results for the PLS regression model were obtained by using three principal components, which explain 100% of the X-Variance (spectral data) and 98.7% of the Y-Variance (coated Acryl-Eze[®] amount) (Table 3). The high variances of the model indicate its validity to predict the enteric coating level even though it was built on

Table 3. Parameter set of the multivariate model³⁰.

Model description	Results
Regression algorithm	PLS
Number of components	3
Calibration range	27–59 μm
Range of wavenumbers	150–1890 cm^{-1}
R ² X	1.000
R ² Y	0.987
RMSEE	2.53 μm
RMSEcv	3.44 μm

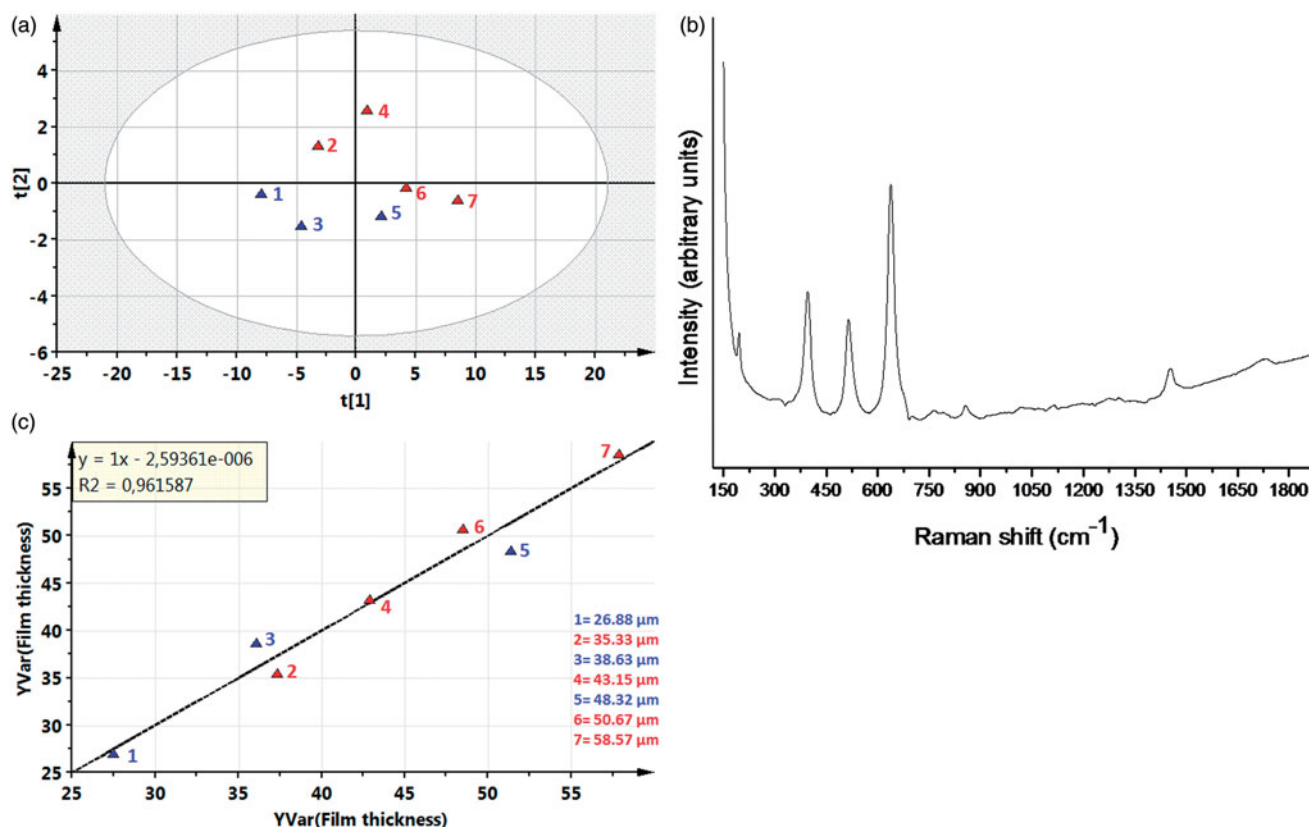


Figure 4. (a) Principal component analysis (PCA) scores plot obtained from SNV preprocessed Raman spectra ($n=3$; mean), (b) p-loadings of PC1 of the PCA model and (c) calibration variance regression model for SNV Raman spectra (PLS).

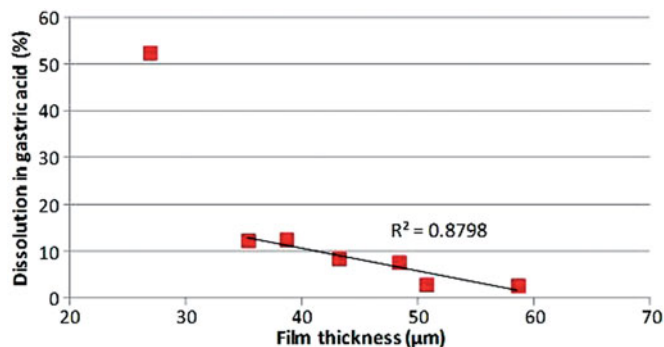


Figure 5. Correlation of film thickness and dissolution in gastric acid after 120 min.

spectra which contains peaks of both pellet layers. The black line represents the linear fit to the data points. The resulting R^2 value of the regression line can be used to quantify the strength of the association between the observed Y and the predicted Y for the pellet samples. The closer the R^2 value is to one the stronger the association between the observed and the predicted variables³¹. The predicted coated thicknesses obtained by the multivariate model fits the real thicknesses measured by the reference method with exception of datapoints 5 and 6 (sample 1 set 1, sample 3 set 2). This might be due to the small differences in coating thickness (2.35 µm) between these two samples. The data points 2 and 3 (sample 4 set 1, sample 2 set 2) showing a coating thickness difference of 3.3 µm are also hard to classify. This leads to the assumption that multivariate models in combination with offline Raman analysis reaches a limit of classification ability in samples which only differ slightly from one another in coating thickness.

Discussion

According to Rantanen, one of the problems with Raman spectroscopy is the small sampling area and penetration depth³². In our study the illumination area was a 28.3 mm² circle, which means that, calculating with a single layer, less than 100 pellets were measured with the Raman probe. This is a significantly lower number of pellets than measured with the Camsizer, once again raising the question of what minimal number of pellets is capable of representing the whole batch regarding film thickness. Nevertheless, Raman spectroscopic data is in good agreement with the film thickness data acquired with digital image analysis, which in turn shows a linear correlation with the polymer weight gain. This again suggests that the structure of the film coatings was not impacted significantly by the differences in the equipment used for their preparation.

No direct linear correlation was observed for the percent of drug dissolved in gastric acid. As can be seen in Figure 5 this is mainly due to the poor performance of Set 2 sample 1. After excluding this data point from the dissolution results the coefficient of determination improved to 0.8798 and 0.6842 for correlation with film thickness and polymer weight gain respectively. These findings correspond with those of Ho et al., whose work showed that weight gain was a poor predictor of dissolution values¹⁴.

Contrary to previous studies done on sustained release systems where film thickness was a good predictor of dissolution^{14,33} delayed release coatings appear to be more complicated. Our results suggest that there might be a threshold value above which a correlation exists. One of the reasons for this may be incomplete film formation. The greater mechanical stress the sample suffered in the bottom spray equipment compared to the Wurster coater could also have contributed to the poor dissolution performance

through the formation of cracks and chips, which in the case of thin coatings (in this case sample 1 set 2) could affect the preparation more adversely than in the case of thick coatings.

Conclusion

In this study a Raman spectroscopic model was built for the measurement of the film thickness of pellets produced in different equipments. Dissolution test results and the existence of a shared film thickness–polymer weight gain correlation indicates that the structure of the film was similar in the samples regardless of which equipment was used for their preparation. Raman spectroscopy proved to be a good tool in measuring the film thickness. Pellets with the lowest film thickness were not gastric resistant. When excluding these pellets from the examination the correlation between film thickness and dissolved fraction after 120 min was good, leading to the hypothesis that a threshold value, possibly representing the polymer film formation and integrity, exists for the correlation to function. This threshold value cannot be derived from spectral or film thickness data alone.

Declaration of interest

The publication is supported by DAAD-MOB/P-MOB/817 (Hungary) and 50430305 (Germany) and by the European Union and co-funded by the European Social Fund. Project title: ‘‘Broadening the knowledge base and supporting the long term professional sustainability of the Research University Centre of Excellence at the University of Szeged by ensuring the rising generation of excellent scientists.’’ Project number: TAMOP-4.2.2/B-10/1-2010-0012.

References

1. Bechgaard H, Hagermann NG. Controlled-release multi-units and single unit doses. A literature review. *Drug Dev Ind Pharm* 1978;4: 53–67.
2. Bodmeier R. Tableting of coated pellets. *Eur J Pharm Biopharm* 1997;43:1–8.
3. Krämer J, Blume H. Biopharmaceutical aspects of multiparticulates. In: Ghebre-Sellassie I, ed. *Multiparticulate oral drug delivery*. New York: Marcel Dekker Inc.; 1994:307–32.
4. Ghebre-Sellassie I. Pellets: a general overview. In: Ghebre-Sellassie I, ed. *Pharmaceutical pelletization technology*. New York: Marcel Dekker Inc.; 1989:1–13.
5. Ghebre-Sellassie I, Knoch A. Pelletization techniques. In: Swarbrick J, Boylan JC, eds. *Encyclopedia of pharmaceutical technology*. New York: Marcel Dekker Inc.; 2002:2067–80.
6. Haddish-Berhane N, Jeong SH, Haghghi K, Park K. Modelling film-coat non-uniformity in polymer coated pellets: a stochastic approach. *Int J Pharm* 2006;323:64–71.
7. Wesdyk R, Yoshi YM, Morris K, Newman A. The effect of size and mass on the film thickness of beads coated in fluidized bed equipment. *Int J Pharm* 1990;65:69–76.
8. Wesdyk R, Joshi YM, De Vincentis J, et al. Factors affecting differences in film thickness of beads coated in fluidized bed units. *Int J Pharm* 1993;93:101–9.
9. Andersson M, Holmquist B, Lindquist J, et al. Analysis of film coating thickness and surface area of pharmaceutical pellets using fluorescence microscopy and image analysis. *J Pharm Biomed Anal* 2000;22:325–39.
10. Larsen CC, Sonnergaard JM, Bertelsen P, Holm P. Validation of an image analysis method for estimating coating thickness on pellets. *Eur J Pharm Sci* 2003;18:191–6.
11. Podczeczek F, Rahman SR, Newton JM. Evaluation of a standardised procedure to assess the shape of pellets using image analysis. *Int J Pharm* 1999;192:123–38.
12. Ho L, Cuppok Y, Muschert S, et al. Effects of film coating thickness and drug layer uniformity on in vitro drug release from sustained-release coated pellets: A case study using terahertz pulsed imaging. *Int J Pharm* 2009;382:151–9.
13. Možina M, Tomažević D, Lebe S, et al. Digital imaging as a process analytical technology tool for fluid-bed pellet coating process. *Eur J Pharm Sci* 2010;41:156–62.

14. Ho L, Müller R, Gordon KC, et al. Applications of terahertz pulsed imaging to sustained-release tablet film coating quality assessment and dissolution performance. *J Control Release* 2008;127:79–87.
15. Ho L, Müller R, Gordon KC, et al. Terahertz pulsed imaging as an analytical tool for sustained-release tablet film coating. *Eur J Pharm Biopharm* 2009;71:117–23.
16. Lee M-J, Seo D-Y, Lee H-E, et al. Inline NIR quantification of film thickness on pharmaceutical pellets during a fluid bed coating process. *Int J Pharm* 2011;403:66–72.
17. Müller J, Brock D, Knop K, et al. Prediction of dissolution time and coating thickness of sustained release formulations using Raman spectroscopy and terahertz pulsed imaging. *Eur J Pharm Biopharm* 2012;80:690–7.
18. Bikiaris D, Koutri I, Alexiadis D, et al. Real time and non-destructive analysis of tablet coating thickness using acoustic microscopy and infrared diffuse reflectance spectroscopy. *Int J Pharm* 2012;438:33–44.
19. Ringqvist A, Taylor LS, Ekelund K, et al. Atomic force microscopy analysis and confocal Raman microimaging of coated pellets. *Int J Pharm* 2003;267:35–47.
20. Kauffman JF, Dellibovi M, Cunningham CR. Raman spectroscopy of coated pharmaceutical tablets and physical models for multivariate calibration to tablet coating thickness. *J Pharm Biomed Anal* 2007;43:39–48.
21. Koller DM, Hanneschläger G, Leitner M, Khinast JG. Non-destructive analysis of tablet coatings with optical coherence tomography. *Eur J Pharm Sci* 2011;44:142–8.
22. Cahyadi C, Karande AD, Chan LW, Heng PWS. Comparative study of non-destructive methods to quantify thickness of tablet coatings. *Int J Pharm* 2010;398:39–49.
23. Romero-Torres S, Perez-Ramos JD, Morris KR, Grant ER. Raman spectroscopic measurement of tablet-to-tablet coating variability. *J Pharm Biomed Anal* 2005;38:270–4.
24. Romero-Torres S, Perez-Ramos JD, Morris KR, Grant ER. Raman spectroscopy for tablet coating thickness quantification and coating characterization in the presence of strong fluorescent interference. *J Pharm Biomed Anal* 2006;41:811–19.
25. Müller J, Knop K, Thies J, et al. Feasibility of Raman spectroscopy as PAT tool in active coating. *Drug Dev Ind Pharm* 2010;36:234–43.
26. Sovány T, Nikowitz K, Regdon Jr G, et al. Raman spectroscopic investigation of film thickness. *Polym Test* 2009;28:770–2.
27. Cita S, Morari C, Vogel E, Maniu D. Vibrational studies of B₆ vitamin. *Vib Spectrosc* 1999;19:329–34.
28. Colorcon®. Acryl-EZE® Aqueous Acrylic Enteric System. Available from: <http://www.colorcon.com/products/coatings/enteric-delayed-release/acryl-eze> [last accessed 18 Nov 2012].
29. de Veij M, Vandenabeelen P, De Beer T. Reference database of Raman spectra of pharmaceutical excipients. *J Raman Spectrosc* 2009;40:297–307.
30. Wirges M, Müller J, Kasa P. From mini to micro scale – Feasibility of Raman spectroscopy as a Process Analytical Tool (PAT). *Pharmaceutics* 2011;3:723–30.
31. Umetrics, Umea, Sweden. SIMCA Help. SIMCA 13.0® Software package.
32. Rantanen J. Process analytical applications of Raman spectroscopy. *J Pharm Pharmacol* 2007;59:171–7.
33. Heinicke G, Schwartz JB. Assessment of dynamic image analysis as a surrogate dissolution test for a coated multiparticulate product. *Pharm Dev Technol* 2006; 11:403–8.

III



Study of the recrystallization in coated pellets – Effect of coating on API crystallinity

Krisztina Nikowitz, Klára Pintye-Hódi, Géza Regdon Jr. *

Department of Pharmaceutical Technology, University of Szeged, H-6720 Szeged, Eötvös utca 6, Hungary

ARTICLE INFO

Article history:

Received 4 July 2012

Received in revised form 22 November 2012

Accepted 13 December 2012

Available online 2 January 2013

Keywords:

Pellet

Coating

Recrystallization

Diltiazem hydrochloride

ABSTRACT

Coated diltiazem hydrochloride-containing pellets were prepared using the solution layering technique. Unusual thermal behavior was detected with differential scanning calorimetry (DSC) and its source was determined using thermogravimetry (TG), X-ray powder diffraction (XRPD) and hot-stage microscopy. The coated pellets contained diltiazem hydrochloride both in crystalline and amorphous form. Crystallization occurs on heat treatment causing an exothermic peak on the DSC curves that only appears in pellets containing both diltiazem hydrochloride and the coating. Results indicate that the amorphous fraction is situated in the coating layer. The migration of drugs into the coating layer can cause changes in its degree of crystallinity. Polymeric coating materials should therefore be investigated as possible crystallization inhibitors.

© 2012 Elsevier B.V. All rights reserved.

1. Introduction

Polymorphs and amorphous materials have generated a great interest in the pharmaceutical industry, although processing and stability issues such as phase transformations significantly hinder their application (Serajuddin, 1999; Zhu et al., 2010). In the case of amorphous materials solid dispersions are the most commonly used solution.

Solid dispersions can be prepared with several methods; the two classical ones are melting and solvent evaporation (Leuner and Dressman, 2000). Supercritical fluid processing can also be used as an alternative (Sethia and Squillant, 2004).

One version of the solvent evaporation method uses a fluid bed chamber to spray the solution of the drug and the carrier, generally polymeric in nature, onto inert cores (Zhang et al., 2008; Sun et al., 2008).

Multilayer pellets are produced in a very similar way. Inert cores can be used in their preparation (Nastruzzi et al., 2000; Sinchaipapad et al., 2004), and the same polymers are frequently used in their production as binders and as coatings. The materials are sprayed onto the cores in a fluid bed chamber either as a (generally aqueous) solution, suspension or as dry powder (Ghebre-Sellassie, 1989; Singh et al., 1995; Vervaet et al., 1995). The polymer binders used in the drug solution or suspension are generally evaluated for interactions with the drug (Türk et al., 2009; Bonferoni et al., 2000).

Incompatibilities aside, coatings have not been widely studied for their influence on the drug layer underneath, although migration of drugs into the coating layer has been described (Heinicke and

Schwartz, 2007; Wouessidjewe, 1997) and their chemical properties can significantly influence drug release (Sadeghi et al., 2003).

In our study we would like to show that when the solid phase behavior of the drug is a factor, coatings must be taken into account. We have formulated a coated multilayer pellet containing the model drug diltiazem hydrochloride in a fluid bed chamber as described in Sovány et al. (2009) and conducted examinations to reveal the possible interactions between the drug and the excipients. We offer and examine the hypothesis that even if no chemical interaction occurs between the drug layer and the coating, in the case of water-soluble drugs changes in crystallinity can be expected due to migration.

2. Materials

Diltiazem hydrochloride (Ph. Eur., a gift from EGIS Ltd., Budapest, Hungary) was used as a model drug, Cellet 500 (Shin-Etsu Chemical Co., Ltd., Tokyo, Japan, granted as a gift from Harke Pharma) as nonpareil core material, Kollidon 25 (donated by BASF, Ludwigshafen, Germany) and Pharmacoat 606 (BASF, Ludwigshafen, Germany) was applied as a binder in the layering of diltiazem hydrochloride, and Acryl-EZE (kindly granted by Colorcon, Dartford Kent, UK), a fully formulated enteric coating dispersion, was used as coating material.

3. Methods

3.1. Preparation of samples – layering of diltiazem hydrochloride

The multiparticulate pellet samples were prepared in a Strea-1 (Niro Aeromatic, Bubendorf, Switzerland) fluid bed chamber.

* Corresponding author. Tel.: +36 62 545 574; fax: +36 62 545 571.

E-mail address: geza.regdon@pharm.u-szeged.hu (G. Regdon Jr.).

In the first, drug-loading step, diltiazem hydrochloride was layered onto nonpareil Cellet 500 cores. A solution of diltiazem hydrochloride and Kollidon 25 or Pharmacoat 606 in a mass ratio of 5:3 and 5:2 respectively was used, as the solution containing only diltiazem hydrochloride did not yield satisfactory loading results on previous occasions. A batch size of 200 g of nonpareils and the above-mentioned solution containing 125 g of API was used. The loading parameters were: inlet temperature 50 °C, outlet temperature 43 °C, fan capacity 4.5, peristaltic pump speed 4 ml/min, air volume 75 m³/h, blow-out pressure 4.4 bar, atomizing pressure 2 bar and nozzle diameter 1 mm.

Between the drug-loading and the following coating the pellets were dried in the spray coater for 10 min. Since the Acryl-EZE contains sodium bicarbonate as an excipient, the equipment had to be completely disassembled and washed to prevent precipitate formation.

At this point samples of the drug-loaded nonpareils were taken for comparison purposes; these are called Samples 1a and 1b from here on.

3.2. Preparation of samples – coating

In the second, coating step, a 20% aqueous dispersion of Acryl-EZE (a fully formulated USP copolymer type C coating system containing 60% polymer and various excipients) was prepared and applied as per the guidelines of the manufacturer. 0.1% of dimeticon was added to prevent foaming during the stirring and coating process. The parameters of the coating were the same as for the drug layering step. Calculated from the amount of coating dispersion, the amount of dry material consumed for 200 g of drug-loaded particles was 60 g and 120 g with an about 8% loss in all cases. The coated pellets will be called Samples 2 and 3 in order of increasing film thickness from here on (Table 1).

Samples were prepared later to outrule interactions. These are labeled Samples A–C and were prepared with the methods described above with one or more of the materials left out as indicated in Table 1.

3.3. Differential scanning calorimetry

Differential Scanning Calorimetry (DSC) was performed with a Mettler–Toledo DSC 821e (Mettler–Toledo GmbH, Switzerland) instrument. DSC curves were evaluated with STARE Software. The starting and final temperatures were 0 °C and 400 °C and heating rate was 10 °C/min. Argon atmosphere was used in all cases. Three parallel examinations were done from all samples. The instrument was calibrated using indium. Samples were measured in a 40 µl aluminium pan.

Table 1
Samples produced.

Sample	API (125.0 g)	Kollidon 25 (75.0 g)	Pharmacoat 606 (50.0 g)	Acryl-EZE (g)
1a	✓	✓	–	–
2a	✓	✓	–	60
3a	✓	✓	–	120
1b	✓	–	✓	–
2b	✓	–	✓	60
3b	✓	–	✓	120
A	✓	–	–	75
B	–	✓	–	120
C	–	–	–	120

API and/or Kollidon 25 or Pharmacoat 606 layered from aqueous solution at 50 °C. Acryl-EZE coated from 20% aqueous dispersion at 50 °C.

3.4. Thermogravimetric analysis

Thermogravimetric Analysis (TGA) was carried out with a Mettler–Toledo TGA/DSC1 (Mettler–Toledo GmbH, Switzerland) instrument. Curves were evaluated with STARE Software. The starting and final temperatures were 0 °C and 400 °C and heating rate was 10 °C/min. Sample weight varied between 10 and 12 mg.

3.5. Powder X-ray diffractometry (XRPD)

The X-ray powder diffraction patterns (XRPDs) were obtained with a Bruker D8 Advance (Bruker AXS, Germany) equipped with a Sycos H-Hot (Ansyco GmbH, Karlsruhe, Germany) programmable plate holder. Results were detected with a Vantec-1 detector. The patterns were recorded at a tube voltage of 40 kV, tube current of 40 mA, applying a step size of 0.01 Å 2θ in the angular range of 3–40 Å 2θ.

3.6. Hot-stage microscopy

Thermomicroscopic investigations were carried out with a Nikon Michrophot FXA polarizing microscope (Nikon Corporation, Tokio, Japan) fitted with a Linkam THMSG-600 heating-freezing stage (Linkam Scientific Instruments, Waterfield, UK). Photographs were taken with a digital camera (UBS 2 UI-1640LE-C, IDS Imaging Development Systems GmbH, Obersulm, Germany). Pellets were carefully crushed and intact coating flakes chosen from the grist.

3.7. Fourier-transformed infrared spectroscopy

FT-IR measurements were performed by an Avatar 330 FT-IR spectrometer (Thermo Nicolet/Thermo Fisher Scientific Inc., Ramsay, Minnesota, USA) equipped with a horizontal ATR crystal (ZnSe, 45°). Spectra were recorded between 4000 and 400 cm⁻¹ at 4 cm⁻¹ optical resolution. Spectra were collected in absorbance mode using the KBr disk method (~0.5 mg powdered sample in 150 mg KBr disk). 256 scans were co-added. Spectra were collected with the EZ Omnic software and analyzed with GRAMS AI.

3.8. Dissolution studies

Dissolution studies were carried out according to the Ph. Eur. standards with a rotating basket (Erweka DT 700, Erweka GmbH, Heusenstramm, Germany), in 1000 ml of simulated gastric acid at 100 rpm at 37 °C for 2 h, then the acidic medium was replaced with 1000 ml of phosphate buffer (pH = 6.8) and the dissolution measured at the same parameters as above. Samples were taken of the gastric acid at 2 h and of the phosphate buffer at 5, 10, 15, 20, 30, 45, 60 and 90 min.

Concentration was measured with a spectrophotometer (Unicam Helios α, Thermo Fisher Scientific Inc., Waltham, USA) at 237 nm, with a bandwidth of 2 nm and a lamp charge of 325 nm by comparison to a calibration curve.

The drug content of the pulverised pellets was determined in phosphate buffer after 2 h at the same parameters as for the dissolution test. Results were analyzed with Microsoft Excel 2007.

4. Results

4.1. Differential scanning calorimetry

The DSC curves of the materials are presented in Fig. 1. The results are consistent with literary data (Zhang et al., 2008; Reverchon et al., 2008; Hekmatara et al., 2006). The endothermic peak signaling the melting of diltiazem HCl can be seen at

214 °C; the second, broad endothermic peak on the curve can be attributed to API degradation. Kollidon 25 and Pharmacoat 606 both exhibit a broad endothermic peak that indicates water loss. No glass transition temperature could be determined for the polymers (Zidan et al., 2012). The T_g of Acryl-EZE is clearly visible, but no other characteristic peaks appear on the curve.

As shown in Fig. 2, an exothermic peak appeared at about 100 °C on the DSC curves of the coated pellets. The T_g of Acryl-EZE did not shift significantly and no other T_g or peak was observed on the curves before the API melting point. The exothermic peaks were always followed by the endothermic peak characterizing the melting of diltiazem HCl.

An amorphous sample of diltiazem HCl was prepared by melting and rapid cooling to measure the T_g . The DSC curve in Fig. 3

exhibits this at 100 °C. Also in Fig. 3 is the curve obtained from a repeated heating of Sample 3a. The exothermic peak appears only during the first heating cycle.

Fig. 4 shows that a similar peak appeared at about 180 °C or directly before the melting point on the curves of the uncoated API-layered pellets depending on the binder used in the sample. No other composition results in exothermic peaks in the curve.

4.2. Thermogravimetric analysis

Fig. 5 shows that no significant weight loss occurs in the thermal range of the exothermic peaks. Significant weight loss starts approximately at the melting point of diltiazem HCl.

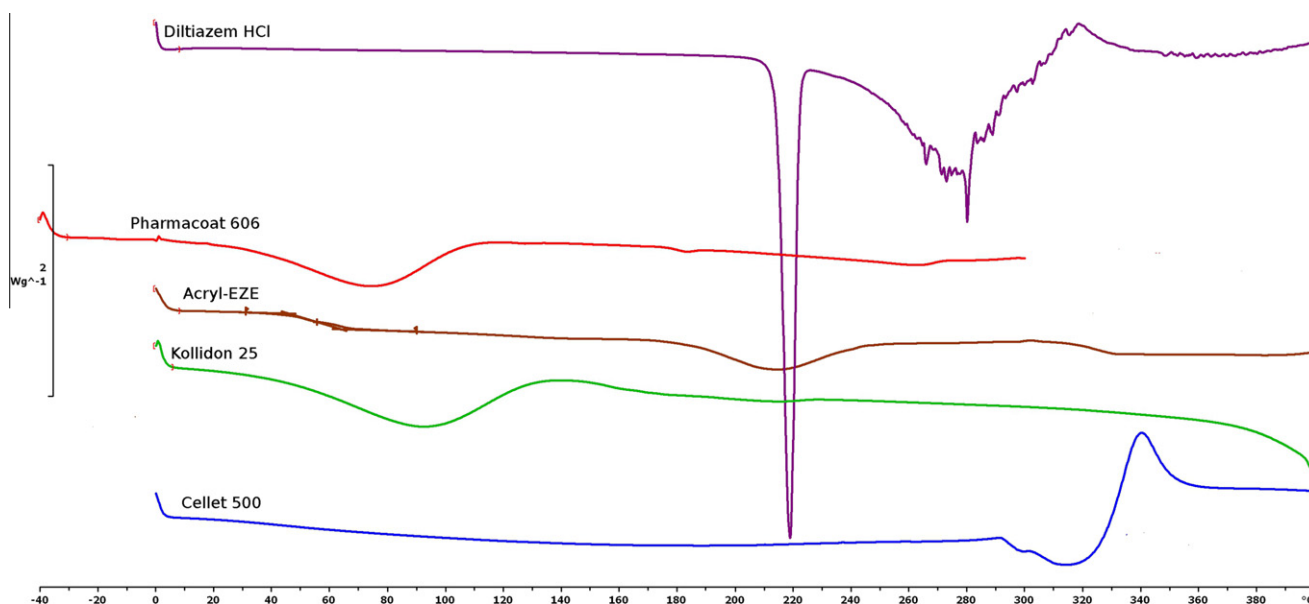


Fig. 1. DSC curves of the base materials.

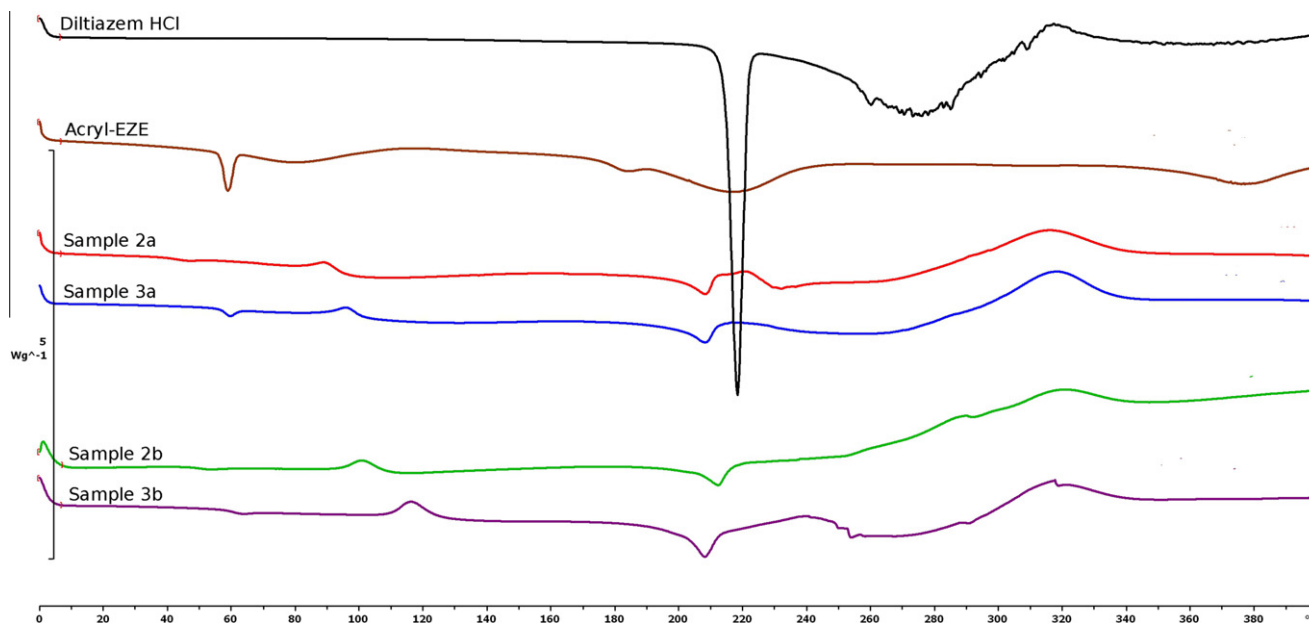


Fig. 2. DSC curves of Samples 2a–3a and 2b–3b.

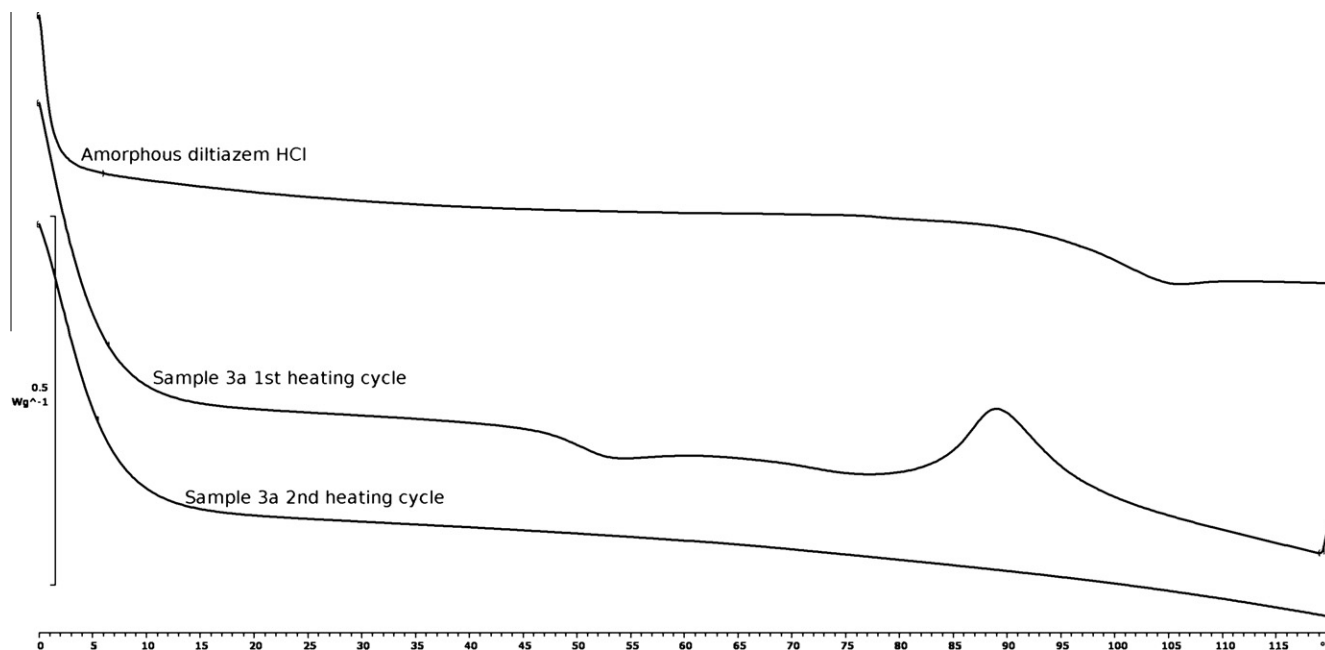


Fig. 3. Thermal behavior of amorphous API.

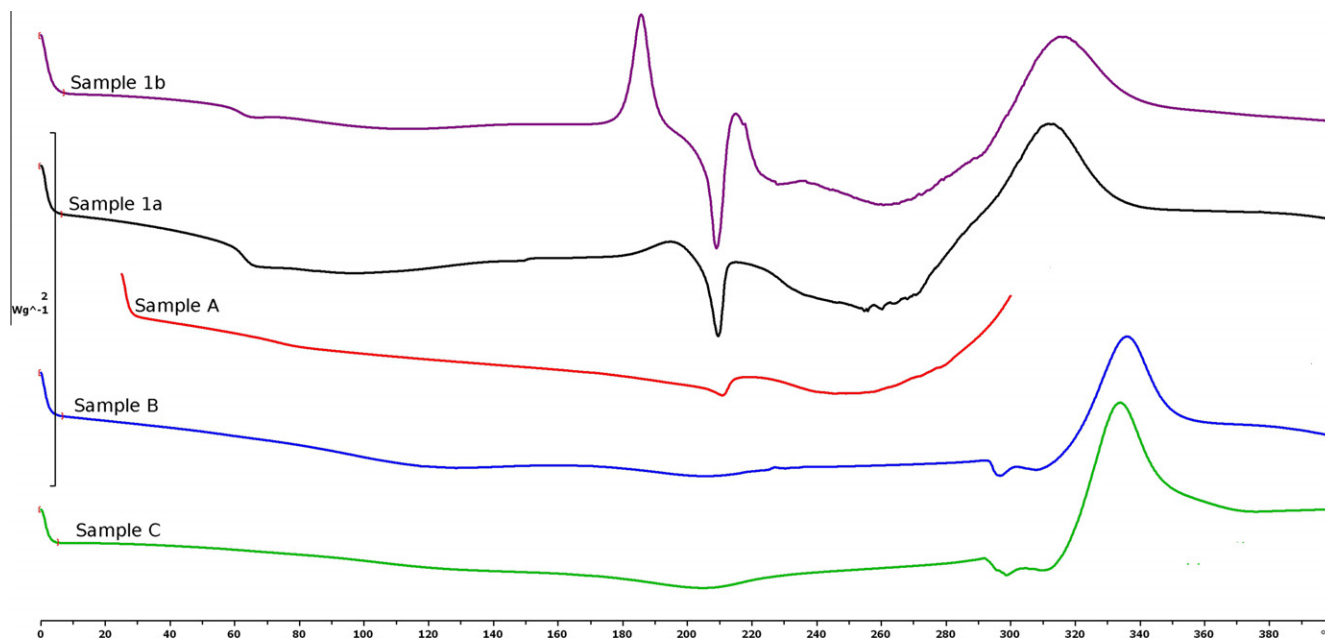


Fig. 4. Thermal analysis of the exothermic peak.

4.3. Powder X-ray diffractometry (XRPD)

As shown in Fig. 6 the XRPD spectrum of diltiazem HCl contains several peaks of different sizes; the larger ones can be detected in the spectrum of Sample 1 at 4.125° , 8.328° , 9.907° , 10.547° , 18.070° , 19.442° , 21.661° and 27.575° 2θ . Cellet 500, Kollidon 25 and Pharmacoat 606 do not produce sharp peaks but appear as broad backgrounds which do not hinder the identification of the sharp peaks from other materials. Acryl-EZE has two sharp peaks in the spectrum; these were identified as talc, listed as an ingredient by the manufacturer.

The XRPD spectra were detected at room temperature at baseline and heated to 120°C and 200°C as they are slightly above the range of the exothermic peaks observed in Figs. 2 and 4. The

results are presented in Figs. 7 and 8. The spectrum of the coated samples contains a sharp peak at 25.648° 2θ , which was identified as titanium dioxide (Parker, 1924), an ingredient of the Acryl-EZE coating system. All coated and the Kollidon-containing uncoated samples contain crystalline API at baseline. In all cases diltiazem peaks have become larger (in some cases, appear) after the heat treatment. Also, in the case of the coated samples almost all of the diltiazem peaks are visible in the spectrum of the heat-treated sample, whereas only the peaks at 9.907° , 10.547° , 15.897° , 18.070° , 19.442° and 21.661° 2θ were prominently present before. In the case of the uncoated samples API peaks only appeared/grew after the 200°C heat treatment. Comparing 120°C and 200°C heat treated (coated) sample spectra, a decrease in API peak heights can be observed.

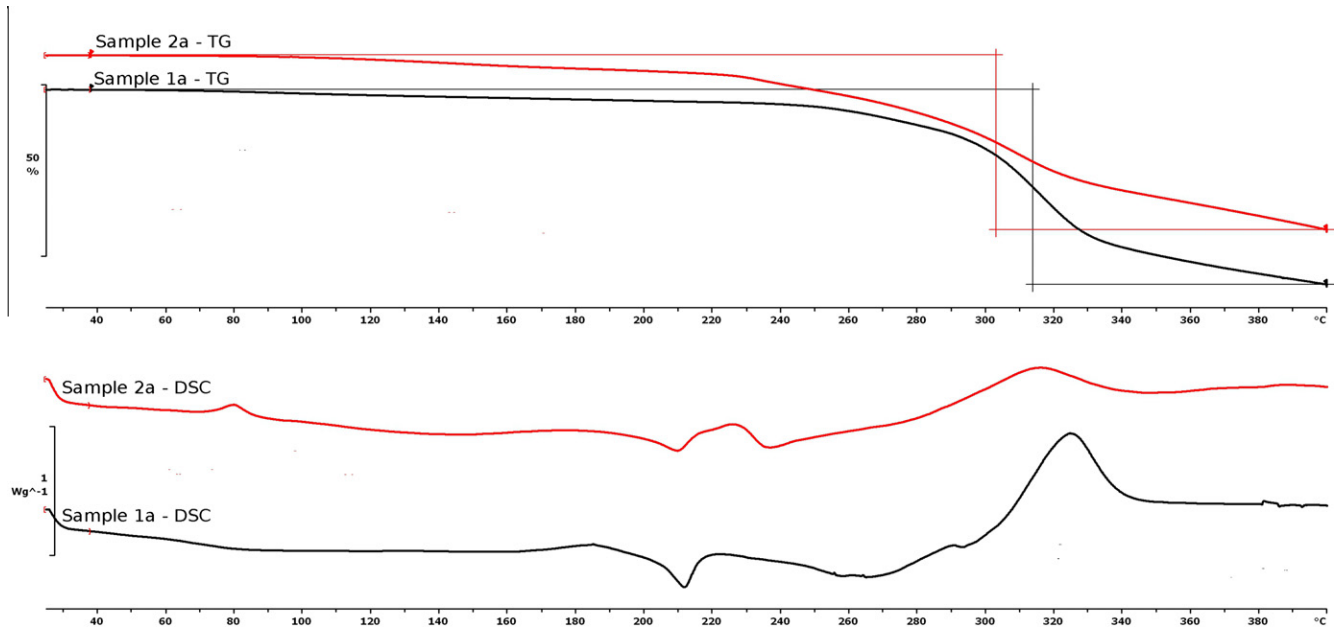


Fig. 5. DSC and TG curves of Samples 1a and 2a.

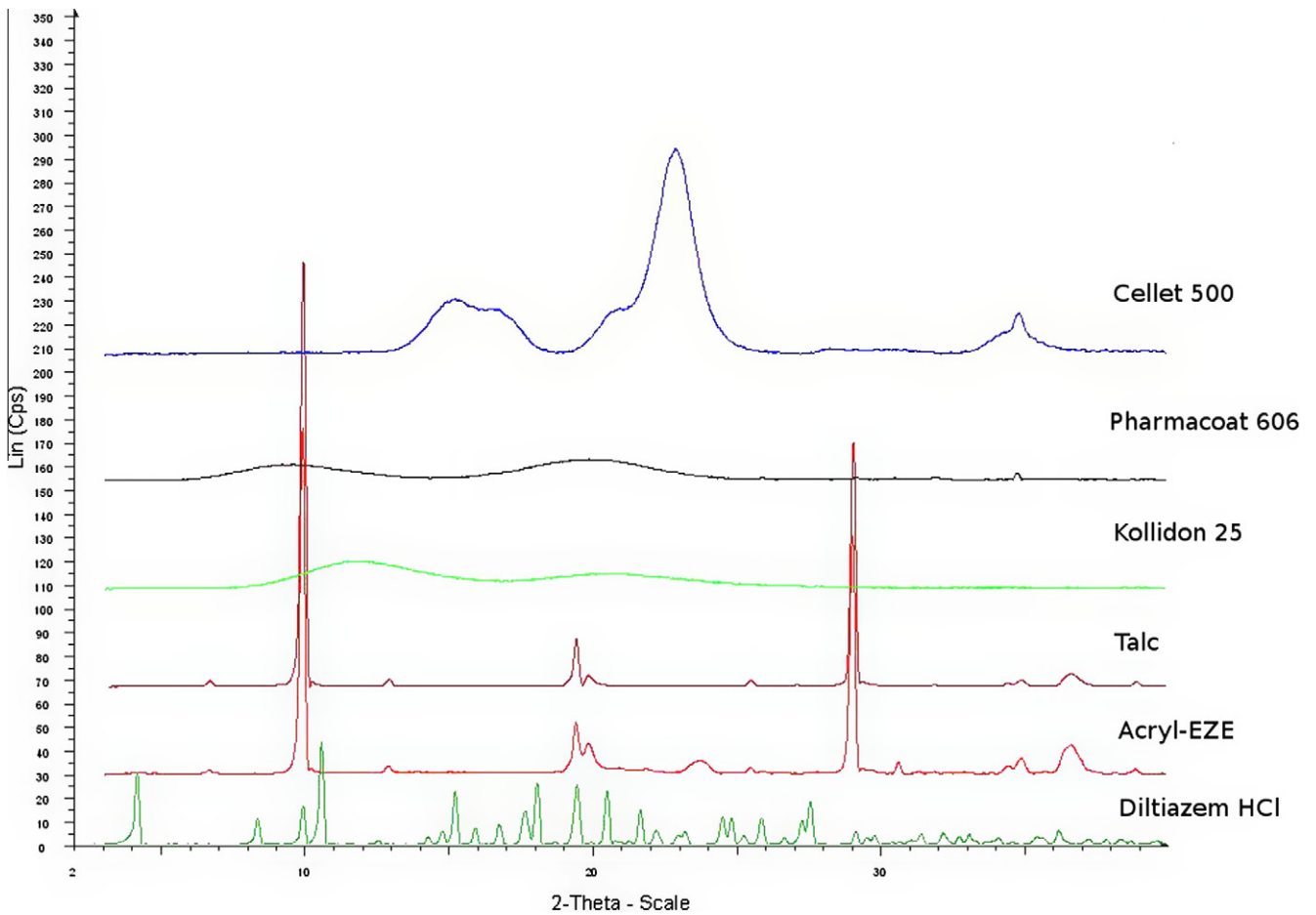


Fig. 6. X-ray spectra of the materials.

4.4. Hot-stage microscopy

Fig. 9, the polarized light microphotograph of a piece of coating taken using crossed Nicols shows that the polymeric film layer

contains some dispersed crystalline material even before the heat treatment (left side). After the heat treatment (right side) the amount of birefringent particles in the coating increased significantly.

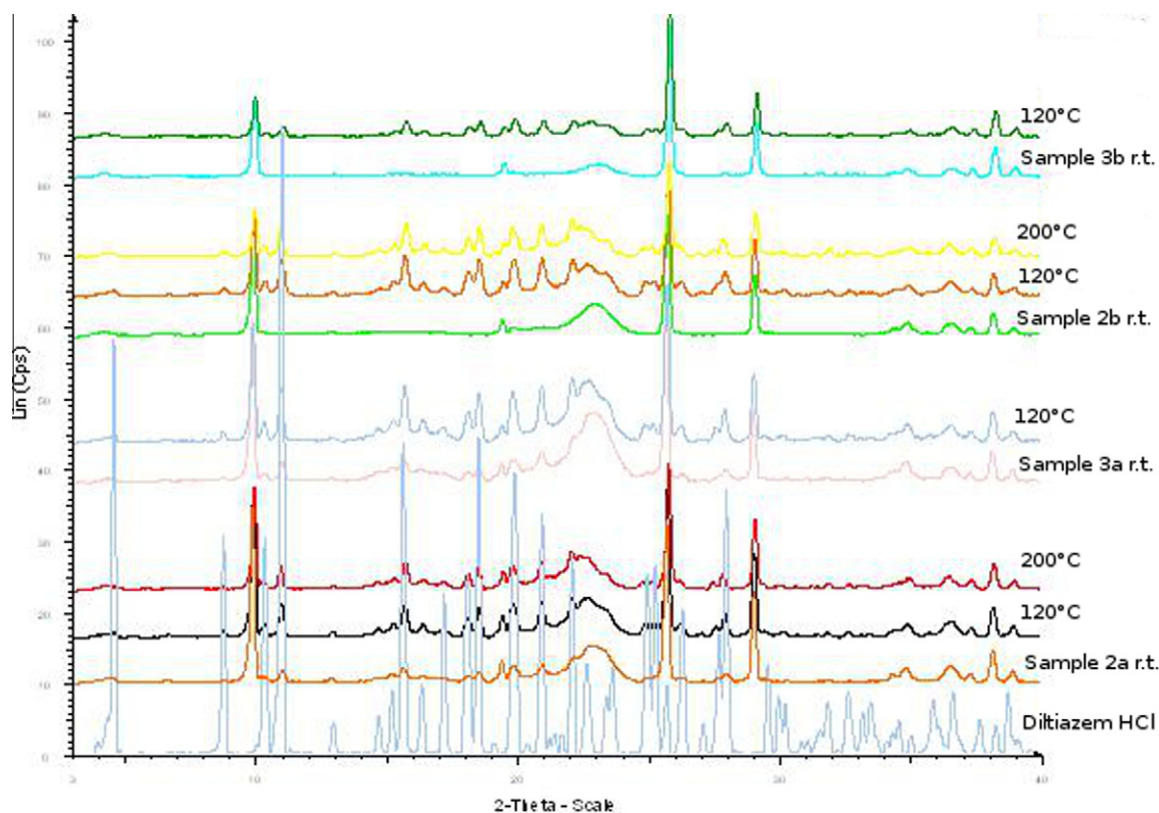


Fig. 7. X-ray spectra of the coated samples before and after heat treatment.

4.5. Fourier-transformed infrared spectroscopy

The FT-IR spectra of a coated sample before and after heat treatment in the DSC equipment is shown in Fig. 10. Both the samples and the physical mixture of binder and API contain a water peak at 3450 cm^{-1} , although the heat treatment appears to have significantly reduced the water content of the sample. Compared to the spectrum of the physical mixture several peaks in the un-treated sample are less prominent (if there at all) and wider, less sharp. Despite this no shifts in peak positions can be observed indicating that no chemical bonds were formed between API and polymers. The spectrum of the heat treated sample appears to be fundamentally the same as the physical mixture spectrum with slight differences that can be attributed to the presence of other excipients. FT-IR spectra of Sample set b have yielded similar results.

4.6. Dissolution studies

The dissolution of the coated samples before and after heat treatment in the DSC equipment is shown in Fig. 11. While the gastroresistance of Samples 2a and 3b improved significantly the change observed in the case of Sample 3a is well beneath the SD value. Sample 2b's coating level proved to be insufficient for significant gastroresistance and thus its dissolution tests were discontinued.

5. Discussion

In Fig. 2 an exothermic peak appeared at about $100\text{ }^{\circ}\text{C}$ on the DSC curves of the coated pellets. The peak only occurred in samples containing both diltiazem hydrochloride and the Acryl-EZE coating (see Fig. 4), suggesting that it is a result of an interaction between these two materials. According to the manual Acryl-EZE contains

sodium bicarbonate, which, unlike the polymers used in the study, has a known interaction with diltiazem hydrochloride (Pillay and Fassihi, 1999): in aqueous media the diltiazem base precipitates. The melting point of diltiazem base is in the same thermal range as the exothermic peak, however, no signs of melting appear on the curves and even though the interaction is known to exist, an undetectable amount of sodium bicarbonate is not likely to produce detectable amounts of diltiazem base in the first place.

The nature of the preparation procedure indicates that a solid dispersion can be formed during API layering that, depending on the composition and parameters, can contain the API in amorphous and/or crystalline form (Zhang et al., 2008). The X-ray analysis confirmed that the transformation causing the exothermic peak at $\sim 100\text{ }^{\circ}\text{C}$ is caused by the recrystallization of the API. In the uncoated samples the amorphous API only recrystallizes upon or close to melting (see Figs. 4 and 8).

Fig. 9 shows that the API migrated into the coating layer and remained in amorphous clusters that later crystallize if subjected to heat treatment. The probable explanation for this is that diltiazem HCl as a highly water-soluble drug dissolved into the droplets of the coating suspension during the coating. The plasticization mechanism described by Mizuno et al. can also play a role in the process (Mizuno et al., 2005). Binder polymers might also play a part in the phenomenon by forming solid dispersions with the API upon layering, from which the amorphous API dissolves more readily than from a fully crystalline API layer (Konno et al., 2008; Van den Mooter et al., 2001; Sun et al., 2008; Zhang et al., 2008). This hypothesis is supported in Fig. 3, as no exothermic peak appears on the DSC curves of the sample prepared without a binder. The migration from the drug layer to the coating probably occurs mostly before a thin uniform coating layer forms on the drug-loaded cores (Mizuno et al., 2005).

Considering the fact that the migration thus affects only a small fraction of the API and the drug layer already contains an

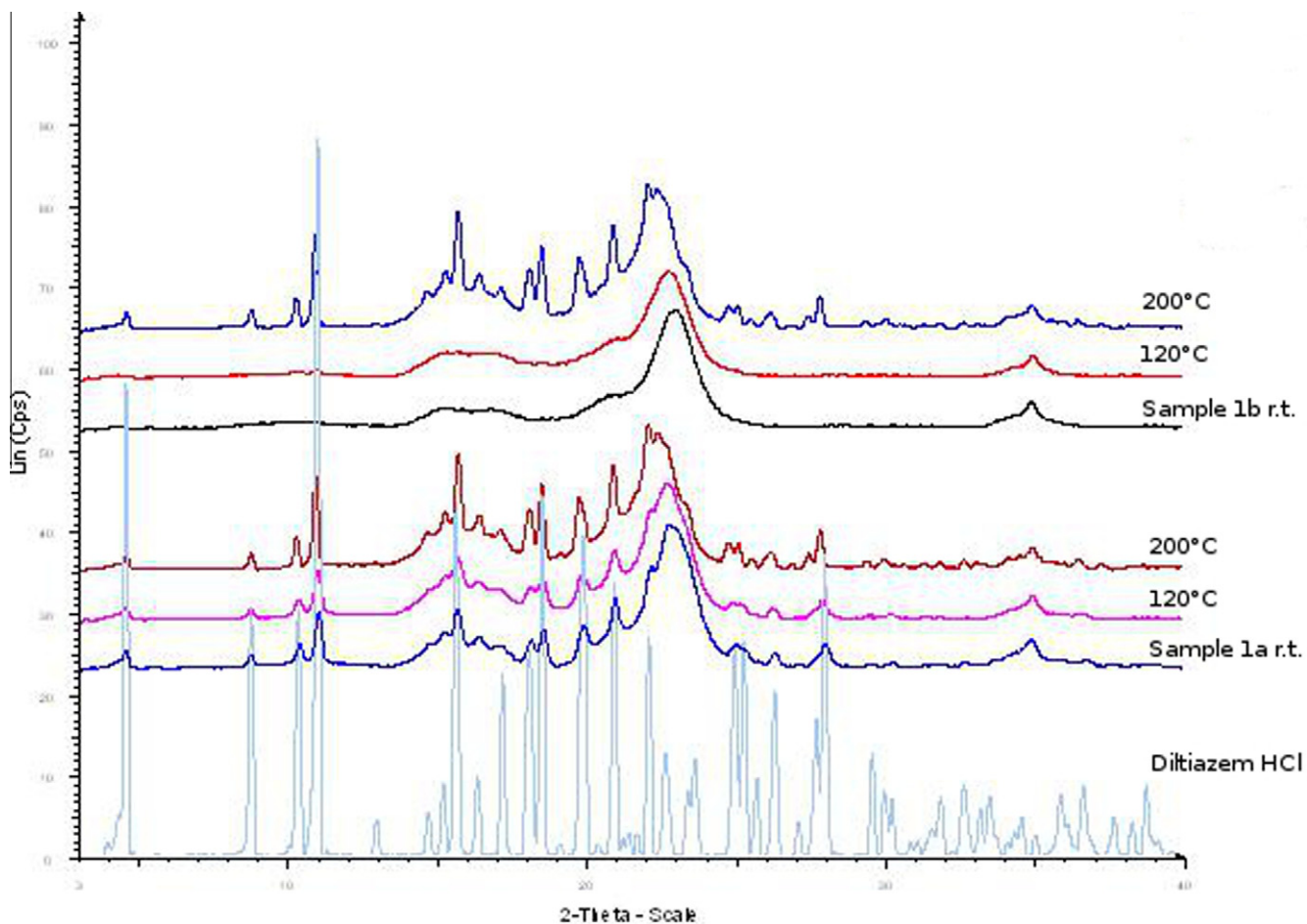


Fig. 8. X-ray spectra of the uncoated samples before and after heat treatment.

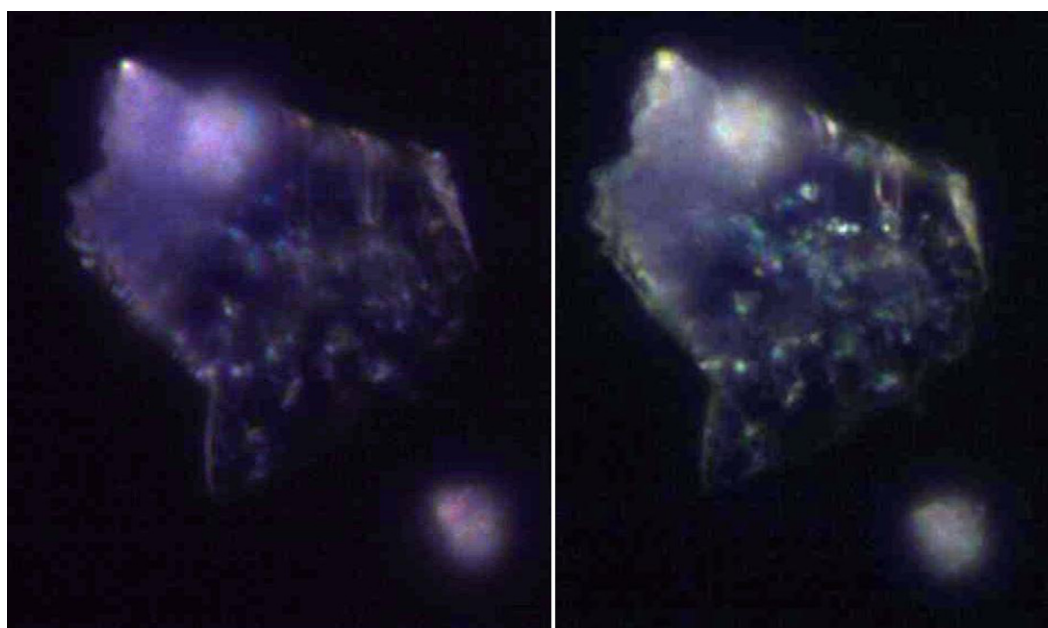


Fig. 9. Polarized light microphotograph of the coating before and after heat treatment.

amorphous fraction, migration does not explain the different recrystallization behavior of the coated and uncoated samples. As

FTIR spectra show no evidence of chemical bonds between polymer and the API in either case only physical inhibition prevents

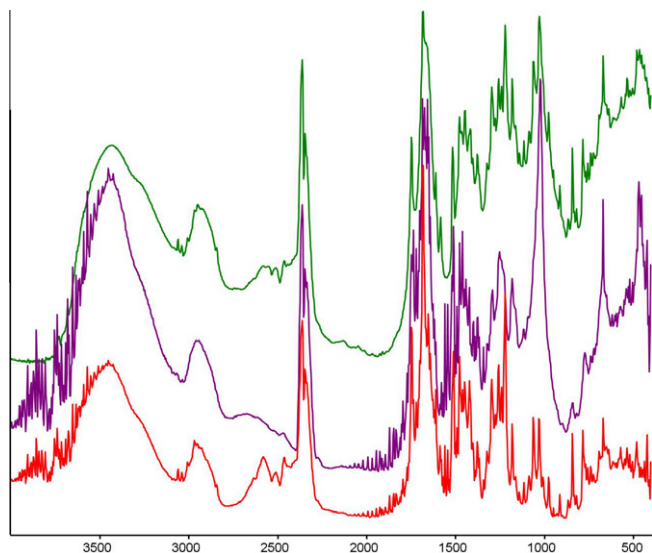


Fig. 10. FT-IR spectrum of Sample 2a after heat treatment, Sample 2a and physical mixture of diltiazem HCl + Kollidon 25 (from top to bottom).

the drug from completely crystallizing during sample preparation and storage (Van den Mooter et al., 2001). In such cases the main reason for recrystallization is the glassy to rubbery state transition of the polymer and the increased molecular mobility of the API (Konno et al., 2008; Van den Mooter et al., 2001). It is known that the physical stability of a drug depends greatly on the preparation method and the polymer carrier (Crowley and Zografi, 2002; Van Eerdenbrugh and Taylor, 2010; Bley et al., 2010). In our case the methods of preparation were the same for all samples but the amorphous API is located partly in the coating layer and partly in the drug layer, which means that if no other underlying mechanism exists, we should observe two phases in the recrystallization: one for the drug layer and one for the coating (or only one if they overlap). However only one was observed and at significantly lower temperatures than in the uncoated samples.

According to our results this phenomenon must be explained by the presence of the coating. The DSC curves of the uncoated

samples in Fig. 5 show a broad endothermic peak that literature attributes to the loss of water in PVP and HPMC, respectively. This peak is not present in the coated samples indicating a quasi-water-tight property of the coating on the timescale of the DSC analysis. The exothermic peak attributed to API recrystallization coincides with the boiling point of water which raises the question: does water play a role in the recrystallization (Wu et al., 2012)?

Several well-described phenomena can be used to explain the possible influence of water on the recrystallization behavior of our coated samples (Baird and Taylor, 2012; Malaj et al., 2010). Many studies proved that water acts as a plasticizer in polymer drug delivery systems; as a plasticizer it can decrease the T_g of the polymer to the observed range – which it cannot do for the uncoated samples as the unhindered evaporation reduces its amount by the time the sample reaches the temperature range in question (Pirayavaraporn et al., 2012). Water can also be contained in the microcrystalline cellulose core. As a highly water-soluble drug, diltiazem hydrochloride can dissolve in the water migrating toward the surface of the pellet from the core and crystallize from the solution. As water boils in the thermal range of the recrystallization peak, the pressure of steam in the pores of the pellet is expected to grow rapidly at the time. Since water also acts as a plasticizer, pores can be expanded essentially removing the physical barrier that stood in the way of recrystallization. The process is well-known and routinely used in the food industry but a similar effect achieved during the use of supercritical or pressurized carbon dioxide in the pharmaceutical industry has been described (Varnalis et al., 2001; Norton et al., 2011; Verreck et al., 2005, 2006, 2007).

These mechanisms can and probably do work independently at the same time. To determine the most important among them and explore its implications regarding the stability of the system, many difficulties will have to be overcome. A method should be devised to measure the position of water and pore size inside the pellet without removing the coating. Studies on stability should take into consideration that the generally used high relative humidity will probably cause an unrelated recrystallization phenomenon by plasticizing the polymer that would not happen at ambient conditions (Malaj et al., 2010).

Similar problems arise when trying to determine the significance of recrystallization on the dissolution behavior of the pellets.

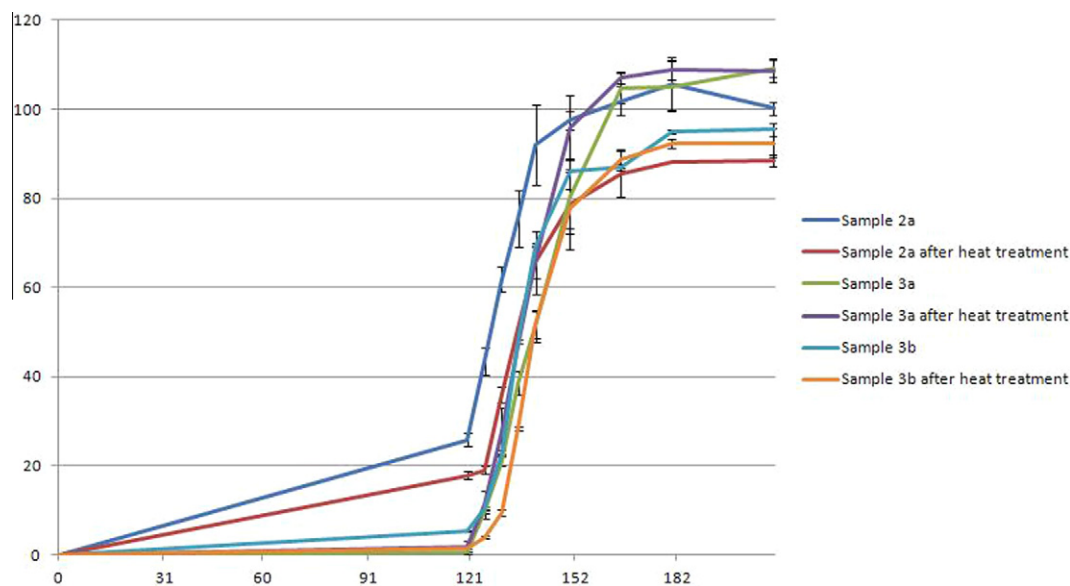


Fig. 11. Dissolution of coated samples before and after heat treatment.

As recrystallization involves heat treatment, it is logical to assume that a curing of the coating also takes place which (while further limiting water evaporation from the sample) would affect the outcome of a later dissolution test (Pirayavaraporn et al., 2012; Muschert et al., 2009). Also if the expansion of the pores described above is significant enough to expand the pellet, the coating polymer would either rupture or, which is more probable given that it transforms into the rubbery state at the temperature involved, would stretch and transform back into the glassy state upon cooling. Both of these mechanisms would result in worsening gastroresistance, unlike the curing effect which has been described to improve results significantly (Muschert et al., 2009; Gendre et al., 2012). The extent of the API migration and the film thickness would probably also influence the results. The preliminary dissolution tests presented in this article suggest that no rupturing occurred in the samples and in some cases the sum of the effects described above could significantly improve gastroresistance.

6. Conclusion

DSC analysis of the coated pellets showed an exothermic peak that is not characteristic of any of the materials used. Further examination revealed that this is due to the recrystallization of amorphous diltiazem HCl present in the film coating. This confirms our hypothesis that water-soluble drugs are subject to significant migration when coated with aqueous systems and thus the polymers used for coating must be taken into account when determining the crystallinity of the API.

Acknowledgements

This work was supported by a grant from “Stiftung Aktion Österreich-Ungarn” and by TÁMOP-4.2.2/B-10/1-2010-0012 (Hungary). The authors acknowledge Professor Ulrich J. Griesser with whom many of the experiments presented here were originally performed. The authors would also like to thank Felix Schubert for his invaluable help in the making of Fig. 9.

References

- Baird, J.A., Taylor, L.S., 2012. Evaluation of amorphous solid dispersion properties using thermal analysis techniques. *Adv. Drug Deliver. Rev.* 64, 396–421.
- Bley, H., Fussnegger, B., Bodmeier, R., 2010. Characterization and stability of solid dispersions based on PEG/polymer blends. *Int. J. Pharm.* 390, 165–173.
- Bonferoni, M.C., Rossi, S., Ferrari, F., Bettinetti, G.P., Caramella, C., 2000. Characterization of a diltiazem-lambda b carrageenan complex. *Int. J. Pharm.* 200, 207–216.
- Crowley, K.J., Zografi, G., 2002. Cryogenic grinding of indomethacin polymorphs and solvates: assessment of amorphous phase formation and amorphous phase physical stability. *J. Pharm. Sci.* 91, 492–507.
- Gendre, C., Genty, M., da Silva, J.C., Tfayli, A., Boiret, M., Lecoq, O., Baron, M., Chaminade, P., Péan, J.M., 2012. Comprehensive study of dynamic curing effect on tablet coating structure. *Eur. J. Pharm. Biopharm.* 81, 657–665.
- Ghebre-Sellassie, I., 1989. Pellets: a general overview. In: Ghebre-Sellassie, I. (Ed.), *Pharmaceutical Pelletization Technology*. Marcel Dekker Inc., New York, Basel, pp. 1–14.
- Heinicke, G., Schwartz, J.B., 2007. The influence of surfactants and additives on drug release from a cationic Eudragit coated multiparticulate diltiazem formulation. *Pharm. Dev. Technol.* 12, 381–389.
- Hekmatara, T., Regdon Jr., G., Sipos, P., Erős, I., Pintye-Hódi, K., 2006. Thermoanalytical study of microspheres containing diltiazem hydrochloride. *J. Therm. Anal. Calorim.* 86, 287–290.
- Konno, H., Handa, T., Alonzo, D.E., Taylor, L.S., 2008. Effect of polymer type on the dissolution profile of amorphous solid dispersions containing felodipine. *Eur. J. Pharm. Biopharm.* 70, 493–499.
- Leuner, C., Dressman, J., 2000. Improving drug solubility for oral delivery using solid dispersions. *Eur. J. Pharm. Biopharm.* 50, 47–60.
- Malaj, L., Censi, R., Mozzicafreddo, M., Pellegrino, L., Angeletti, M., Gobetto, R., Di Martino, P., 2010. Influence of relative humidity on the interaction between different aryl propionic acid derivatives and poly(vinylpyrrolidone) K30: evaluation of the effect on drug bioavailability. *Int. J. Pharm.* 398, 61–72.
- Mizuno, M., Hirakura, Y., Yamane, I., Miyaniishi, H., Yokota, S., Hattori, M., Kajiyama, A., 2005. Inhibition of a solid phase reaction among excipients that accelerates drug release from a solid dispersion with aging. *Int. J. Pharm.* 305, 37–51.
- Muschert, S., Siepmann, F., Cuppok, Y., Leclercq, B., Carlin, B., Siepmann, J., 2009. Improved long term stability of aqueous ethylcellulose film coatings: importance of the type of drug and starter core. *Int. J. Pharm.* 368, 138–145.
- Nastruzzi, C., Cortesi, R., Esposito, E., Genovesi, A., Spadoni, A., Vecchia, C., Menegatti, E., 2000. Influence of formulation and process parameters on pellet production by powder layering technique. *AAPS Pharm. Sci. Technol.* 1, 14–25.
- Norton, A.D., Greenwood, R.W., Noble, I., Cox, P.W., 2011. Hot air expansion of potato starch pellets with different water contents and salt concentrations. *J. Food Eng.* 105, 119–127.
- Parker, R.L., 1924. Zur Kristallstruktur von Anastas und Rutil. (II. Teil. Die Anastasstruktur). *Zeitschrift fuer Kristallographie, Kristallgeometrie, Kristallphysik, Kristallchemie* 59, 1–54.
- Pillay, V., Fassihi, R., 1999. Electrolyte-induced compositional heterogeneity: a novel approach for rate-controlled oral drug delivery. *J. Pharm. Sci.* 88, 1140–1148.
- Pirayavaraporn, C., Rades, T., Tucker, I.G., 2012. Determination of moisture content in relation to thermal behaviour and plasticization of Eudragit RLPO. *Int. J. Pharm.* 422, 68–74.
- Reverchon, E., Lamberti, G., Antonacci, A., 2008. Supercritical fluid assisted production of HPMC composite microparticles. *J. Supercrit. Fluids* 46, 185–196.
- Sadeghi, F., Ford, J.L., Rajabi-Siahboomi, A., 2003. The influence of drug type on the release profiles from Surelease-coated pellets. *Int. J. Pharm.* 254, 123–135.
- Serajuddin, A.T., 1999. Solid dispersion of poorly water-soluble drugs: early promises, subsequent problems, and recent breakthroughs. *J. Pharm. Sci.* 88, 1058–1066.
- Sethia, S., Squillant, E., 2004. Solid dispersion of carbamazepine in PVP K30 by conventional solvent evaporation and supercritical methods. *Int. J. Pharm.* 272, 1–10.
- Sinchaipanid, N., Chitropas, P., Mitrevej, A., 2004. Influences of layering on theophylline pellet characteristics. *Pharm. Dev. Technol.* 9, 163–170.
- Singh, S.K., Dodge, J., Durrani, M.J., Khan, M.A., 1995. Optimization and characterization of controlled release pellets coated with an experimental latex: I. Anionic drug. *Int. J. Pharm.* 125, 243–255.
- Sovány, T., Nikowitz, K., Regdon Jr., G., Kása Jr., P., Pintye-Hódi, K., 2009. Raman spectroscopic investigation of film thickness. *Polym. Test.* 28, 770–772.
- Sun, N., Wei, X., Wu, B., Chen, J., Lu, Y., Wu, W., 2008. Enhanced dissolution of silymarin/polyvinylpyrrolidone solid dispersion pellets prepared by a one-step fluid-bed coating technique. *Powder Technol.* 182, 72–80.
- Türk, C.T., Haşçıçek, C., Gönül, N., 2009. Evaluation of drug-polymer interaction in polymeric microspheres containing diltiazem hydrochloride. *J. Therm. Anal. Cal.* 95, 865–869.
- Van den Mooter, G., Wuyts, M., Bleton, N., Busson, R., Grobet, P., Augustijns, P., Kinget, R., 2001. Physical stabilisation of amorphous ketoconazole in solid dispersions with polyvinylpyrrolidone K25. *Eur. J. Pharm. Sci.* 12, 261–269.
- Van Erdenbrugh, B., Taylor, L.S., 2010. Small scale screening to determine the ability of different polymers to inhibit drug crystallization upon rapid solvent evaporation. *Mol. Pharm.* 7, 1328–1337.
- Varnalis, A.I., Brennan, J.G., MacDougall, D.B., 2001. A proposed mechanism of high-temperature puffing of potato. Part I: The influence of blanching and drying conditions on the volume of puffed cubes. *J. Food Eng.* 48, 361–367.
- Verreck, G., Decorte, A., Heymans, K., Adriaensen, J., Cleeren, D., Jacobs, A., Liu, D., Tomasko, D., Arien, A., Peeters, J., Rombaut, P., Van den Mooter, G., Brewster, M.E., 2005. The effect of pressurized carbon dioxide as a temporary plasticizer and foaming agent on the hot stage extrusion process and extrudate properties of solid dispersions of itraconazole with PVP-VA 64. *Eur. J. Pharm. Sci.* 26, 349–358.
- Verreck, G., Decorte, A., Li, H., Tomasko, D., Arien, A., Peeters, J., Rombaut, P., Van den Mooter, G., Brewster, M.E., 2006. The effect of pressurized carbon dioxide as a plasticizer and foaming agent on the hot melt extrusion process and extrudate properties of pharmaceutical polymers. *J. Supercrit. Fluid.* 38, 383–391.
- Verreck, G., Decorte, A., Heymans, K., Adriaensen, J., Liu, D., Tomasko, D.L., Arien, A., Peeters, J., Rombaut, P., Van den Mooter, G., Brewster, M.E., 2007. The effect of supercritical CO₂ as a reversible plasticizer and foaming agent on the hot stage extrusion of itraconazole with EC 20 cps. *J. Supercrit. Fluids* 40, 153–162.
- Vervaeke, C., Baert, L., Remon, J.P., 1995. Extrusion-spheronisation: a literature review. *Int. J. Pharm.* 116, 131–146.
- Wouessidjewe, D., 1997. Aqueous polymethacrylate dispersions as coating materials for sustained and enteric release systems. *STP Pharm.* 7, 469–475.
- Wu, J.X., Xia, D., van den Berg, F., Amigo, J.M., Rades, T., Yang, M., Rantanen, J., 2012. A novel image analysis methodology for online monitoring of nucleation and crystal growth during solid state phase transformations. *Int. J. Pharm.* 433, 60–70.
- Zhang, X., Sun, N., Wu, B., Lu, Y., Guan, T., Wu, W., 2008. Physical characterization of lansoprazole/PVP solid dispersion prepared by fluid-bed coating technique. *Powder Technol.* 182, 480–485.
- Zhu, L., Jona, J., Nagapudi, K., Wu, T., 2010. Fast surface crystallization of amorphous griseofulvin below T_g. *Pharm. Res.* 27, 1558–1567.
- Zidan, A.S., Rahman, Z., Sayeed, V., Raw, A., Yu, L., Khan, M.A., 2012. Crystallinity evaluation of tacrolimus solid dispersions by chemometric analysis. *Int. J. Pharm.* 423, 341–350.

III

Rétegzéses technológia elve és alkalmazási lehetősége multipartikuláris rendszerekben

Nikowitz Krisztina, Hódi Klára, ifj. Regdon Géza

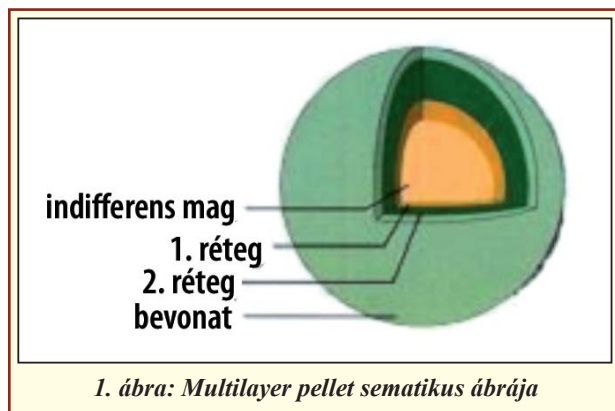
Bevezetés

A módosított hatóanyag-leadású készítmények térnyerésével számtalan új gyógyszerforma alakult és alakul ki. A jelenség nagy győztese az úgynevezett multipartikuláris rendszerek, amelyek (a hagyományos gyógyszerformákkal szemben) sok kisebb, egyedi hordozóegységben tartalmazzák a hatóanyagot. Legelterjedtebb formájuk a kapszulába töltött pelletek, de tablettává préselve is forgalomba kerülnek [1].

A pelletek többnyire egyenletes felületű, ennek következtében jó folyási tulajdonságokkal rendelkező, tömött szerkezetű, közel gömb alakú granulátumok. A hagyományos gyógyszerformákkal szemben előnyük a sokoldalú alkalmazhatóság, a megnövekedett abszorpció és a csökkent irritáció, a nem kívánt hatóanyag-felszabadulás kockázatának csökkenése, valamint az inkompatibilitások elkerülése [1-11].

A pelletek előállításának lehetséges módja a felépítési technológia (pl. rotofluid granulálás), valamint az extrudálás-szferonizálás. Mindkét esetben lehetséges további rétegek felvitele a pelletre az ún. rétegzéses eljárással [11-13].

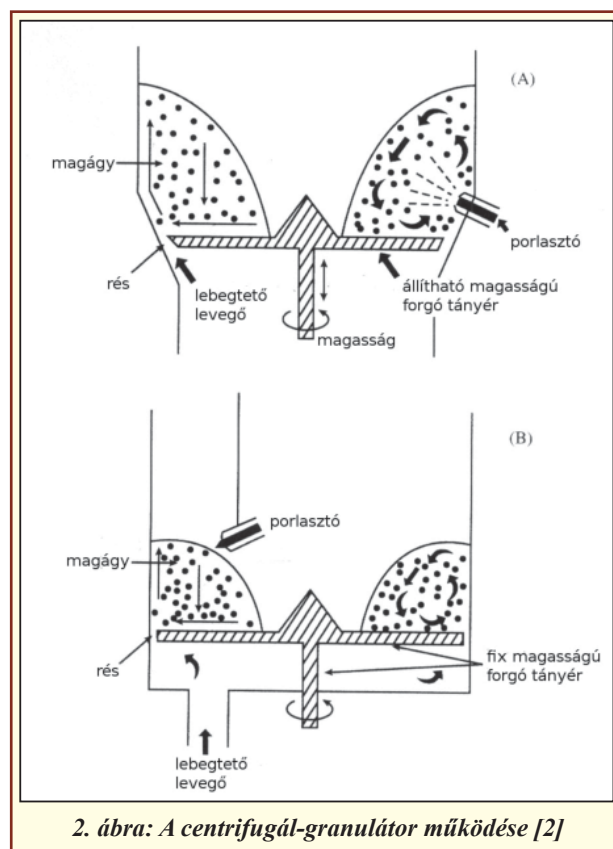
A rétegzéses eljárás során a ható- és segédanyagokat rétegekben visszük fel egy korábban elkészített magra. A mag lehet inert (ezek általában cukrok, cukorszármazékok, vagy készülhet cellulózból stb.), illetve tartalmazhat hatóanyagot is. A felvitt rétegek számában és funkciójában is lehet különbség. Az **I. ábrán** egy indifferens maggal készült rétegzett pellet szerkezete látható. A rétegek száma és vastagsága meg kell feleljen a hatóanyag anyagi sajátosságainak, terápiás adagjának, ill. az adott alkalmazási célnak.

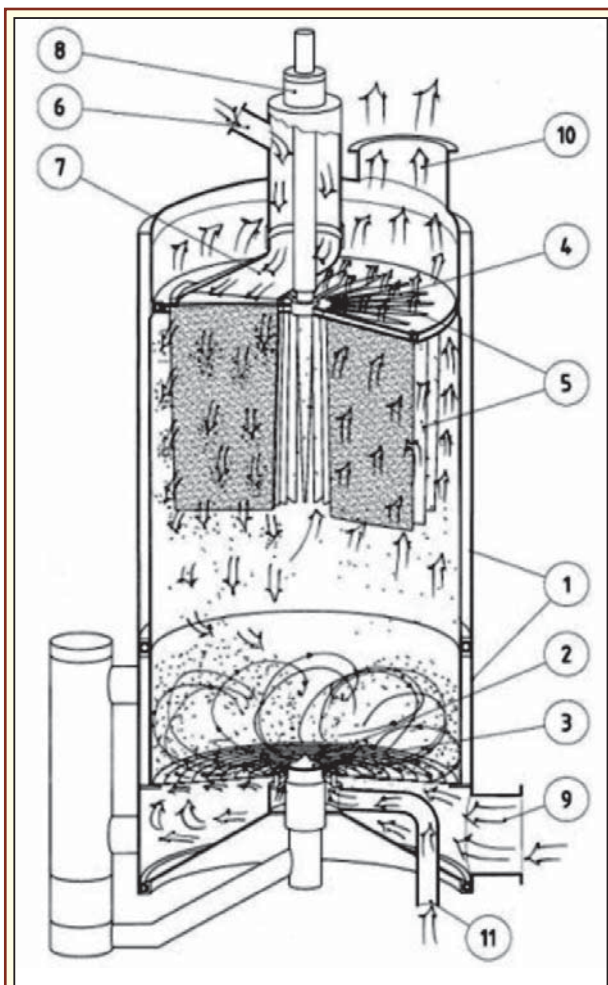


Működési elvek és berendezések

A rétegzéses eljárásához többféle berendezés használható. Kezdetben a cukros drázsírozásra használt üstöt alkalmazták, azonban ez több szempontból nem volt ideális megoldás. A porlasztáshoz és a szárításhoz használt levegő eltávozása csak az üst száján keresztül lehetséges, ahová szűrő nem építhető be, így a kis tömegű apró szemcsék eltávozása komoly gondot, a visszatartása pedig komoly feladatot jelent. Ezenkívül a rétegzett anyag egyenletes eloszlása az üst alakjától és dőlésszögétől függ, így a holtterek keletkezésével is számolni kell.

Az előbb felvázolt problémák kiküszöbölése céljából, ill. a nagyobb hatékonyság érdekében hamar átérttek a centrifugál-granulátorok, ill. a rotofluid granulátorok alkalmazására. Az ilyen típusú berendezésekben közös, hogy ideális esetben a magok nedvesedése és száradása folyamatosan egyensúlyban van és igen rövid idő alatt végbemegy, így a hatóanyag





3. ábra: Az Innojet Ventilus készülék működése

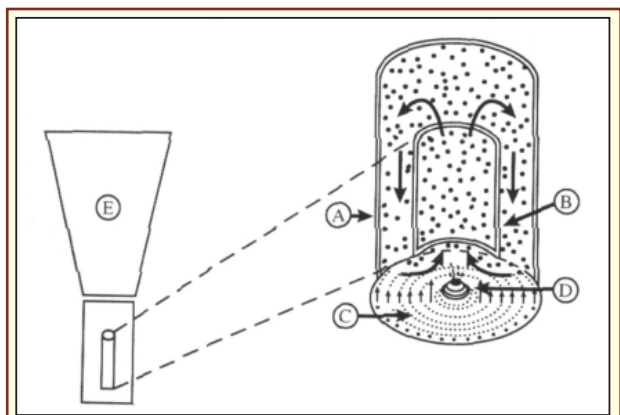
Jelmagyarázat: 1 – külső fal; 2 – alsó tányér levegőnyílásokkal; 3 – Rotojet porlasztó; 4 – Sepajet porvisszavezető rendszer; 5 – szűrőtartó elem; 6 – szűrőtisztító levegő; 7 – szűrők feletti rotor; 8 – szűrők feletti rotor meghajtása; 9 – lebegtető levegő bevezetése; 10 – levegő kivezetése; 11 – centrálisan bevezetett levegő

száradása a magok felületén gyorsan megtörténik, ezzel csökkentve az anyagvesztést. A gyors száradás és az ebből következő kis nedvességtartalom miatt a magoknak nincs alkalmuk összetapadni [2].

A centrifugál-granulátorokban a szemcsék összetett mozgást végeznek (lásd 2. ábra): a tányér szélén fölfelé haladó levegőáram hatására a magok megemelkednek, a tányér közepe felé esnek, majd leérkezve a centrifugális erő ismét a tányér szélé felé taszítja őket, így folyamatosan mozgásban vannak. A tányér forgása eközben szintén hat a szemcsékre, így azok önmagába visszatérő, spirál alakú utat járnak be [2, 14, 15].

A fent vázolt berendezés egyik legfontosabb jellemzője, hogy „nyitott” üzemi technológiájú, míg a hasonló elven működő, de „zárt” elvű készülékek az ún. „Rotofluid” berendezések; a gyógyszeripar elsősorban ezeket használja.

Az Innojet új berendezésében (lásd 3. ábra) már a tányér forgatása helyett a tányért alkotó koncentrikus



4. ábra: A fluidizációs bevonó és részei

Jelmagyarázat: A – műveleti tér fala; B – térelválasztó kolonna; C – perforált lemez; D – porlasztó; E – expanziós kamra [2]

fémlemezek közötti réseken irányítottan kiáramló levegő kényszeríti az anyagot a berendezés szélé felé. Az eljárás előnye az egyenletes levegőáramlás és a sokoldalú felhasználhatóság. Ipari szempontból a berendezés könnyű szerelése és tisztítása, valamint a felépítéséből következő lineáris léptéknövelhetősége emelhető ki.

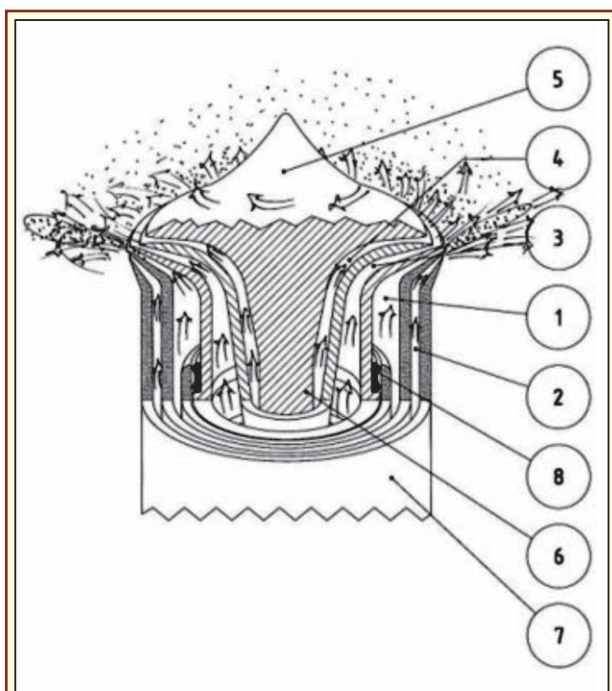
A leggyakrabban használt berendezés fluidizációs elven működik, amelyben az alulról jövő levegőáram emeli fel a magokat a kolonnában, majd azok a sebességcsökkenés miatt visszahullanak a berendezés aljára. Ennek bevonásra és rétegzésre optimalizált változata a Wurster módszer (lásd 4. ábra). A berendezésben térelválasztóként egy csövet helyeznek el. A magok felfelé történő mozgása irányítottan a cső belsejében, lefelé esése a cső körül történik. A lehullott magokat a nagy sebességgel áramló levegő szívó hatása visszahúzza a cső alá, így a magok folyamatosan mozgásban maradnak [2, 16].

A fluidizációs berendezésnek több módosított változata született. A pulzáló fluidágyas berendezésben a levegő áramlása a perforált lemeznek egyszerre csak egy részére koncentrált, és időben váltakozva mozgatja át a teljes magágyat [17].

Rétegzéses hatóanyag-felvitel

A különböző rétegek felvitele az anyagok tulajdonságaitól függően többféleképp történhet. Vízen jól oldódó hatóanyagok esetében az oldatos, rosszul oldódó anyagok esetében a szuszpenziós felvitel, vagy a porrétegzés alkalmazható. A szerves oldószerek használata környezetvédelmi és költséghatékonysági okokból, valamint az oldószermaradványok jelentette problémák miatt kizorulóban van [2, 18].

Oldatok és szuszpenziók rétegzésénél a hatóanyagot minél magasabb koncentrációban érdemes felvinni, mert az oldószer eltávolításának sebessége határozza meg a művelet idejét, energiaigényét és a részecskeno-



5. ábra: Rotojet porlasztó működési elve

Jelmagyarázat: 1 – folyadék réteg; 2 – alsó porlasztó levegő; 3 – felső porlasztó levegő; 4 – felső védő levegőréteg, 5 – védőkúp; 6 – meghajtó tengely; 7 – külső védőburkolat; 8 – tömítés

vekedés sebességét. Szuszpenziók esetében célszerű minél kisebb szemcseméretben alkalmazni a hatóanyagot, mivel a kialakuló felület egyenletessége a szemcsemérettel fordítottan arányos, valamint a nagyobb részecskék hajlamosabbak letöredezni a magokról [2, 19].

Porok rétegzése esetén a hatóanyagot szilárd formában adagolják a berendezésben lévő magok felületére, miközben a kötőanyagot tartalmazó folyadékot porlasztva juttatják a rendszerbe. A por kis szemcsemérete miatt általában glidánsok alkalmazására is szükség van [20-21].

A műveletben használt porlasztó általában a berendezés alján helyezkedik el, és a levegőáramlással azonos irányba (függőlegesen felfelé) porlaszt. Laboratóriumi méretű berendezésekben általában egy porlasztó üzemel a berendezés közepén, míg nagyobb gépek, üzemi berendezések esetében a porlasztók egyenlő távolságra, koncentrikus körökben találhatók. Utóbbi megoldás hátránya, hogy a porlasztók egyikénél fellépett probléma a termék teljes mennyiségére van hatásos, így a potenciális veszteség nagyobb.

A készülékeknél említett Innojet berendezésben a fúvókának nem a csúcsán, hanem a peremén található a folyadékot és a porlasztó levegőt adagoló részek (lásd 5. ábra). A vízszintes porlasztó két ellentétes irányú nyalábban porlaszt, a termék egyenletes nedvesítését a porlasztófej forgása biztosítja.

A magok folyamatos mozgása miatt a felszínükön

képződő réteg folyamatos erózióknak van kitéve, amely részben az ütközésekből, részben a levegő áramlásából ered. Minél gyorsabb a magok mozgása, annál erősebb és több ütközés zajlik a magok, illetve a magok és a berendezés falai között, és minél nagyobb a levegőáram, annál gyorsabban, akár még a magok elérése előtt távozik a hatóanyag a rendszerből, illetve annál nagyobb eséllyel sodorja le a gyengén kötött hatóanyagot a mag felszínéről [2]. Ezért fontos a levegőáram és a többi paraméter megfelelő szinkronizálása.

A kitermelés növelése érdekében szinte minden esetben alkalmaznak kötőanyagokat. Ezek általában alacsony molekulatömegű polimerek, amelyeket a folyékony fázisban oldva visznek be a rendszerbe. Kezdetben a folyadék alkotta hidak, majd a száradás után a feloldódott hatóanyagból vagy a polimer kötőanyagból képződött szilárd hidak tartják a helyén a hatóanyagréteget [2].

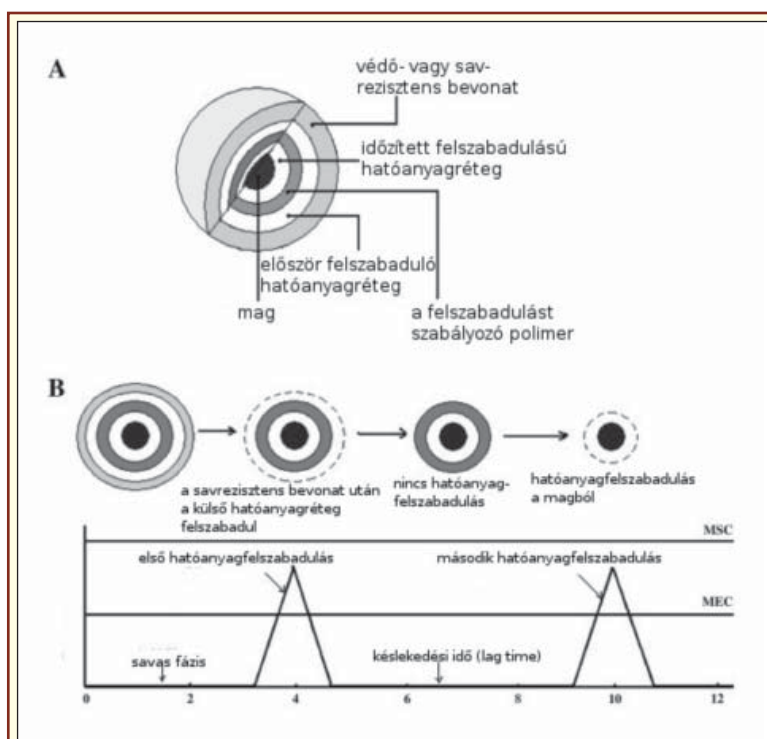
Egy magra több különböző hatóanyag is rétegezhető, az inkompatibilitások figyelembe vételével akár egyszerre, akár egymást követően. Több pumpa megfelelő programozásával akár egy rétegen belül is fokozatosan változó összetételt érhetünk el. Egymással inkompatibilis hatóanyag- illetve bevonatrétegek közé elválasztó réteget iktatnak, ami megakadályozza a kritikus komponenseket tartalmazó rétegek érintkezését [22].

Bevonatként – amennyiben szükséges – a tabletták bevonásánál megszokott anyagok jöhetnek szóba. Megfelelő polimerek, ill. több különböző bevonatréteg alkalmazásával módosított hatóanyag-leadó (nyújtott, késleltetett, pulzáló stb.) rendszerek hozhatók létre.

Kritikus paraméterek

Minden eljárásnál különös figyelmet kell fordítani a kritikus paraméterek meghatározására, művelet közbeni folyamatos ellenőrzésükre. A kritikus paraméterek köre nemcsak az anyagi rendszerek összetételétől függ, hanem az egyes technológiák, előállítási elvek esetében is jelentős eltéréseket mutathat, ezért meghatározásuk különösen fontos [23].

A hagyományos drázsírozó üstnél az üst alakja, a forgástengely dőlésszöge, a terelőlapátok állása és a forgási sebesség, míg a centrifugál-granulátor és a fluidizációs berendezés esetében a porlasztó levegő nyomása, a szárító levegő hőmérséklete, a levegő nedvességtartalma, a por ill. a folyadék adagolási sebessége, a fúvóka átmérője számítanak elsősorban kritikus paraméternek. A centrifugál- ill. rotofluid granulátorokban a rétegzett anyag egyenletes eloszlását elsősorban a tányér megfelelő forgási sebességével lehet biztosítani, de fontos paraméter a szárító levegő térfogata és sebessége, a fúvóka átmérője, valamint a sarzsméret is. A szárító levegő sebessége bizonyos berendezéseken a tányér és a berendezés fala közötti rész nagyságának változtatásával szabályozható [24].



6. ábra: Rétegzéssel kialakított pulzáló rendszer sematikus ábrája [23]

A fluidizációs berendezésekhez általában több különböző lyukméretű perforált lemez tartozik, így a szárító levegő mennyisége bizonyos keretek között változtatható. Természetesen mód van az áramlási sebesség szabályozására is. Kritikus paraméter továbbá a szuszpenzióban történő hatóanyag-felvitel esetén a hatóanyag szemcsemérete is [2, 25].

A rétegzéses eljárás a komoly felszereltség mellett is nagy szakértelmet kíván, hiszen a termék minőségét rengeteg paraméter befolyásolja. A kritikus paraméterek folyamatos ellenőrzése ezért kiemelten fontos [23].

A rétegzéses eljárás számos jelentős gyógyszer-technológiai probléma megoldására alkalmazható. Segítségével egyszerűen állíthatók elő a hatóanyag amorf formáját tartalmazó szilárd oldatok, mivel a kötőanyagként használt polimerek egy része kristályosodást gátló tulajdonságokkal is rendelkezik [26-27]. Sokoldalúan módosítható a termék hatóanyag-leadása mind a segédanyagok, mind az egyes rétegek megfelelő megválasztásával. Egy készítményben feldolgozhatóvá válik számos, akár egymással inkompatibilis hatóanyag is, és az egyes hatóanyagok leadása időben és egymáshoz viszonyítva pontosan szabályozható. A rétegzéses eljárással előállított pelletek később több gyógyszerformában is feldolgozhatók.

Gyógyászati alkalmazásuk

Magyarországon jelenleg elsősorban nyújtott hatóanyag-leadású ill. savrezisztens készítmények kerülnek így forgalomba. A rétegzéses eljárás ezenkívül

különösen alkalmas pulzáló hatóanyag-leadás elérésére: a pelletek legkülső bevonatrétege oldhatatlanságával vagy savrezisztens mivoltával biztosítja a kezdeti késleltetett kioldódást az alatta levő hatóanyagrétegből, majd a hatóanyagréteg feloldódása után az ez alatt található bevonatréteg késleltető hatása érvényesül, majd kioldódik az alatta levő hatóanyagréteg, és így tovább, egészen az inert magra közvetlenül felvitt hatóanyagrétegeig.

Ezek gyakorlati megvalósításához általában rupturáló bevonatokat, illetve esetenként az azokra rétegzett oldhatatlan, de permeábilis filmeket használnak. Az FDA által Pulsys néven engedélyezett ilyen típusú készítmény amoxicillint tartalmaz [3, 23].

Ígéretes kísérletek történtek rétegzéses eljárással készített úszó rendszerek előállítására [28-29]. Bizonyos oldhatatlan permeábilis polimerek alkalmasak arra, hogy az alattuk elhelyezkedő efferveszcens rétegben termelődő gázt csapdába ejtve akár 24 órán keresztül is lebegésben tartsák a

pelletteket. A polimer a kioldódást a megszokott módon befolyásolja.

A rétegzett pelletet – mint a pelletet általában – kapszulába tölthetők vagy tablettává préselhetők. A rétegzett pelletekből préselt tabletták előállítása sok kihívással jár. A multipartikuláris rendszerek előnyeinek megtartása érdekében az egyes pelletet a préselés során nem veszíthetik el egyediségüket, illetve a megfelelő hatóanyag-kioldódást biztosító bevonataik nem sérülhetnek. A kész termék ugyanakkor rendelkezik a tabletták kényelmes bevehetőségével, esetleges felelősségével, valamint gyors szétesésénél fogva nyelési nehézségeket sem okoz [30-31]. Az így előállított készítmények általában módosított hatóanyag-leadásúak, külföldön MUPS megjelöléssel kerülnek forgalomba. A tablettázás nehézségeinek elkerülésére a pelletet gyorsan széteső gélmátrixba inkorporálásával is kísérleteznek [32].

Összefoglalás

Összességében elmondható, hogy a rétegzéses eljárás számtalan, (Magyarországon) még kihasználatlan lehetőséget rejt magában, amelyek gyakorlati felhasználásához és a megfelelő beteg tájékoztatáshoz elengedhetetlen a háttérben levő technológia ismerete. A rétegzéses eljárást ugyan nem egyedül a gyógyszeriparban alkalmazzák, de működése minden iparágban azonos műszaki elven zajlik, így alapvetően azonos problémákat vet fel. Természetesen a gyógyszeripari alkalmazás az a terület, ahol a benne rejlő lehetőségeket a legjobban lehet kihasználni.

Köszönetnyilvánítás

A TÁMOP-4.2.1/B-09/1/KONV-2010-0005 azonosító számú, „Kutatóegyetemi Kiválósági Központ létrehozása a Szegedi Tudományegyetemen” című projekt az Európai Unió támogatásával, az Európai Regionális Fejlesztési Alap társfinanszírozásával valósul meg.

IRODALOM

1. Dey, N.S., Majumdar, S., Rao, M.E.B.: *Tropical Journal of Pharmaceutical Research* 7, 1067-1075 (2008). – 2. Ghebre-Sellassie, I., Knoch, A.: Pelletization techniques in: J. Swarbrick, J.C. Boylan, Editors, *Encyclopedia of Pharmaceutical Technology*, Marcel Dekker Inc., New York and Basel, 2002. – 3. Dashevsky, A., Mohamad, A.: *Int J Pharm* 318, 124-131 (2006). – 4. Follonier, N., Doelker, E., Cole, E.T.: *J Control Release* 36, 243-250 (1995). – 5. Hirshey Dirksen, S.J., D'Imperio, J.M., Birdsall, D., Hatch, S.J.: *Curr Med Res Opin* 18, 371-380 (2002). – 6. Krause, J., Breitzkreutz, J.: *Pharmaceutical Medicine* 22, 41-50 (2008). – 7. Ghebre-Sellassie, I.: Pellets: A general overview in: I. Ghebre-Sellassie, Editor, *Pharmaceutical Pelletization Technology*, Marcel Dekker Inc., New York and Basel, 1989. – 8. Krämer, J., Blume, H.: Biopharmaceutical aspects of multiparticulates in: I. Ghebre-Sellassie, Editor, *Multiparticulate oral Drug Delivery*, Marcel Dekker Inc., New York, Basel and Hong Kong, 1994. – 9. Kleinebudde, P., Knop, K.: Direct pelletisation of pharmaceutical pellets in fluid-bed processes in: Salman, A.D., Hounslow, M.J., Seville, J.P.K., Editors, *Handbook of Powder Technology: Granulation vol. II*, Elsevier, London, 2007. – 10. Trivedi, N.R., Rajan, M. G., Johnson, J.R., Shukla, A.J.: *Crit Rev Ther Drug* 24, 1-40 (2007). – 11. Vervaet, C., Baert, L., Remon, J.P.: *Int J Pharm* 116, 131-146 (1995). – 12. Nastruzzi, C., Cortesi, R.,

Esposito, E., Genovesi, A., Spadoni, A., Vecchia, C., Menegatti, E.: *AAPS PharmSciTech* 1, 9 (2000). – 13. Sinchaipanid, N., Chitropas, P., Mitrevaj, A.: *Pharm Dev Technol* 9, 163-170 (2004). – 14. Kása, P. jr., Hódi, K., Révész, P., Erős, I.: Pelleték előállítása centrifugálganulátorban, *Acta Pharm. Hung.* 70, 41-44 (2000). – 15. Beretzky, Á., Antal, I., Karsai, J., Erős, I., Hódi, K.: *Acta Pharm. Hung.* 78, 37-43 (2008). – 16. Turton, R., Cheng, X.X.: *Powder Technol* 150, 78-85 (2005). – 17. Nitz, M., Taranto, O.P.: *Chem Eng Process* 47, 1412-1419 (2008). – 18. Rafati, H., Ghassempour, A., Barzegar-Jalali, M.: *J Pharm Sci* 95, 2432-2437 (2006). – 19. Muschert, S., Siepmann, F., Cuppok, Y., Leclercq, B., Carlin, B., Siepmann, J.: *Int J Pharm* 368, 138-145 (2009). – 20. Pearnchob, N., Bodmeier, R.: *Int J Pharm* 268, 1-11 (2003). – 21. Smikalla, M., Mescher, A., Walzel, P., Urbanetz, N. A.: *Int J Pharm* 405, 122-131 (2011). – 22. El-Malah, Y., Nazzal, S.: *Int J Pharm* 337, 361-364 (2007). – 23. Roy, P., Shahiwala, A.: *J Control Release* 134, 74-80 (2009). – 24. Ar Rashid, H., Heinämäki, J., Antikainen, O., Yliruusi, J.: *Eur J Pharm Biopharm* 51, 227-234 (2001). – 25. Rácz, I., Selmecezi, B.: *Gyógyszertechnológia; Medicina kiadó, Budapest, 2001.* – 26. Sun, N., Wei, X., Wu, B., Chen, J., Lu, Y., Wu, W.: *Powder Technol* 182, 72-80 (2008). – 27. Zhang, X., Sun, N., Wu, B., Lu, Y., Guan, T., Wu, W.: *Powder Technol* 182, 480-485 (2008). – 28. Sharma, S., Pawar, A.: *Int J Pharm* 313, 150-158 (2006). – 29. Sungthongjeen, S., Paeratakul, O., Limmatvapirat, S., Puttipatkhachorn, S.: *Int J Pharm* 324, 136-143 (2006). – 30. Abdul, S., Chandewar, A.V., Jaiswal, S.B.: *J Control Release* 147, 2-16 (2010). – 31. Türkoğlu, M., Varol, H., Çelikok, M.: *Eur J Pharm Biopharm* 57, 279-286 (2004). – 32. Schmidt, C., Bodmeier, R.: *Int J Pharm* 216, 9-16 (2001).

Nikowitz, K., Hódi, K., Regdon, G. jr.: **Principle and possible use of layering technology in the production of multiparticulate systems**

SZTE Gyógyszertechnológiai Intézet, 6720 Szeged, Eötvös u. 6.
e-mail: geza.regdon@pharm.u-szeged.hu

IV



Study of the preparation of a multiparticulate drug delivery system with a layering technique

Krisztina Nikowitz, Péter Kása Jr., Klára Pintye-Hódi, Géza Regdon Jr.*

Department of Pharmaceutical Technology, University of Szeged, H-6720 Szeged, Eötvös utca 6, Hungary

ARTICLE INFO

Article history:

Received 31 March 2010

Received in revised form 14 July 2010

Accepted 4 September 2010

Available online 24 September 2010

Keywords:

Multiparticulate

Enteric coating

Acryl-EZE

Dissolution

ABSTRACT

The properties of a fully formulated enteric coating system were examined on a model multiparticulate formulation. Samples containing the model drug diltiazem hydrochloride were made in a fluid bed chamber with different amounts of Acryl-EZE, a ready-to-use coating dispersion. The effects of the film thickness on the dissolution profile were determined. While all samples yielded satisfactory release results in simulated intestinal fluid, the results in simulated gastric acid were worse than expected. The scanning electron microscopic images suggested that coating problems were not responsible for this behaviour.

© 2010 Elsevier B.V. All rights reserved.

1. Introduction

The highly water-soluble model drug diltiazem hydrochloride is a first-line antihypertensive and antianginal agent. In the treatment of hypertension a once-daily dosage is preferred in consequence of compliance issues. The extended-release diltiazem capsules available on the market typically consist of rapid-release, delayed-release and, for some products, immediate-release particle fractions [1].

Multiparticulate drug delivery systems consist of multiple discrete drug-containing units, typically thousands of spherical pellets that are filled into one capsule. The individual pellets in a multiparticulate system can sometimes be divided into fractions according to their size, coating, release properties, drug content, etc., offering a wide range of possibilities for drug development. Multiparticulate drug delivery systems are increasingly gaining favor on the market, as their multiple-unit nature furnishes several benefits over the more traditional single-unit dosage forms [2,3]. These include a lower irritative effect due to the decreased local concentration, less individual differences in plasma concentration than with tablets [4], a reduced risk of dumping, improved bioavailability [4], a large scale of products to be covered (in terms of both dosage forms and release kinetics) and an easy-to-solve approach to interactions [5,6]. Disadvantages include the large number of variables, multiple-step manufacturing, high production costs, greater excipient requirements and the need for advanced technology and trained operating personnel [7].

Pellets can be produced by the direct pelletization of the drug and the excipients (matrix pellets) and the use of nonpareil seeds with one or multiple layers of drug (layered pellets) [8,9]. Both types of products can be further coated; in our case this was done with an acrylic-based film-coating product. In the latter case, the quality and thickness of the film layer can be greatly influenced by the drug layer underneath [10]. Besides the surface characteristics and distribution, this also means that the chemical characteristics of the film layer can vary because of the drug. It has been documented that diltiazem is associated with the hydrophobic sites of cationic polymer coatings and is retained during dissolution [11].

A number of ready-to-use coating dispersions are available on the market for the achievement of various release profiles. Their use eliminates the need for the development and preparation of the coating suspension and they have therefore gained acceptance in the pharmaceutical industry [12].

In our experiments, we used the solution layering technique to make the multilayered pellets described below. Solution layering is a process during which the active pharmaceutical ingredient (API) and the excipients (typically binders and coating materials) are either dissolved or suspended and sprayed onto the continuously drying cores. The method can be used to dose multiple, even incompatible APIs together and the further processibility of the pellets is good, thanks to the narrow size distribution, the good flow behaviour and the dense surface [6].

In our experiments, we evaluated the possibility of a multiparticulate delayed-release diltiazem product. We also investigated the use of fully formulated coating systems as a possible method of reducing the manufacturing steps. Our future goal is to formulate a sustained-release capsule in which the delayed-release product

* Corresponding author. Tel.: +36 62545576; fax: +36 62545571.

E-mail address: geza.regdon@pharm.u-szeged.hu (G. Regdon).

described below can be used as a fraction as the release directly on the absorption site is expected to yield better results in extending the release time of the formulation.

2. Materials

Diltiazem hydrochloride (Ph. Eur.) was used as a model drug, Cellet 500 (Shin-Etsu Chemical Co., Ltd., Tokyo, Japan) as nonpareil core material, Kollidon 25 (BASF, Ludwigshafen, Germany) was applied as a binder in the layering of diltiazem hydrochloride, and Acryl-EZE (Colorcon, Dartford Kent, UK), a fully formulated enteric coating dispersion, was used as coating material.

3. Methods

3.1. Preparation of samples – layering of diltiazem hydrochloride

The multiparticulate pellet samples were prepared in a Strea-1 (Niro Aeromatic, Bubendorf, Switzerland) fluid bed Wurster chamber. In the equipment cores were fluidized by filtered and heated air. The cores' fast upward movement takes place inside a partition column and slower downward movement on its sides. Liquid is sprayed onto the cores from below. Schematic figure (Fig. 1) taken from Chan et al. [13].

In the first, drug-loading step of the process, diltiazem hydrochloride was layered onto the nonpareil Cellet 500 cores. In accordance with the results of our preliminary examinations, a solution of diltiazem hydrochloride and Kollidon 25 in a mass ratio of 5:3 with a total solid content of 40% was used, as the solution containing only diltiazem hydrochloride did not yield satisfactory loading results. A batch size of 200 g of nonpareils and the above-mentioned solution containing 197 g of dry material was used. The loading parameters were: inlet temperature 50 °C, outlet temperature 43 °C, fan capacity 4.5, peristaltic pump speed 4 ml/min, air volume 75 m³/h and nozzle diameter 1 mm.

Between the drug-loading and the following coating step the pellets were dried in the spray coater for 10 min. Since the Acryl-EZE contains sodium bicarbonate as an excipient, the equipment had to be completely disassembled and washed to prevent precipitate formation.

At this point samples of the intermediate product were taken for comparison purposes; these drug-containing uncoated pellets are called Sample 1 from here on.

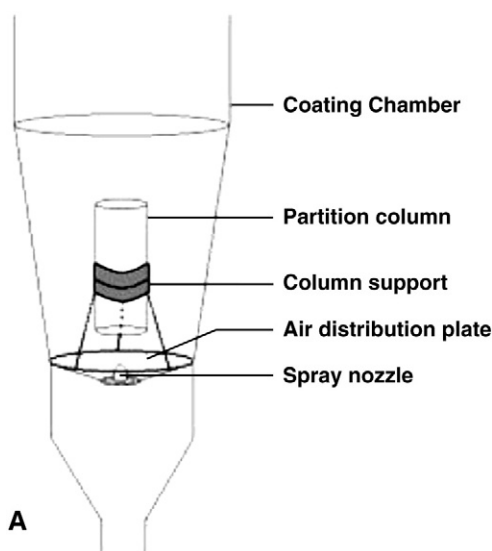


Fig. 1. Schematic picture of the Strea 1 fluid bed chamber.

3.2. Preparation of samples – coating

In the second, coating step, an Acryl-EZE dispersion (a fully formulated USP copolymer type C coating system containing 60% polymer and various excipients) was prepared and applied, following the guidelines provided by the manufacturer, as a 20% aqueous dispersion. A small amount (0.1%) of dimeticone was added to prevent foaming during the stirring and coating process. The parameters used for the coating were the same as for the drug layering step.

Different amounts of coating dispersion were sprayed onto 200 g of drug-layered pellets in the Strea equipment. Four batches were prepared with different amounts of coating dispersion for each. The amount of the dry material consumed for 200 g of drug-loaded particles was 59.5 g, 79.5 g, 99.3 g and 125.0 g, respectively with an about 8% loss. The drug-layered pellets were pre-heated at a reduced atomizing pressure for 10 min, coated at a gradually increasing spray rate and dried in the equipment for 10 min afterwards. The coated pellets will be called samples 2 to 5 in order of increasing dry material consumed for the film coating from here on (Table 1).

3.3. Measurement of layer thickness

An image analysis method (Leica Quantimet 500 MC, Leica Cambridge Ltd, Cambridge, UK) was used to determine the thickness of the layers on the pellets. The mean thicknesses were calculated via the mean diameters of the particles, determined by measuring 300 particles of each batch with a stereomicroscope (Zeiss, Oberkochen, Germany). Film thickness was also examined with Raman spectroscopy; the results of that work were published independently [14].

3.4. Scanning electron microscopy

Photographs of every batch were taken with a scanning electron microscope (SEM) (Hitachi 4700, Hitachi Ltd., Tokyo, Japan) and possible coating problems were identified. A sputter coating apparatus (Polaron E5100, Polaron Equipment Ltd., Greenhill, UK) was used to induce the electric conductivity on the surface of the samples. The air pressure was 1.3–13 mPa.

3.5. Dissolution of diltiazem hydrochloride from pellets

Dissolution studies were carried out according to the Ph. Eur. standards with a rotating basket (Erweka DT 700, Erweka GmbH, Heusenstramm, Germany), in 1000 ml of simulated gastric acid at 100 rpm at 37 °C for 2 h, then after draining the vessel of the acid it was replaced with 1000 ml of phosphate buffer pH = 6.8 and the dissolution measured at the same parameters as above. Samples were taken of the gastric acid at 2 h and of the phosphate buffer at 5, 10, 15, 20, 30, 45, 60 and 90 min.

Concentration was measured with a spectrophotometer (Unicam Helios α , Thermo Fisher Scientific Inc., Waltham, USA) at 237 nm, with a bandwidth of 2 nm and a lamp charge of 325 nm by comparison to a calibration curve.

Table 1
Samples produced.

Samples	Coating dispersion (g)	Dry material consumed (g)
Sample 1	none (only contains the drug on the nonpareil core)	none
Sample 2	300	62.40
Sample 3	400	79.48
Sample 4	500	99.34
Sample 5	600	124.96

The drug content of the pulverised pellets in the phosphate buffer was determined after 2 h at the same parameters as for the dissolution test.

4. Results and discussion

4.1. Preparation of the samples

The fan capacity and the fluid feed rate proved to be the most important parameters in our studies. A too low fan capacity often resulted in the particles sticking to the inner surface of the vertical cylinder. Agglomeration of the particles was never completely overcome but when discontinuous spraying was employed the agglomerates broke down into individual particles shortly after the spraying process was paused [15]. This method has the disadvantage of an excessively long coating time but decreasing the fluid feed rate increased the coating time even more and did not eliminate agglomeration completely. Use of a higher fluid feed rate resulted in one large agglomeration that blocked the inside of the cylinder and the experiment had to be discontinued.

4.2. Measurement of layer thickness

As illustrated in Fig. 2, two diameters of each sample were measured (white and grey boxes) and the mean (dotted line) and median (uninterrupted line) calculated. Both the mean and median lines show that the particle size increased from that of the nonpareil core in each sample. As the median represents the value that separates the lower half of the sample from the upper half, the shift of the median toward one end of the scale and its difference from the mean value means that the samples exhibited an increasingly skewed distribution; this corresponded with the observation that larger particles tended to receive a thicker coating than smaller ones [16], which is a known occurrence and is mainly due to the fact that between equal masses of particles the one consisting of larger spheres has the smaller surface area. The increase in size was mostly due to the addition of the drug layer, but Fig. 2 clearly reveals the shift in the graph with the amount of coating dispersion used. The mean thickness of the film coating is presented in Table 2.

The roundness distribution of the particles, where roundness was calculated as the quotient of two diameters, (Fig. 3) did not change significantly during the process, suggesting that no serious coating problems occurred.

4.3. Scanning electron microscopy

The characteristics of the drug-loaded pellets are clearly depicted in Fig. 4. It can be observed that the API forms a relatively uniform

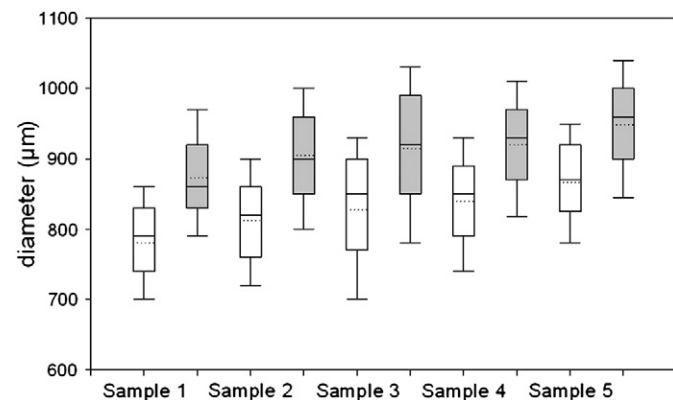


Fig. 2. Size distribution (breadth and length) of coated particles.

Table 2
Film thicknesses of samples.

Samples	Coating dispersion (g)	Film thickness (mean; μm)
Sample 1	none (only API)	none
Sample 2	300	15.5
Sample 3	400	23.5
Sample 4	500	28.9
Sample 5	600	44.4

drug layer on the core, though recrystallization causes some unevenness and cracking in the layer.

The coating covered the uneven drug layer adequately for all the samples (Fig. 5), but thinner coatings displayed the same uneven surface, and higher-resolution images demonstrated coating problems, such as layers, craters and a rough surface.

The results of the morphological tests indicated that the thickest coating layer yielded the best quality of surface.

4.4. Dissolution of diltiazem hydrochloride from pellets

It is clear from Fig. 6 that every sample underwent 100% drug release by 60 min in the pH 6.8 dissolution medium. Sample 2, with the thinnest coating film layer, however, yielded more than 10% drug release in the acidic medium, despite the enteric coating used. Samples 3, 4 and 5 furnished progressively better results, with no release exceeding 2.50%. Previous studies showed that the minimum film thickness for achieving gastro-resistance (less than 5% over 2 h in gastric acid) in aqueous enteric Eudragit coatings is about 50 μm in tablets [17] and 15% weight gain in pellets [18]. With Arcyl-EZE a thinner coating (about 30 μm thick and 13% polymer weight gain) was sufficient.

The standard deviation due to the coating problems tended to be inversely proportional to the thickness of the film on the pellets.

The standard deviations were unusually high. One explanation for this is the rupture of the film coating, which occurs more often in thinner coatings. The diagram further indicated that thinner film coatings also had a tendency to dissolve more quickly, with higher drug release patterns early on. Thicker film coatings seem to hinder dissolution (not prevent it, as the film dissolves at pH 6.8), but give a

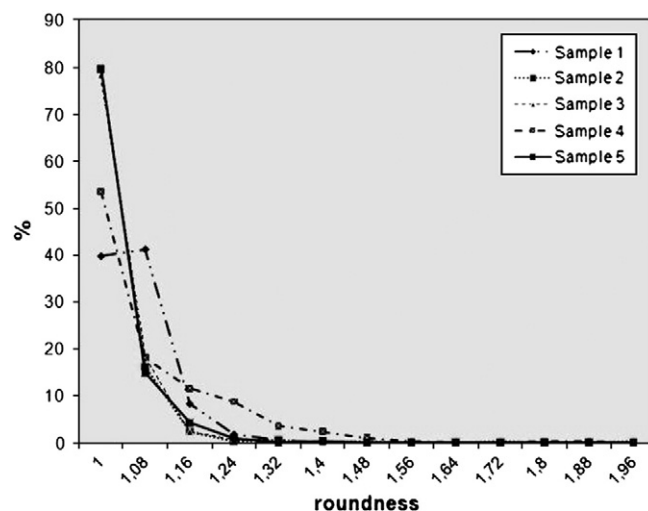


Fig. 3. Roundness distribution of particles.

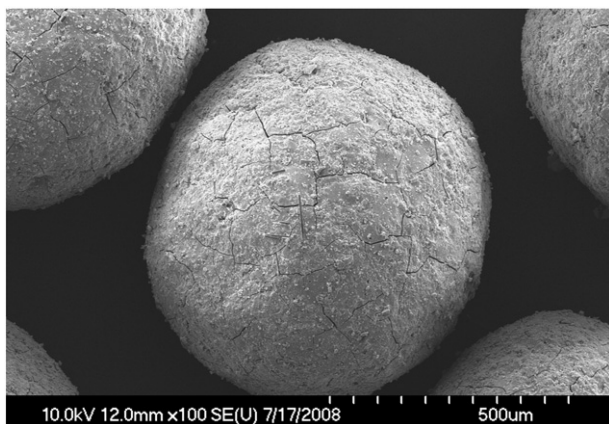


Fig. 4. SEM picture of Sample 1 (10.0 kV, $\times 100$ SE(U)).

more even dissolution profile, as revealed in the progressively lower standard deviation values.

5. Conclusions

Our investigations permit the conclusion that Acryl-EZE is suitable for the making of delayed-release multilayer pellets without the use of additional excipients. The film thickness is easily determined through image analysis.

Dissolution studies led to the finding that the film thickness directly influenced the rate and extent of dissolution in an acidic medium, and with an observable tendency to hinder dissolution in an alkaline medium, but this tendency was not highly pronounced because of the large standard deviations.

For every sample, the drug release in acidic medium greatly exceeded our expectations based on the film thickness. This may have been due to drug migration into the film layer. This idea is supported by the very good solubility of diltiazem and by the fact that the drug release in acid is dependent on the film thickness.

Declaration of interest

The authors report no declarations of interest.

Acknowledgements

The authors of this work wish to thank BASF SE for the generous donation of Kollidon 25, Colorcon Ltd. for the supply of Acryl-EZE, Egis

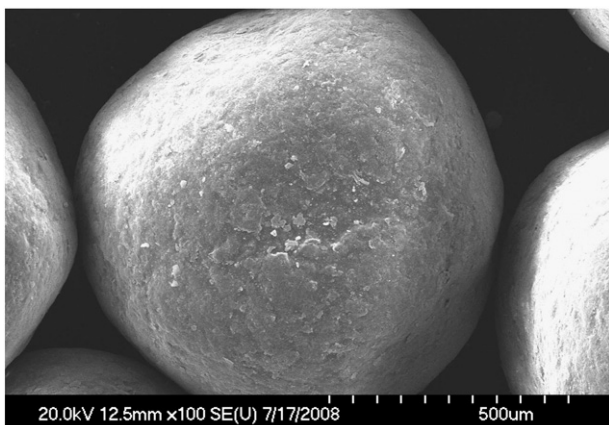


Fig. 5. SEM picture of Sample 5 (10.0 kV, $\times 100$ SE(U)).

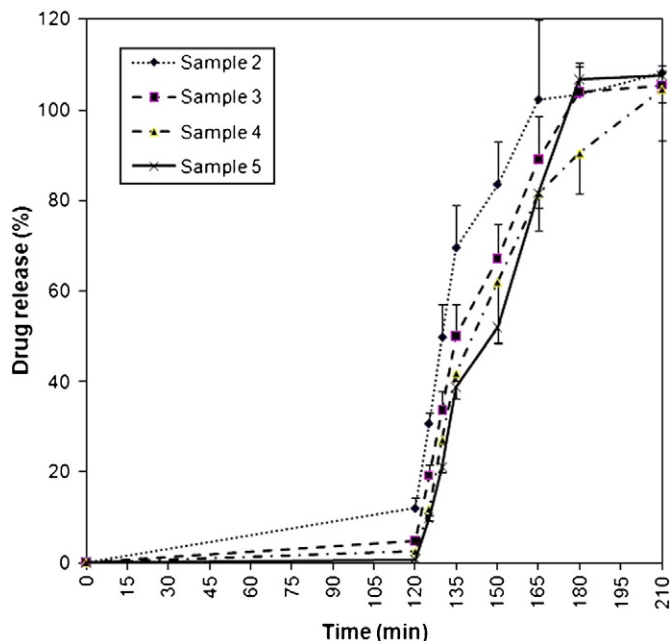


Fig. 6. Drug release of the coated pellets in simulated gastric and intestinal fluid.

PLC for their gift of diltiazem hydrochloride, and Syntapharm for their support with the nonpareil cores.

References

- [1] V.K. Sharma, J. Hussain, H.F. Khorakiwala, US Patent 6635277 – Composition for pulsatile delivery of diltiazem and process of manufacture. October 21, 2003. Available at: <http://www.patentstorm.us/patents/6635277/description.html>. Accessed on 13 January 2009.
- [2] H. Bechgaard, N.G. Hagermann, Controlled-release multi-units and single unit doses. A literature review, *Drug Dev. Ind. Pharm.* 4 (1978) 53–67.
- [3] R. Bodmeier, Tableting of coated pellets, *Eur. J. Pharm. Biopharm.* 43 (1997) 1–8.
- [4] J. Krämer, H. Blume, Biopharmaceutical aspects of multiparticulates, in: I. Ghebre-Sellassie (Ed.), *Multiparticulate Oral Drug Delivery*, Marcel Dekker Inc., New York, 1994, pp. 307–332.
- [5] I. Ghebre-Sellassie, Pellets: a general overview, in: I. Ghebre-Sellassie (Ed.), *Pharmaceutical Pelletization Technology*, Marcel Dekker Inc., New York, 1989, pp. 1–13.
- [6] I. Ghebre-Sellassie, A. Knoch, Pelletization techniques, in: J. Swarbrick, J.C. Boylan (Eds.), *Encyclopedia of Pharmaceutical Technology*, Marcel Dekker Inc, New York, 2002, pp. 2067–2080.
- [7] P. Roy, A. Shahiwala, Multiparticulate formulation approach to pulsatile drug delivery: current perspectives, *J. Control. Release* 134 (2009) 74–80.
- [8] C. Nastruzzi, R. Cortesi, E. Esposito, A. Genovesi, A. Spadoni, C. Vecchia, E. Menegatti, Influence of formulation and process parameters on pellet production by powder layering technique, *AAPS PharmSciTech* 1 (2000) 9 (Available at: <http://www.aapspharmstech.org/view.asp?art=pt010209&pdf=yes>. Accessed on 13 January 2009).
- [9] N. Sinchaipanid, P. Chitropas, A. Mitrevej, Influences of layering on theophylline pellet characteristics, *Pharm. Dev. Technol.* 9 (2004) 163–170.
- [10] E.L. McConnell, C.B. Macfarlane, A.W. Basit, An observational study on the influence of solvent composition on the architecture of drug-layered pellets, *Int. J. Pharm.* 380 (2009) 67–71.
- [11] G. Heinicke, J.B. Schwartz, The influence of surfactants and additives on drug release from a cationic Eudragit coated multiparticulate diltiazem formulation, *Pharm. Dev. Technol.* 12 (2007) 381–389.
- [12] M. Nitz, O.P. Taranto, Film coating of theophylline pellets in a pulsed fluid bed coater, *Chem. Eng. Proc.* 47 (2008) 1412–1419.
- [13] L.W. Chan, E.S.K. Tang, P.W.S. Heng, Comparative study of the fluid dynamics of bottom spray fluid bed coaters, *AAPS PharmSciTech* 7 (2006) 37.
- [14] T. Sovány, K. Nikowitz, G. Regdon Jr., P. Kása Jr., K. Pintye-Hódi, Raman spectroscopic investigation of film thickness, *Polymer Testing* 28 (2009) 770–772.
- [15] D. Wouessidjewe, Aqueous polymethacrylate dispersions as coating materials for sustained and enteric release systems, *STP Pharma* 7 (1997) 469–475.
- [16] R. Wesdyk, Y.M. Joshi, N.B. Jain, K. Morris, A. Newman, The effect of size and mass on the film thickness of beads coated in fluidized bed equipment, *Int. J. Pharm.* 65 (1990) 69–76.
- [17] K. Thoma, K. Bechtold, Influence of aqueous coatings on the stability of enteric coated pellets next term and tablets, *Eur. J. Pharm. Biopharm.* 47 (1999) 39–50.
- [18] E.R. Bendas, J.W. Ayres, Leaky enteric coating on ranitidine hydrochloride beads: dissolution and prediction of plasma data, *Eur. J. Pharm. Biopharm.* 69 (2008) 977–985.



Dr. Krisztina Nikowitz
Ph.D. student

e-mail: niko@pharm.u-szeged.hu
Date and place of birth: 1984, Budapest

Qualifications, academic degrees
• Pharmacist diploma, 2009

Place of work, post
• Ph.D. student, SZTE, Department of Pharmaceutical Technology, Szeged, Hungary

Research activity

- Preparation and evaluation of film-coated dosage forms and free films
- Physical–chemical and thermoanalytical investigations



Dr. Péter Kása Jr. Ph.D.
Assistant professor

e-mail: p.kasa@pharm.u-szeged.hu
26th September, 1959, Szeged

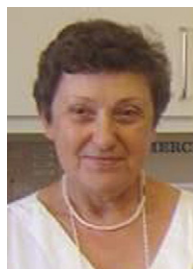
Qualifications, academic degrees
• 1983 Pharmacist diploma
• 1989 Specialist in pharmaceutical technology
• 2002 Ph.D. degree
• Since 2003 assistant professor

Place of work

- Since 1987, Univ. of Szeged, Department of Pharmaceutical Technology

Research

- Preformulation investigations of raw and auxiliary materials
- Preparation of
 - granules, pellets with centrifugal granulator
 - low and high API content tablets and medicated chewing gum tablets with direct compression
- Investigation of compression procedure
- Preparation optimisation with different artificial neural networks
- Light and SEM investigations



Dr. Klára Pintye-Hódi DSc.
Professor
e-mail: klara.hodi@pharm.u-szeged.hu
Date and place of birth: 19.08.1943, Kétegyháza

Qualifications, academic degrees
• Pharmacist diploma, 1968
• Candidate of Pharmaceutical Sciences at the Hungarian Academy of Sciences 1983
• Ph.D. degree, 1996
• Habilitation, 1996
• DSc. 2006

Place of work, post

- Professor, University of Szeged, Department of Pharmaceutical Technology, H-6720 Eötvös u. 6. Szeged, Hungary

Research activity

Development of solid dosage forms with required biological efficiency

- preformulation studies
- study of processing of solid dosage forms
- development and preparation of tablets, pellets and coated forms
- preparation of fast dissolving disintegrated tablets
- preparation of modified release capsules and tablets
- development of matrix systems (mucoadhesive films, granules and tablets)



Dr. Géza Regdon Jr. Ph.D.
Associate professor
e-mail: geza.regdon@pharm.u-szeged.hu
Date and place of birth: 1959, Szeged

Qualifications, academic degrees
• Pharmacist diploma, 1982
• Ph.D. degree, 1996
• Habilitation, 2004

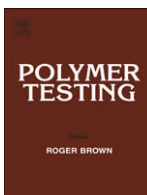
Place of work, post

- Associate professor, University of Szeged, Department of Pharmaceutical Technology, Szeged, Hungary

Research activity

- Preparation and evaluation of film-coated dosage forms and free films
- Coating of crystals and granules with different layer thicknesses and with multilayers by means of fluidization
- Physical–chemical (surface free energy, free volume, FTIR) and thermoanalytical investigations (DSC, MTDSC, TG, kinetic evaluations)
- Factorial design, release and stability tests

V



Short Communication: Test Method

Raman spectroscopic investigation of film thickness

T. Sovány, K. Nikowitz, G. Regdon, Jr., P. Kása, Jr., K. Pintye-Hódi*

Department of Pharmaceutical Technology, University of Szeged, Szeged 6720, Hungary

ARTICLE INFO

Article history:

Received 19 March 2009

Accepted 5 May 2009

Keywords:

Film thickness

Image analysis

Raman spectroscopy

Pellets

ABSTRACT

The determination of film thickness is of prime importance in the quality assurance of coated pharmaceutical preparations. The rapid measurement of this parameter is problematic for multi-particulate pellet systems. The aim of this study was to apply the Raman spectroscopic method for the determination of the thickness of polymer coating on pellets. The change of Raman intensity was compared with measured film thickness, which was calculated from the change of the geometric parameters of the pellets, measured with an image-analyzing system. The results revealed that despite some difficulties Raman spectroscopy is a suitable method for the fast and accurate determination of film thickness on multi-particulate systems.

© 2009 Elsevier Ltd. All rights reserved.

1. Introduction

The thickness of the film coating on solid dosage forms exerts a large effect on the drug dissolution profile of the preparation. For this reason, the determination of this parameter is of prime importance in the quality assurance of controlled release dosage forms. Traditionally, the film thickness can be determined via the addition of a specific amount of coating material, or by measurement of the geometric parameters. Geometric measurements can easily be performed on tablets, but measurements on granules or pellets are more difficult due to their size. Such measurements can be made only with image-analyzing techniques, which are accurate, but time demanding [1]. In recent years, the use of fast and powerful nondestructive methods such as interferometry [2] or spectroscopic methods (NIR, FTIR, Terahertz) has come into focus [3], which can be used for on line monitoring of the technological process [4,5], particularly as regards tablet coatings. In the case of pellet systems, this measurement is more problematic due to the size ratio of the particles and the laser spot. The present study relates to the applicability of Raman spectroscopy for the measurement of the thickness of films on pellets.

2. Experimental

The multi-particulate pellet samples were prepared in a Strea-1 fluid bed Wurster chamber (Niro Aeromatic Ltd., Switzerland). In the first step, the API was layered onto the surface of indifferent (without API) cores. Dilthiazem HCl (Ph. Eur.) and Kollidon 25 (BASF, Germany), in a relative mass ratio of 5:3, were dissolved in water to give a total solid content of 40%. The liquid was layered onto the surface of preheated Cellet 500 (ShinEtsu, Japan) cores at 50 °C. The other coating conditions for all batches were: nozzle diameter 1 mm, peristaltic pump speed 4 rpm, fan capacity 4.5, air volume 75 m³/h and outlet temperature 43 °C. The dry material consumed was 197 g for 200 g of core. The pellets were further fluidized for 10 min after layering.

Table 1

Film thickness and corresponding peak integrals of products.

	Film thickness (μm)	Integrals		
		Peak 1	Peak 2	Peak 3
Sample 1	0	0	0	0
Sample 2	15.5	9158	5369	22,155
Sample 3	23.5	11,471	7669	24,926
Sample 4	28.9	11,805	9174	26,077
Sample 5	44.4	13,876	10,416	30,428

* Corresponding author. Tel. +36 62545576; fax: +36 62545571.
E-mail address: klara.hodi@pharm.u-szeged.hu (K. Pintye-Hódi).

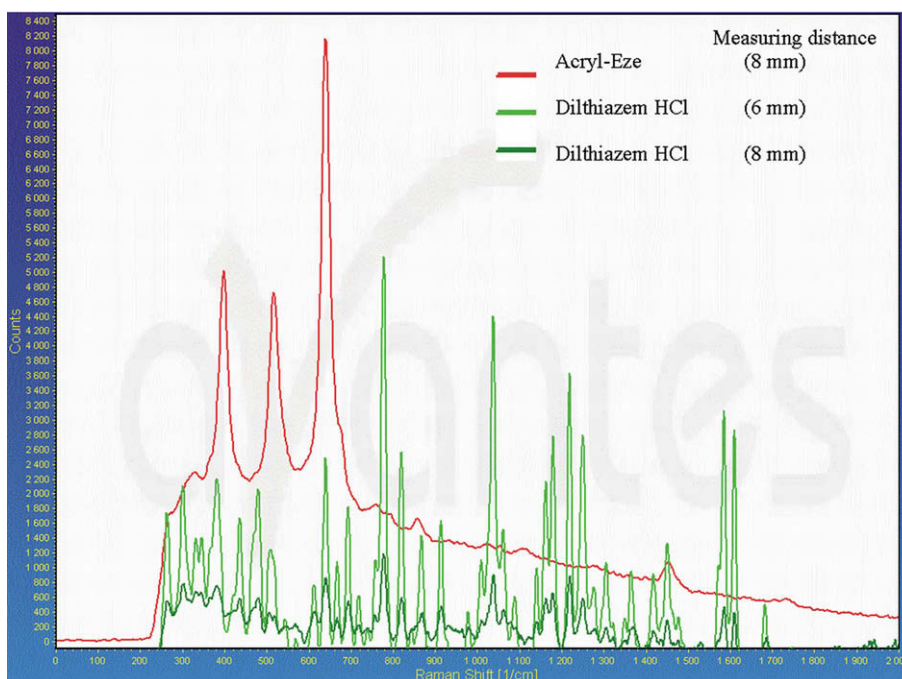


Fig. 1. Raman spectra of materials with different measuring distance.

After a 10-min drying time, the coating material was sprayed under the same conditions as above. The coating liquid was a 20% aqueous dispersion of Acryl-Eze (Colorcon, UK), a 1:1 copolymer of methacrylic acid and methyl methacrylate, generally used for enteric coating of dosage forms. The consumed dry material, from Samples 2 to 5 was 59.5 g, 79.5 g, 99.3 g and 125.0 g, respectively.

3. Results and discussion

3.1. Measurement of film thickness

Film thickness was determined from the results of image-analyzing measurements. Samples were taken after the layering of the active pharmaceutical ingredient and

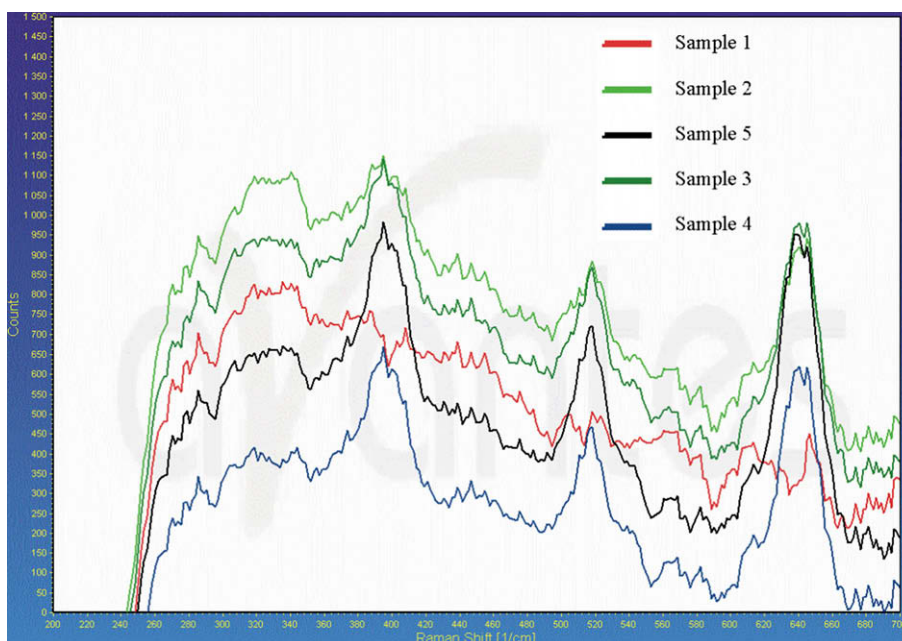


Fig. 2. Raman spectra of the samples.

after coating. The geometrical parameters of 300 particles were determined with a stereomicroscope (Zeiss, Switzerland) and a Quantimet 500 MC image-analyzing system (Leica Cambridge Ltd., UK). The mean film thickness was calculated from the difference between the mean particle diameters of the particles before and after coating. The image analysis demonstrated that the roundness of pellets was good, with calculated values in the range 1.07–1.21. However, there was a small difference between the smaller and the larger diameter of the particles. These were around 780 μm and 860 μm respectively for every batch after layering. The further measurements revealed that the film thickness of the coating layer, which was 15.5, 23.5, 28.9 and 44.4 μm for the various samples (Table 1), correlated well ($R^2 = 0.975$) with increasing amount of the coating material.

3.2. Raman spectrometry

The Raman spectra were detected off-line with an AvaSpec 2048 CCD-array Raman spectrometer (Avantes BV, The Netherlands) using a standard 785 nm laser. Two problems occurred during the spectroscopic measurements. The spectra were taken from bulk samples with a fiber optic detector, where the spot size was about three times larger than the individual particles of the sample. The scattering of the laser light on the rough surface weakened the intensity of the Raman signal, so an increase in the number of scans was necessary. Each spectrum was calculated as the average of 25 scans, which required about 2 min measurement time. The other problem was that the API exhibits many characteristic peaks in the Raman shift range 250–1700 $1/\text{cm}$, which partially overlap with the characteristic peaks of the coating material at 398, 516 and 640 $1/\text{cm}$ (Fig. 1). However, the results indicated a strong influence of the measuring distance of the detector on the peak intensities. The optimal distance was 6 mm for the API and 8 mm for the coating material. This difference is a great advantage during the measurements, which were performed with an 8 mm detector distance, because the weakening of the signal of the API (Fig. 1) helps the determination of the film thickness. Especially in the case of coated samples, because under these circumstances the

signals of the API were hidden in the noise, the peaks of the coating material could be determined alone without subtracting the spectra from each other (Fig. 2). The integral values of the peaks were calculated after baseline correction. The integral values (Table 1) exhibited a strong correlation with the film thickness: the R^2 values of the calibration curves were 0.943, 0.892 and 0.996 respectively for the different peaks. This tendency clearly indicates that the estimation of the film thickness based on the Raman spectra improves with the improvement of the signal/noise ratio.

4. Conclusions

It may be concluded that Raman spectrometry is a suitable method for the estimation of film thickness. The measurement requires only a short time as compared with other methods. The disturbing effects of the different materials can be eliminated through selection of the optimal measuring conditions. This permits monitoring of the film thickness even during the coating process.

Acknowledgements

This work was supported by a Sanofi-Aventis scholarship. We would like to thank Katalin Vakli and the Avantes Company for the Raman spectrometer.

References

- [1] Zs. Muskó, K. Pintye-Hódi, P. Szabó-Révész, P. Kása Jr., I. Erős, D. Deák, Measurement of film thickness on the surface of coated pellets and its influence on drug dissolution rate, *Pharmazie* 55 (2000) 465–466.
- [2] H.M. Shabana, Determination of film thickness and refractive index by interferometry, *Polym. Test.* 23 (2004) 695–702.
- [3] A.J. Fitzgerald, B.E. Cole, P.F. Taday, Nondestructive analysis of tablet coating thicknesses using terahertz pulsed imaging, *J. Pharm. Sci.* 94 (2005) 177–183.
- [4] J.J. Moes, M.M. Ruijken, E. Gout, H.W. Frijlink, M.I. Ugwoke, Application of process analytical technology in tablet process development using NIR spectroscopy - blend uniformity, content uniformity and coating thickness measurements, *Int. J. Pharm.* 357 (2008) 108–118.
- [5] S.H. Tabasi, R. Fahmy, D. Bensley, C. O'Brien, S.W. Hoag, Quality by design, part II - application of NIR spectroscopy to monitor the coating process for a pharmaceutical sustained release product, *J. Pharm. Sci.* 97 (2008) 4067–4086.